SPIQ-FS Dataset

Version 0

Estimation of marginal damage costs from reactive nitrogen emissions to air, surface waters and groundwater

Steven Lord

Environmental Change Institute, University of Oxford

Content reviewer:

Citation: **Lord, S. (2020) Estimation of marginal damage costs from reactive nitrogen emissions to air, surface waters and groundwater. Documentation of the SPIQ-FS Dataset Version 0. Environmental Change Institute, University of Oxford.**

 Research funded by Quadrature Climate Fund.

Summary

Marginal damage costs in international dollars (US$2020 Purchasing Power Parity) per kg in N-weight of NH_3 (ammonia) emissions to atmosphere, per kg in N-weight of NO_x (nitrogen oxide & dioxide) emissions to atmosphere, per kg in N-weight of Nr (reactive nitrogen) run-off to surface waters, and per kg in N-weight of Nr (reactive nitrogen) leached to groundwater are estimated for 171 countries. The damage costs estimate 2020 present value of present and future economic losses from 1 kg of the respective atmospheric or aquatic reactive nitrogen emission in 2020.

The marginal damage costs for each country and each form of reactive nitrogen emission are provided as random variables of loss in parametric form in Table 7 on page 64. Two parameters, mu and sigma, are estimated for a lognormal distribution of probable US$2020 PPP present values given 1 kg of atmospheric or aquatic reactive nitrogen emission. The samples from which the parametric forms are derived and the correlation matrix for covariance of loss across countries are available in the SPIQ-FS dataset.

Use for economic loss

The objective of the SPIQ-FS dataset is to enable estimates of economic risk due to food system activities and the economic potential of food system transformation. The intended use involves aggregation across countries and quantities, for example, in global studies of dietary change or for multinational company or value chain estimates of impact.

The marginal cost estimates should not be used for local or site-specific studies.

The estimate represents aggregated economic loss to a present or future economy (e.g. reduction in Gross Domestic Product (GDP) or consumption as an income-equivalent welfare loss) but no transfers between individual economic actors or sectors (e.g. payments from households to the health sector for health costs).

The average present value of probable US$2020 PPP marginal economic loss given 1 kg of atmospheric or aquatic reactive nitrogen emission for each country and each form of reactive nitrogen emission is reported in Table 6 on page 60. The average value should be used to calculate the average value of total economic losses across multiple countries and quantities since it is additive.

To calculate risk in total economic losses within a country from one form of nitrogen pollution, the distribution of probable US$2020 PPP marginal economic loss given 1 kg of atmospheric or aquatic reactive nitrogen emission in Table 7 should be multiplied by the quantity of emissions. This may overestimate the uncertainty in total economic losses for a large quantity of emissions and may underestimate the uncertainty for a small quantity of emissions given only the knowledge that the emission occurs within the country[1].

---

[1] Over- or under-estimation may result since it is unclear whether 1 kg of emission of NH_3, say, by food system activities represent independent lotteries of economic loss. When aggregating to a total economic loss for n kg emitted, the sum of n random variables each with lognormal distribution given by Table 7 as a representation of the uncertainty in total economic loss should not be used without a sufficient argument for independence within the impact pathways of each unit of emission. For example, the total economic impact of CO_2 (carbon dioxide) emissions in 2050, treating each emission as a random draw from the distribution of economic loss for

To calculate risk in total economic losses across multiple forms of nitrogen pollution, other impact quantities such as Greenhouse Gas (GHG) emissions, and multiple countries, the correlation matrices in the SPIQ dataset should be used to reconstruct a joint distribution of probable US$2020 PPP present values for the impact quantities[2]. Samples from the joint distribution of marginal damages should be multiplied by their respective quantities for each country and then added. The resulting set is a sample of total economic losses. Economic risk or economic potential is generally underestimated without using joint sampling.

It is not recommended to use the average values in Table 6 separate from the uncertainty estimate in Table 7.

Use for economic potential

The marginal damage costs in Table 7 and any totals for economic losses calculated using them **do not include the value (benefits) provided to society from 1 kg of atmospheric or aquatic reactive nitrogen emission**. There is no comparison with a counterfactual to estimate the balance of value between avoided damages from nitrogen emissions and the costs to abate nitrogen emissions. Abatement costs include the option of 'paying the cost' of losing the production value from nitrogen use.

Reducing nitrogen emissions will not 'save the costs' to the global economy of amounts calculated using the values in Table 6 on page 60 and Table 8 on page 68. Damage costs should be paired with abatement costs and counterfactuals to determine the economic risk from food system activities and the economic potential in food system transformation.

The simplest use with a counterfactual is two or more scenarios which, all else being equal, have the same value from production with different quantities of nitrogen emissions. In this case, a change in overall economic value is estimated by the marginal damage costs multiplied by the change in the respective atmospheric or aquatic reactive nitrogen emission.

Methodology and caveats

Impact pathway

---

1 metric ton of CO2 emitted and summing the random variables, will result in a gross error if economic loss is not independent between each emission due to a common component in the impact pathway (e.g. a systematic underestimate in the chemistry of radiative forcing). For nitrogen pollutions, emissions share common biological responses in exposed ecosystems and human populations and can share similar factors related to impact such as temperature, humidity, and precursors to particulate production. Large quantities of emissions from spatially separated sources across countries with heterogeneity in factors related to impact is discussed in the text. Uncertainty for marginal damage costs when quantities are unspecified is not fully resolved in SPIQ Version 0.

[2] Covariance in economic losses due to joint emission or production of impact quantities from food system activities, for example 1 kg of NH3 emission in country i and 1 metric ton of CO2 emitted in country j, is estimated in the document "SPIQ-FS Version 0: double counting and estimation of correlations between impact quantities". The parametric form given in Table 7 represents what is called the marginal distribution of a joint distribution across countries and quantities of marginal damages for the impact quantities associated to food system activities. Determination of the correlations considers spatial and temporal coincidence of impact. All SPIQ-FS Version 0 damages are for impact quantities produced in 2020. A later version may consider joint distribution across countries and quantities and years of emission/production.

Ammonia (NH_3) emissions to atmosphere create ammonium compound particulate matter. Exposure of human populations occurs through wide dispersal with subsequent health effects and gross productivity losses. Wet and dry deposition of ammonium compounds and ammonia on terrestrial and aquatic systems can cause acidification and biodiversity loss. Deposition is a secondary source of atmospheric emissions or run-off causing acidification and eutrophication. Acidification can cause crop losses and damage to ecosystem services produce economic loss.

Nitrogen oxide & dioxide (NO_x) emissions to atmosphere interact producing particulate matter and tropospheric ozone. Exposure of human populations occurs through wide dispersal with subsequent health effects and gross productivity losses. Dispersed ozone damages plant tissue directly. Wet and dry deposition of particulate matter and reactive nitrogen compounds such as nitric acid on terrestrial and aquatic systems can cause acidification and biodiversity loss. As for ammonia, deposition is a secondary source of atmospheric emissions or run-off causing acidification and eutrophication. Acidification and ozone exposure can cause crop losses and damage to ecosystem services produce economic loss.

From direct application on cropland and grassland, or from atmospheric deposition on cropland, grassland, forests, other terrestrial biomes, surplus Nr leaches from soil into groundwater or is transported in surface run-off into riverine systems. Soluble nitrate (NO_3^-) is the main species. Nitrate consumed in drinking water produces subsequent health effects and gross productivity losses. Nitrogen in surface freshwater can be retained in inland waterways and connected ecosystems, causing acidification, biodiversity loss and eutrophication. Nitrogen not retained and exported to coastal environment causes acidification, biodiversity loss and eutrophication and can be a source of secondary atmospheric emissions.

Secondary emission of N_2O from nitrification and denitrification processes associated the atmospheric NH_3 or NO_x emissions, or reactive nitrogen emissions to surface water and groundwater, are assumed to be quantified within GHG emissions.

Calculation and uncertainty

Attribution of human and ecosystem damage from the nitrogen cascade of NH_3 or NO_x emitted to air from agricultural activities, or reactive nitrogen leached to groundwater or entering surface waters as run-off, come from a limited set of studies. Most marginal estimates are based on calculations for the European Union (EU) nitrogen assessment. Transfer to other countries involves modification of exposure and ecosystem damage factors, with a large amount of uncertainty.

Marginal damages from NH_3 and NO_x air pollution are adjusted by scaling a low-resolution regression model of exposure and vulnerability. Spatial datasets on global deposition are used to estimate differences between countries in the face of atmospheric emissions and secondary impacts from deposition and run-off.

Marginal damages from run-off to surface water are adjusted using proportional average costs of lost ecosystem services. Spatial datasets on inland retention and export to coastal systems of nitrogen are used to determine differences in loads to ecosystems between countries, and spatial dataset are used to estimate the differences in habitats and value of their ecosystem services.

Marginal damages from concentration of nitrate in groundwater are adjusted using proportional costs of lost life years.

The variation between countries is large, from US$2020 PPP >100 per kg of Nr run-off in countries with high proportion of reactive nitrogen export to high value coastal systems to US$2020 PPP < 10 per kg with high retention of nitrogen in lower value inland aquatic. US$2020 PPP >30 per kg of NH_3-N is expected in countries with high population density and presence of acidic precursors for ammonium particle formation to US$2020 PPP < 10 in countries with low population density and inhibitors of particle formation. Large variation is due to primary factors such as population density and the nitrogen cascade, where the "fate" of emitted nitrogen varies greatly between countries. The greatest variance between countries is in the estimate of the marginal damage cost of Nr surface run-off. Spatial datasets based on modelling show huge variation between nitrogen retained in inland water systems and export to coastal systems. Where a country has a high proportion of riverine export of Nr to coastal systems, the valuations in the Ecosystems Service Valuation Dataset (ESVD) for many countries has much higher values for coral reefs and coastal systems than retention in inland wetlands. Damage costs for run-off to surface waters are also the most uncertain, due to high uncertainty for the economic value of losses of inland water and coastal ecosystem services.

Our mean values for health damages from NH_3 and NO_x are lower than other studies, which (a) are from EU countries with a higher population density compared to most countries in the rest of the world, (b) use value of a statistical life, and (c) are not average marginal damage cost to be used at a country level but estimated at a higher resolution. Despite having lower mean values, the uncertainty represented in Table 7 spans an order of magnitude and includes the estimates based on value of a statistical life.

Caveats include using broad assumptions for transport from the EU nitrogen assessment to other countries. Transboundary effects of run-off and deposition for smaller countries within proximity to large nitrogen emitters may be large. Detailed spatial modelling of the fate of nitrogen, and the connection to surrounding socio-economic systems is recommended to improve the estimates and reduce uncertainty, though, even with this modelling, attribution between services lost and the load of nitrogen to human and natural systems is still a challenge. Potential improvements will be afforded by a greater emphasis on spatially explicit modelling in SPIQ-FS Version 1.

Damage costs in the SPIQ-FS dataset are not valuable for direct comparison of countries. The costs represent primarily the externalised costs of nitrogen use for market corrections in the economies where the costs are borne.

Global perspective

For perspective, national estimates of NH_3 and NO_x atmospheric emissions from the agricultural sector from EDGAR5.0 and agricultural contribution to total run-off and groundwater leaching from IMAGE-GNM across 171 countries are paired with the marginal damage costs (Section 4.4.3 from page 37 and Section 4.10.2 from page 75).

Estimated global costs of nitrogen use for agriculture are over US$2020 PPP 1 trillion, with a greater than 5% chance that costs are over US$2020 PPP 3 trillion. China represents over 30% of the total damage costs with an expected loss of US$2020 PPP 390 billion. How much of this estimated economic loss can be recovered from transforming agricultural production and food systems is unclear without global modelling studies of abatement and the respective costs of nitrogen emissions.

The large uncertainty in ecosystem service losses from surface run-off, and the dominance of several countries in terms of quantity of run-off (China, Brazil, India, Russia, United States) give the global distribution of losses a long tail (Figure 11 on page 79).

Annex A

Contents

4 Nitrogen

4.1 Quantities associated to impact

The food system is associated to ~80% of anthropogenic ammonia (NH3) emissions and ~20% of anthropogenic NOx emissions into the atmosphere [1-6] (Figure 1). Both forms of reactive nitrogen (Nr) emissions to the atmosphere are associated to human health damage from inhalation of particulate matter [7] and ecosystem damage from subsequent atmospheric deposition on terrestrial, riverine, and marine environments [8].

The food system is associated to ~80% of anthropogenic Nr emissions into inland waterways [2, 9] (Figure 1). Some of the emission to inland waterways transport through riverine systems to coastal and marine environments. Most of the direct Nr emissions to waterways are soluble nitrate $NO3^-$ direct from fertiliser and manure run-off and leaching, as well as human waste from consumed food. The smaller components are run-off from land deposition, or direct deposition on riverine, coastal, or marine systems of agricultural atmospheric Nr emissions as well as atmospheric NOx from burning fossil fuels for energy and transport (some of which is attributable to energy use in the food system [10]). Excess soluble Nr impacts ecosystems through eutrophication and acidification, and impacts humans and animals through nitrate pollution of drinking water [8].

Release into the atmosphere of N2O (nitrous oxide) from soils, fertilizer application, and manure, and the costing of N2O emissions, is considered in Annex A – GHG. Atmospheric and aquatic transmission of ammonia, nitrates and nitrogen oxides can result in terrestrial and marine deposition of Nr and secondary N2O emissions before and during denitrification [11]. In 2016, 1.3 Tg N yr^{-1} of N2O emissions were from secondary anthropogenic N deposition compared to ~5.5 Tg N yr^{-1} of net primary anthropogenic N2O emissions [12]. ~70% of anthropogenic N2O emission is attributable to the food system through primary emissions (Figure 1) and secondary emissions from deposition (not shown).

4.1.1 Food system sources of N emissions

Nitrogen is embedded in crops from natural atmospheric deposition, biological N fixation, crop residues and recycling manure, and synthetic fertilizer application. It is embedded in livestock products through consumption of grass and feed. Human N intake of embedded N in crop and livestock products is excreted in faeces or urine. The transport of embedded N through crop and livestock products has been called virtual N.

Subtracting manure losses from vegetal food production, livestock is responsible for 63% (67 Tg N yr^{-1}) of estimated food system 2010 N emissions [13] (Figure 1) while providing 17% of global calories and 33% of global protein (FAOSTAT, 2014) [14]. 61% (41 Tg N yr^{-1}) of livestock N emissions are attributed to crop-based feed. 31% (21 Tg N yr^{-1}) of livestock N emissions are attributed to manure. Livestock production dominates the flux of N in the food system (Figure 1). Emissions from processing livestock (1 Tg N yr^{-1}), and the fate of virtual nitrogen embedded in meat and dairy products (4 Tg N yr^{-1}), are minor and make up most of the remaining 8%.

Vegetal-based food is responsible for 35% (33 Tg N yr^{-1}) of estimated food system 2010 N emissions (Figure 1). 26 Tg N yr^{-1} is emitted from production of vegetal foods and 7 Tg N yr^{-1} is emitted from human waste. Vegetal sources provide 82% of global calories and 60% of global protein (FAOSTAT, 2014).

Annex A

Aquaculture's contribution to food system N emission is presently small. China is responsible for >66% of global aquacultural production. Estimates of Chinese aquaculture NH3 air emissions are 0.54 Tg N yr^{-1}, and Noy deposition to coastal sediment 2.1 Tg N yr^{-1} [15] – making terrestrial sources of food production and human waste greater emitters than aquaculture. Aquaculture is responsible for <2% of food production N2O emissions [12]. Global seafood consumption provides 1% of global calories and 7% of global protein (FAOSTAT, 2014).

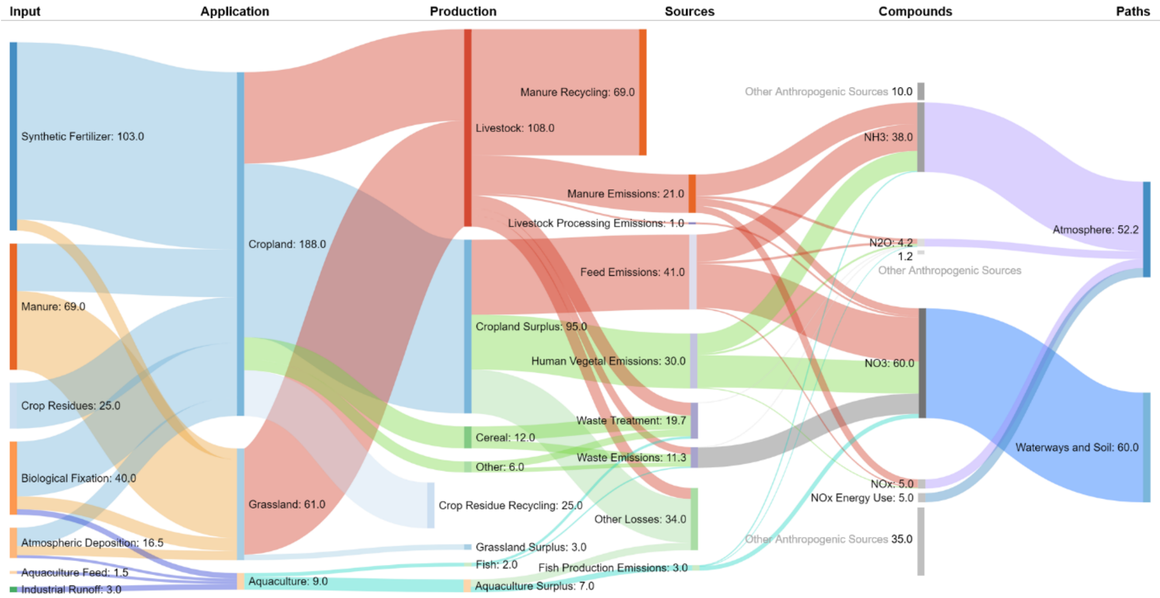

Figure 1: Source: Author. Units Tg N yr^{-1}. NH3, NOx and NO3- emissions of the global food system 2010, with division of fluxes between grassland, cropland, livestock and non-livestock feed and foods, and aquaculture. Derived from 2010 livestock accounting from [13], extrapolated with 2010 total flux accounting from [2, 9], and consistent with crop factors from [16]. Aquaculture extrapolated from [15]. Consistency with other studies examined in [4, 5, 16, 17]. N2O emissions primary and secondary from [12]. Waste water treatment N2O from [18]. Excludes Nr emissions from food system energy use and transport. Waste emissions are from untreated waste of consumed food, with treatment factors from [19]. Fertiliser rates for grassland are scaled from [20] and with grassland surplus excluding manure. Grassland surplus high uncertainty. Other crop surplus losses include non-food crop uses. Uncertainties on fates of other losses from cropland surplus exist within anthropogenic input Nr run-off and leaching into water ways (estimated 75 Tg N yr^{-1} in [21] and 110 in Tg N yr^{-1} in [9], though it is unclear whether the total in [21] is before or after water treatment). NO3- in waterways and groundwater is most of input Nr from run-off and leaching. Around 40% of Nr input to waterways is transported to coastal and marine environments, though there is large uncertainty in denitrification sinks during transport from soils, water bodies, vegetation and groundwater [22]. An estimated 12 Tg N yr^{-1} of N run-off from fertiliser, manure and secondary deposition acts as additional N input to aquaculture, whose surplus is not shown (believed to be stored in excess N held in coastal waters and N transport to ocean [15]). 4.2 Tg N yr^{-1} in N-weight of N2O emissions matches the ~6.8 Mt N2O emissions attributed to the food system [23], see Annex A – GHG Figure 1. NOx emissions from energy use in the food system indicated in compound column. Secondary emissions from nitrogen cascades not shown (see Damage costs below). From atmospheric deposition of food system NH3 and NOx emissions from manure, fields, waste, and aquaculture, an estimated 0.65 Tg N yr^{-1} (1 Mt) of secondary N2O emissions would be attributed to the food system [1-3, 12]. In 2010 livestock dominated the flux of Nr through: absorption of N in crop-based feed, emissions from production of the crop-based feed, and manure. Without attributing manure losses from vegetal food production, livestock is responsible for 63% (67 Tg N yr^{-1}) of estimated food system 2010 N emissions [13]. Livestock production has accelerated in the decade 2010-2020. After livestock, fertiliser emissions for vegetal-based human food and human waste are the largest emission sources. Total 2010 anthropogenic atmospheric emissions of NH3, N2O and NOx added for reference to food system emissions (NH3 total 48 Tg N yr^{-1} and NOx total 45 Tg N yr^{-1} from EDGAR 4.3.2 [6], N2O total 5.4 Tg N yr^{-1} from [12]).

Processing and manufacturing of food products result in <2% of food system direct N emissions from release of embedded N, mostly to waterways. Attribution of N impacts for processors, manufacturers, and retailers, is through "Scope 2" emissions of NOx from energy and transport, upstream “Scope 3” Nr emissions from agriculture, and downstream “Scope 3” Nr waste emissions post-consumption.

High resolution satellite data of atmospheric NH_3 emissions can pinpoint concentrated emissions in proximity to human concentrations and ecosystems. Satellite data suggests that NH_3 emissions databases may underestimate livestock and fertiliser manufacturing emissions [24].

Fossil fuel production and use emits NO_x and NH_3 to the atmosphere. Therefore, energy use for inputs, production, manufacturing, retail, and transport of food is an attributable source of additional NO_x and NH_3. The food system was responsible for ~15% of 2010 fossil fuel energy use globally [10]. 15% of the approximately 36 Tg N yr^{-1} 2010 NO_x atmospheric emissions from fossil fuel use [4] is ~5 Tg N yr^{-1}, compared to NO_x ~5 Tg N yr^{-1} estimated from manure and field emissions [13].

4.1.2 Ammonia (NH_3) emissions in energy use for retail and manufacturing

Burning of fossil fuels has proportionally greater NO_x than NH_3 emissions by N-weight. Hence NH_3 emissions from energy use across the food system are <2% of those from direct agricultural NH_3 emissions [25]. Direct agricultural emissions of NH_3 (including emissions not attributed to the food systems, e.g. biofuel) are >80% of global NH_3 emissions [1, 4] so capturing changes in agricultural NH_3 emissions is generally more important for changes to impact. NH_3 emissions from attributable energy use can be ignored for most large-scale impact studies. For small-scale studies, NH_3 emissions from energy use in transport, retail, and manufacturing should be examined for their contribution to impact even if proportionally lower than agricultural emissions. NH_3 emissions from combustion generally occur in closer proximity to human populations and closer to resident atmospheric NO_x and sulfur oxide (SO_x) (see below under atmospheric pathway of NH_3 emissions). This implies a greater amount of $PM_{2.5}$ production per N-weight closer to human population density than an agricultural NH_3 emission, and a greater cost per tonne of NH_3 emitted.

4.2 Air, water, and soil pathways of Nr emissions and damages

Sources for primary emissions of Nr to atmosphere are described in (Figure 1). A complex of secondary chemical reactions in the atmosphere and from deposition on land and ocean is called the nitrogen cascade [2] (Figure 2). Nr products that deposit on land, waterways, and ocean (as NH_x and NO_y) result in damage to ecosystems [8] and secondary emissions of NH_3, NO_x and N_2O [26] before denitrification [27]. Nr is being produced more rapidly than it is being converted back to inert N_2 (78% of the atmosphere). In ecosystems that may be some distance from primary emission sources (Figure 4), Nr is accumulating in the environment [8]. The ocean is a major sink [28]. Impact from the nitrogen cascade may increase in the future as terrestrial and marine sinks of Nr saturate.

A consequence of the nitrogen cascade, and a complication for costing impacts, is that the same nitrogen emission produces compounds that can damage human health and ecosystems several times (Figure 2 b. and Table 3 in [2] illustrate), and in several forms of nitrogen compounds from primary emission and secondary deposition (which can lead to tertiary emissions of NH_3, NO_x and N_2O to air).

a. Nitrogen Cascade (Fowler 2013)

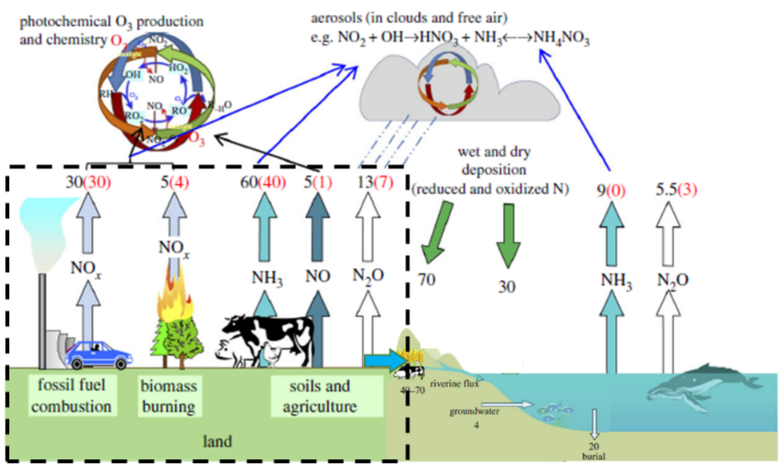

b. Nitrogen Cascade (Sutton and Billen, 2011)

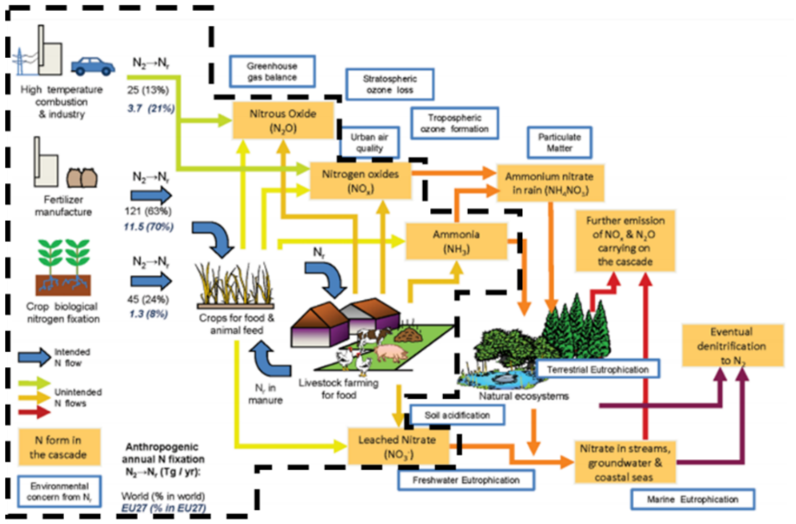

Figure 2: Two representations of the nitrogen cascade. Panel a. adapted from [2]. Panel b. from the European Nitrogen Assessment [29]. The dashed box in each panel represents the scope of Figure 1, i.e. Nr flux to primary emissions. In Panel a, red values indicate global 2010 anthropogenic Nr emissions according to [2]. In Panel b. roman numerals indicate global anthropogenic Nr flux, and italic numerals indicate EU-27, for 2011. For damage costing, a representation of the nitrogen cascade from primary emissions is given in Figure 5.

4.2.1 NH3 atmospheric primary emission

Ammonia (NH3) is a major component in producing particulate matter PM2.5 (as ammonium nitrate when binding with NOx and ammonium sulphate when binding with SOx) [8]. NH3 emitted to atmosphere undergoes chemical reactions or is dispersed within 24 hours, but the PM2.5 produced is transported over days or weeks in the atmosphere [30] and inhaled by humans and animals. It is estimated that ammonium, sulphate, and nitrate, form about a third of global particular matter (PM2.5) [31]. A 2021 United States (US) attribution study found food production responsible for ~16000 of 2015 US air pollution deaths [32] (Figure 3), which is 16% of deaths of the US total attributable to air pollution [33]. NH3 emissions attributed to food production were responsible for ~75% deaths in the study and 12% of total US air pollution deaths [32]. Dust (tillage and soil erosion from livestock) was the next major contributing factor (22% of air pollution deaths attributable to food production) and 3% of total. Dust should be considered under the costs of soil erosion. Deaths in the US study were highly spatially concentrated according to population density and proximity of agricultural production.

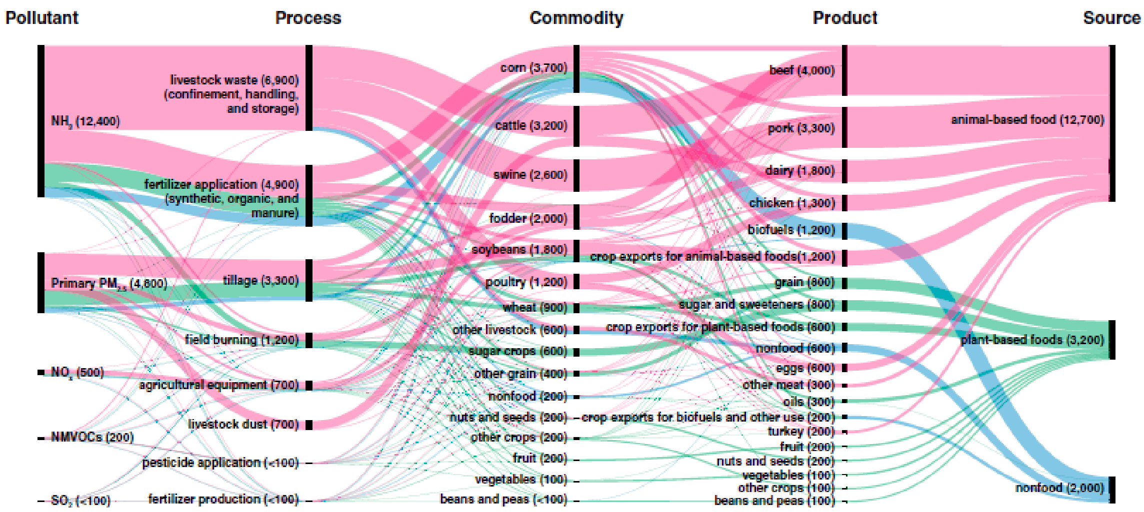

Figure 3; Source and caption: Fig 1 in [32]. "Annual premature US deaths attributed to increased atmospheric PM2.5 from US agriculture. Five alternate categorizations (columns) are shown: pollutant, process, commodity, product, and source. Pollutants include primary PM2.5 and secondary PM2.5 formed from precursor gases (NH3, NOx, NMVOCs, and SO2). The height of each black bar within each column corresponds to the number of attributed deaths; deaths within each column sum to 17,900."

Attributable deaths from NOx emissions were low in the US study (<1%). Fossil fuel use for fertiliser production and agricultural equipment were counted, but not transport, manufacturing and retail in the food sector. NOx and SOx emission have been regulated for transport, energy, and manufacturing, in many countries, including the US. NH3 has not. A Chinese study (1970-2008) attributed ~43% of total damages from atmospheric Nr emission to agricultural NH3 and ~7% to food system NOx emissions including energy use [34]. At larger scales and for full scope of the value chain, the NH3 emissions will be expected to produce >80% food system human health damage costs compared to NOx. At smaller scales and partial scope, the ratio of NH3 and NOx damages depends on the proximity of sources of combustion, burning, and energy use compared to agricultural emissions (e.g. Figure S7 in [34]).

When redeposited on land and waterways ammonia produces soil acidification and nitrates that contribute to biodiversity loss and eutrophication [1, 25, 35]. This is further described below. Secondary emission of N2O occurs from deposition, leading to climate impacts.

4.2.2 NOx atmospheric primary emissions

Atmospheric reactions involving emitted NOx increase tropospheric ozone (O3) [2]. O3 acts as a GHG producing radiative forcing, has human health impacts, and losses to crop yields [8, 36-38]. NOx creates smog and binds with NH3 to produce ammonium nitrate and other particulate matter that induces human health impacts [8]. In addition to NOx emissions from energy and transport use in the food system, direct NOx exposure of agricultural or food manufacturing workers, or food preparation from biomass burning, has human health impacts [39, 40]. Deposition of Nr from the nitrogen cascade of emitted atmospheric NOx contributes to secondary damage pathways.

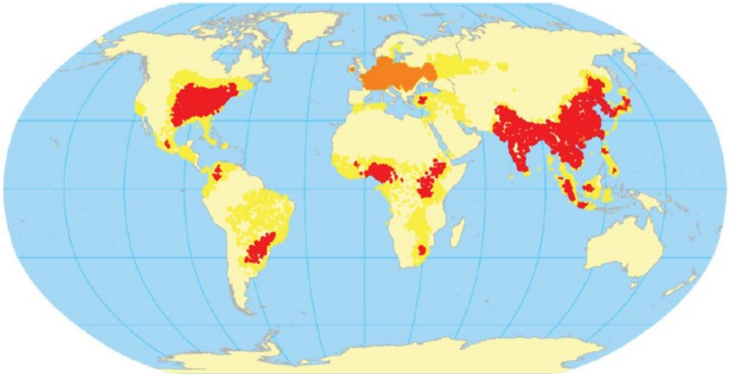

Figure 4: Source and caption: Figure 1 in [8]. "Distribution of atmospheric Nr deposition and exceedance of deposition levels in the period 2000–2030 on Protected Areas (PAs) under the Convention on Biological Diversity. Red PAs show an exceedance of 10 kg N ha^{-1} yr^{-1} and deposition in 2030 higher than 2000. Orange PAs show a current exceedance, but deposition in 2030 lower than 2000. Yellow PAs might be under threat since Nr deposition exceeds 5 kg N ha^{-1} yr^{-1}, but is increasing over the period 2000–2030."

4.2.3 Nr secondary atmospheric deposition to land

Atmospheric Nr from primary NH3 and NOx emissions is deposited widely on terrestrial and aquatic ecosystems as ammonia, nitrous oxides, ammonium compounds, nitrites, nitrous acid, nitrates, and nitric acid (NHx and NOy) [41]. Nr compounds delivered to terrestrial systems cause impact through reactions with soil and vegetation, re-emission into the atmosphere, or in waterways and then marine systems through run-off. Deposition can be wet (with precipitation) or dry; mechanisms which generally deposit similar amounts of Nr [42]. Most natural systems are N-limited, meaning that biomass increases with additional Nr, and are vulnerable to acidification.

Damage in terrestrial ecosystems arise from acidification of soils [43] and changes to vegetation [44]. Ecosystem services in natural forests and grasslands are impacted by acidification through biodiversity loss in soils, change in soil structure, and inhibited growth [45]. N sensitive plants and microbiomes are reduced and growth is elevated for nitrophiles, changing the balance of vegetation and eventually the ecosystem fauna and flora [44, 46].

Acidification of cropland soils [47] results in direct agricultural losses and reduction in soil biodiversity, enhancement of existing stressors, contributes to soil erosion, and can effect carbon and nitrogen fluxes [48].

4.2.4 Nr primary and secondary emissions to water ways and soils

From direct application on cropland and grassland, or from atmospheric deposition on cropland, grassland, forests, other terrestrial biomes, surplus Nr leaches from soil into groundwater or is transported in surface run-off into riverine systems [2, 9].

Leaching or run-off can be the dominant source of Nr pollution, depending on the site [49]. Accumulation in soil, N pools and leaching can occur over decades and become a primary source in N water pollution [49]. Other study sites show correlations between wet Nr deposition and riverine Nr concentrations; regression implying a >20% contribution of deposition to total riverine export from the study catchment [50, 51].

The main form of Nr transported in groundwater and surface freshwater is soluble nitrate NO3- [52]. Nitrate NO3- is either consumed by humans and fauna in extracted groundwater, or from surface freshwater polluted by both run-off and re-combination with groundwater [8, 9]. Ingestion of NO3-

through contaminated groundwater has been associated to infant methemoglobinemia, colorectal cancer and thyroid disease [53, 54]. However, the human health and economic effects of and nitrate are less well understood than exposure to particulate matter and ozone [55]. The major exposure of nitrate, except in very high concentrations in drinking water, is through vegetable consumption [56].

Around 40% of Nr input to freshwater is transported to marine environments, though there is large uncertainty in denitrification sinks during transport [22]. Depending on the climate conditions, specifics of the water body and the nature of the Nr deposition in the catchment (synthetic fertilizer or manure management), Nr will either be denitrified in ecosystems along the water way, or collect in freshwater bodies, or reach coastal systems. Excessive Nr can cause freshwater and coastal eutrophication and acidification [9].

Acidification

Acidification of freshwater bodies, wetlands, coastal and marine environments results in inhibited growth and losses to invertebrates and fish [57]. Freshwater wetland and bodies can be more vulnerable due to lower acid neutralizing capacity [8, 57]. Species composition at the base of the food chain is shifted toward acid-tolerant macrophytes and phytoplankton, resulting in biodiversity loss and alterations in higher trophic levels.

Coastal and ocean acidification from deposited ammonium compounds (acidifying) and ammonia (alkalising) is small compared to acidification through CO2 drawdown, but amplified in coastal regions with the greater concentration of Nr from leaching and run-off [58]. Though coastal and ocean environments have higher acid neutralizing capacity, and marine organisms are more acid tolerant, high value ecosystem services and biodiversity in coastal systems such as coral reefs can be impacted [59].

Eutrophication

Freshwater bodies and coastal systems can experience aquatic eutrophication, resulting in a loss of ecosystem services to humans, directly, or a loss of services through effects on surrounding ecosystems [60, 61]. As with terrestrial vegetation, Nr loading results in species selection and biodiversity loss. Eventually, low-diversity algal or bacterial populations can dominate surface waters, limiting sunlight and depleting oxygen from water below the surface. Hypoxic (low oxygen) and anoxic (no oxygen) water stratifies below the surface killing plants, communities in sediment, coral reefs in coastal systems [62], and animals, resulting in “dead zones” [63, 64].

Eutrophication does not occur in the open ocean. Most of the accumulation of anthropogenic Nr in the ocean is from atmospheric deposition [28]. The effects of an ~3% increase in annual marine biological production attributed to anthropogenic deposition and transport of Nr [28], including an ~0.4% increase in ocean carbon sequestration [65], are discussed in correlations in Section 4.5 below.

Surplus Nr in riverine and coastal systems, from primary water emission or secondary atmospheric deposition, provides an increasing background Nr input to aquaculture (estimated globally at ~12 Tg N^{-1} [15], with 66% of this input to Chinese coastal environments). Growth in coastal food sources from the increased Nr input produces financial gain from aquaculture enterprise but can turn to collapse and financial loss with hypoxic events. Indicating, as with other environmental marginal costings, the non-linear nature of marginal costs as a function of total emissions to the aerial or water catchment of the impacts.

Aquatic eutrophication is increased by the anthropogenic emission of other soluble nutrients, particularly phosphorous [66, 67]. Eutrophication can reduce denitrification in sediment, resulting in positive reinforcement and increasing Nr saturation [68].

4.3 Attribution and Damage costs

Estimates of the damage costs of NH3, NOx, and NO3 primary emissions require sophisticated modelling of the nitrogen cascade to determine the exposure of humans and ecosystems to intermediate quantities such as aerosol particulates, response factors such as the vulnerability of exposed populations to respiratory stress, and costs such as economic consequences of respiratory disease. N2O damage arises from residence in the atmosphere. Damage costs for the climate change effects of N2O are discussed in Annex A – GHG. The major pathways to damages from Nr emissions, described in the previous section and assessed in synthesis studies (see e.g. Figure 2 in [8] and Figure 2 in [69]), are summarised in Table 1 and Figure 5.

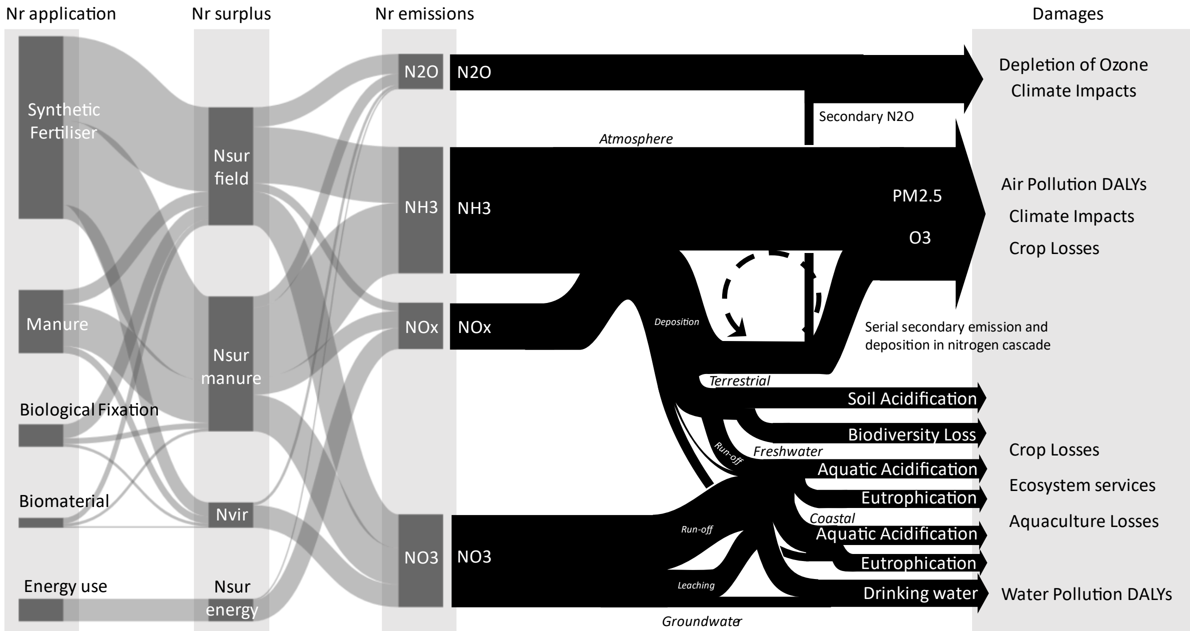

Figure 5: Source: Author. Representation of atmospheric, terrestrial, and aquatic impact pathway of primary Nr emissions summarised in Table 1. Primary atmospheric emissions of NH3 and NOx have some joint interaction to form particulate matter. NOx emissions produce tropospheric ozone. NHx and NOy compounds deposit on land, water bodies, and marine environments. Deposition can produce secondary vaporization and emissions of N2O, NH3 and NOx. Deposited Nr produces terrestrial, freshwater, and coastal impacts, and contributes to the direct flow of, mainly, soluble primary emissions of NO3- into the environmental through run-off to riverine systems and leaching into groundwater of applied Nr and Nr from waste. Connection of impact pathway of primary emissions to origins in Figure 1 shown by emissions factors between application, surplus, and emissions. Ambiguity and variance in costing impacts of Nr can arise through the quantity of impact being treated as an implied input of Nr (e.g. kg of synthetic fertiliser used or manure, kW of fossil fuel sourced energy used), Nr surplus from application (e.g. Tg N surplus to fields from inputs, Tg N embedded in outputs as virtual Nr). Both the matrices of emission factors (EF - grey) that translate from implied inputs to Nsur, and Nsur to Nr emissions, and the amount of damages from Nr emissions (black), are context dependent.

Costing of marginal damages from Nr emissions have concentrated on the European Union [70, 71], the United States [72], and China [73]. Detailed damage estimates have concentrated on climate impact, crop losses from tropospheric O3 [38], and human health impacts of air pollution, due to the maturity of atmospheric Chemical Transport Models (CTMs) and economic estimates [74, 75]. Attribution of multicausal outcomes such as disease and damage to humans from particulate matter, ozone, or other intermediaries of impact from Nr emissions, is based on assembled evidence from univariate control studies or regression analysis [76, 77]. Some CTMs have reduced complexity and attribution to health impact in the form of Disability-Adjusted Life Years (DALYs) built into the model [78]. Attribution of Nr pollution in waterways is highly variable with the most robust estimates using spatially explicit hydrological models [49, 79]. Some costings do not include ecosystem losses from secondary deposition and run-off [80], because of the uncertainty and less developed methods for attributing Nr emissions to loss of ecosystem services and costing the loss of services [81].

Total average damage costs attributed to agricultural Nr emissions for the US (US$2008 210 billion), EU (US$2008 190 billion) and China (US$2008 54 billion) for Nr emissions are >1.4% GDP in 2008 for each region respectively [34, 70, 72, 73]. In the US and EU the cost of agricultural Nr emissions exceeded the value of agricultural commodities produced.

The study [72] of the US did not estimate abatement costs. Other studies indicate an average 30% abatement of N application in agriculture would optimise the value to society of N application [34, 70, 82]. The optimality in [70] was determined by using an abatement cost of atmospheric Nr pollution in IIASA's GAIN model, no abatement cost of run-off of leaching of Nr was included. In [82] the abatement cost was given by the loss of agricultural yield. Without a more complete examination of abatement measure for N (see mitigation costs below), it is unclear whether more detail in N efficiency measures offer cheaper abatement and hence a higher optimal reduction target.

4.3.1 Unit of marginal damages

Costings of Nr usually involve an estimate of the damage cost per unit of input, surplus, or emission at a location, and multiplication by the quantity of inputs, surplus, or emissions at that location. The marginal cost per unit has been estimated at the level of all these quantities, e.g. damage per kg (per hectare) of fertiliser input [83] ([84]), dollars of damage or abatement per unit of surplus [85, 86], and dollars of damage per kg of emission [70]. Even if emissions occurred at the same locations, to be comparable, costings between inputs, surplus, and emissions as the unit quantity for marginal damages would need to be converted by the Emission Factors (EF) of the specific fertilisers, productions processes, management practices, and locations [87].

Location factors can include climatic or soil conditions that can result differences in quantities of NH3 or NO3- emitted from Nr surplus, higher rates of denitrification, etc. EFs are used by actors (e.g., IPCC Tier 1) to simplify calculation of Nr emissions for national accounts and at farm level [88].

The EF matrices are generally not invertible. The damage cost per unit of emission of NH3 and NOx to air, and Nr to soil and surface water at a spatial location is less dependent on the contextual factors of the actor and their operations, and more suitable to standardise. We provide estimates of damage costs per unit of emission below. Tables of EFs for atmosphere are available and open source [89]. EFs for run-off and leaching emissions are less well developed [49]. Calculating Nr emissions using EFs should be the responsibility of emitting parties as part of disclosure of nitrogen impacts.

Unlike climate damages from GHG emissions, actors need to be aware of appropriately estimating the damage cost per unit of Nr emission at the location of emission. For an example, for a "Scope 3" damage cost exercise, there may be large variation between the upstream damage cost per unit of rural NOx emissions from crop and manure management practices, and downstream urban NOx emissions from combustion.

Annex A

Table 1: Major impact pathways of NH3, NOx and NO3 emissions for damage cost estimates.

Emission	Intermediatory	Effect	Impact	Cost
NH_3	Ammonium (NH_4) compounds formed through atmospheric reactions	Air pollution (PM2.5)	Human respiratory DALYs	Disease
	Deposition of NHx (see below)			
NOx	Tropospheric ozone (O_3) formed through atmospheric reactions	Air pollution	Human respiratory DALYs	Disease
	-	-	Physiological impairment of plant growth	Crop losses
	Deposition of NOy (see below)			
	Deposition on land of cascade from NH_3 and NOx air emissions	Reactions from deposited Nr	Acidification (cropland)	Crop losses
	-	-	Acidification (non-cropland soils)	Ecosystem Services
	-	Increased Biological Production	Biodiversity Loss (terrestrial)	Ecosystem Services
			Fertilisation	Crop gains
	Run-off or leaching of Nr deposition on land (see below)			
NO_3	Run-off or leaching from (a) Production or processing, (b) Deposition of Nr compounds on land, and (c) Deposition on water of cascade from NH_3 and NOx air emissions	Increases nitrates in drinking water – ground and surface (NO_3^-)	Human toxicity DALYS	Disease
	-	Reactions from deposited Nr	Acidification (freshwater)	Ecosystem Services
	-	-	Acidification (coastal)	Ecosystem Services
	-	Increased Biological Production	Eutrophication (freshwater)	Ecosystem Services
	-	-	Eutrophication (coastal)	Ecosystem Services

4.3.2 Variance in marginal damages

Specifics of fertiliser composition, productions processes, management practices, and climatic and soil conditions, in addition to volume of agriculture activities, creates variation in the amount of emissions. The marginal damages are functions of emissions, in that higher emissions are expected to contribute greater costs per tonne of emission from increased background exposure of humans and ecosystems. Spatially explicit marginal damage costs may be functions of total Nr emissions at differential spatial aggregate levels. The total emissions at the same site, the total Nr emissions to the same water catchment, and the total Nr emissions received by exposed human populations, may all increase in the marginal costs of damage. The relationship is not linear, the increase of damage costs at extreme levels of local emissions, without high aggregate levels in the surrounding region, is unclear. Once local damages saturate the rate of change of marginal damages depends on the extent of the spread of dead zones [64], longer distance transport from high concentrations of particulate matter [90], or contagion from ecosystem loss [91].

Marginal costs vary with additional spatial and contextual factors involved in a chain of exposure, response, and economic impact that are only weakly associated to the quantity of Nr emissions. Exposure includes exposure of humans and ecosystems to intermediate quantities such as aerosol particulates, which may be more abundant from the same unit of NH3 emission because of climatic conditions. Response includes factors such as the vulnerability of exposed populations to respiratory stress, such as coincident exposure to NOx from rubbish burning or biomass burning for cooking, or coincident Cardio-Vascular Disease (CVD) risks from Non-Communicable Diseases (NCDs). Economic impacts of respiratory disease can vary due to safety nets, insurance, and other factors.

Studies on the marginal damage cost of Nr emissions for the European Union [70] and the United States [72] use fixed marginal damage costs for components of the nitrogen cascade without spatial variation across the EU member states of 2008 and across the contiguous US. The study [72] used most marginal damage estimates from [70] and [69]. Variation in the total damages in [70] arises from estimated variation in the totals for emissions, deposition and run-off. Since proportion of deposition and terrestrial run-off of 1 tonne of NH3 or NOx primary atmospheric emission are components of the impact pathway in Figure 5, then spatial variation in deposition and run-off is one component of variation in marginal damage cost of Nr emission of a unit of NH3, NOx to atmosphere, or Nr to waterways.

A more complete examination of the variation in marginal damage costs due to location of emissions, environmental conditions of the emission, variation in the amount of intermediates such as ammonium compounds and ozone from 1 tonne of NH3 or NOx primary atmospheric emission, deposition, and variation in the distribution of downwind or downstream exposure of vulnerable people or ecosystems, is considered in [83]. Additional variation in the components of Figure 5 were represented at a county level for Minnesota in the US [83]. Marginal damage costs for N application varied from \$0.001 /kg to >\$10 / kg, indicating the high degree of variance in marginal damage costs.

To scale to global spatially explicit marginal damage costs for NH3, and NOx and NO3- that capture the range of damage costs highlighted by [83], reduced complexity models of atmospheric transport (such as the Intervention Model for Air Pollution (InMAP) [78]) with data on background precursors to ammonium compound formation, coupled to hydrological models of transport of run-off (e.g. Soil & Water Assessment Tool (SWAT) [92]) can calculate spatially explicit exposure from a unit of emission. The exposure levels can be integrated against spatially explicit distributions of the receivers of impacts (human population density, crops, ecosystems). Human health response to

PM2.5 and ozone is well quantified, as are crop values. The economic effect of ecosystem service loss from acidification and eutrophication may need an additional calculation using a model such as InVEST [93].

4.3.3 Summary of difference between damage costs of GHG emissions and Nr emissions

Ignoring distributional issues of asymmetric cost-bearing of damages, costing GHG emissions does not have the spatial variability of costing Nr emissions. There is one global marginal damage cost estimate for CO2 emission at any spatial location on the surface of the earth. Other comparisons between the marginal damage costs of GHG emissions and Nr emissions [83]:

- (C) Costs associated with the global atmospheric pool and global change in radiative forcing and hence temperature and precipitation. (N) Costs associated with local N pools and transport through and on air, land, surface water, ground water and coastal waters, with local changes in intermediaries and through multiple local terrestrial and aquatic chemical and biological processes that produce impact.
- (C) The most damaging impacts are in the future, and uncertainty is mostly associated to comparing future economic costs to economic benefits in the present. (N) With the exception of leaching of NO3- from soil to groundwater, which can take decades, the damage from present Nr emissions can be observed in nearer term impacts on humans and ecosystems within a generation. Major uncertainty is associated to spatial variability and complexity of the impact pathways, which can include intercountry spatial issues of comparison of value (e.g. transboundary damage from Nr emission) rather than temporal issues.

4.3.4 Ambiguity in damage costing

Present damage costs from [70] and [69] use a range of valuation methods to estimate economic damages. For example, crops use market value, nitrate sometimes uses water treatment cost (an abatement cost for DALYs) instead of economic damage from DALYs. Abatement costs are generally lower than damage costs. Costing DALYs from human health loss ranges from Willingness To Pay (WTP), which are generally higher than an indicator of damage to the economy such as productivity losses. Conceptually, these damage costs are not interchangeable, some represent realised costs absorbed into an economy (losses or treatment), and others directly or indirectly stated preferences of individuals where there is large uncertainty whether the stated amounts would be paid.

Without a specific effort to be consistent within each end impact on social preferences, damages, or abatement, ambiguity from the valuation method in current estimates must be absorbed in the uncertainty in marginal damage costs of Nr emissions. WTP is treated as a potential overestimate of economic damages, and abatement values treated as a potential underestimate of damages, though the reverse is also possible.

4.3.5 Calculation of marginal damage costs

Calculating global spatially explicit marginal damage costs using coupled models was not available for the study. Instead, we used the only costs estimates published ([70] [72]) for components of the nitrogen cascade. Table 2 lists the marginal damage cost components of the impact pathway and their estimated range [70] [72]. The references give prices for studies in the European Union between 1995 and 2005 without adjustment for purchasing power. In Table 2 we therefore inflated to US$2020 and extended the lower range for increase in purchasing power from 2005 (inflation and rise in consumer price indices), and the upper range from 1995.

Annex A

*Table 2: EU damage costs from [70] for components of the nitrogen cascade (with sources of estimation Table S1 in [70]). Range inflated to equivalent purchasing power in US$2020 PPP. N2O damage costs included in Annex A GHG, and adjustments to marginal social costs of GHG emissions due to interactions between the N and C cycles factor into the correlations discussed in Section 4.5. *=high uncertainty in estimates of ecosystem damage through water pathways, see text.*

Damage	Nr emission	Component of Pathway	Sym-bol	Estimate US$2020 PPP kg^{-1}	
				min	**max**
Air Pollution Human Health DALY (PM2.5)	NH3	Air	$m_{a,NH3}$	**4**	**50**
Ecosystems (acidification, eutrophication, biodiversity)	NH3	Deposition on Land	$m_{l,Nr}$	**2***	**15***
Ecosystems (acidification, eutrophication, biodiversity)	NH3	Deposition on Surface water	$m_{w,Nr}$	**5***	**25***
Air Pollution Human Health DALY (PM2.5 and O3)	NOx	Air	$m_{a,NOx}$	**20**	**70**
Crop loss (O3)	NOx	Air	$c_{a,NOx}$	**2**	**5**
Ecosystems (acidification, eutrophication, biodiversity)	NOx	Deposition on Land	$m_{l,Nr}$	**2***	**15***
Ecosystems (acidification, eutrophication, biodiversity)	NOx	Deposition on Surface water	$m_{w,Nr}$	**5***	**25***
Ecosystems (acidification, eutrophication, biodiversity)	Nr	Run-off to Surface water	$m_{w,Nr}$	**5***	**25***
Human health (drinking water)	Nr (nitrate)	Leaching to Groundwater	$m_{g,Nr}$	**0**	**10**
Climate change	N2O	Air	*SC-N2O*	*GHG*	*GHG*
Human health (UV radiation from stratosphere O3 depletion)	N2O	Air	-	-	-
Interactions between N and C cycles, effect on N and C fluxes (emissions, sequestration, denitrification, and radiative forcing)	NH3, NOx	-	-	*corr*	*corr*

European and US total damage cost estimates of N pollution are calculated by estimating the amount of air emissions, deposition on land and surface water from NH3 and NOx air emissions, primary leaching and run-off to water sources and multiplying them using the marginal costs in Table 2. To form country level estimates of marginal damage costs for NH3 and NOx food system emissions to air:

(a) Global datasets of nitrogen emission and deposition were used to estimate the weight in kg of Nr compounds deposited on land and surface water resulting from 1kg of NH3 or NOx emitted to air, and the amount in kg of 1kg of Nr run-off and shallow groundwater leaching that is retained in riverine systems and the amount exported to coastal water systems.

(b) Population density, total NH3, NOx and SOx emissions, as well as temperature are primary factors for exposure to air particulate matter [94] [83] [95]. We fitted a statistical model to existing explicit modelling of damages across US states [95], allowing us to transfer $m_{a,NH3/NOx}$ to country level adjustment to air pollution costs $m_{i,a,NH3/NOx}$ for country i. Crop losses are also adjusted by relative proportions of total value in international dollars Purchasing Power Parity (PPP) of crops $c_{i,a,NOx}$ using data on the producer price index from Food and Agriculture Organisation Statistical Database (FAOSTAT).

(c) From lack of data we adjust $m_{l,Nr}$ and $m_{w,Nr}$ from Table 2 to estimates for $m_{i,l,Nr}$ and $m_{i,w,ret,Nr}$ and $m_{i,w,exp,Nr}$ for country i that assumes a constant disutility of ecosystem service losses to Nr deposition on land and Nr surface water run-off that is retained in riverine systems and exported to coastal systems, respectively. Similarly, $m_{g,Nr}$ has a country level adjustment $m_{i,g,Nr}$ that maintains constant disutility of human health loss to nitrate pollution [96].

Compared to air emissions and human health impacts, there are few studies on acidification, eutrophication, and biodiversity costs from Nr run-off and leaching [70, 97-99]. The estimate in Table 2 for $m_{w/I,NH3/NOx/Nr}$ comes from a sole study on restoration costs and the upper margin is arbitrarily set in [70] at 5 times the restoration amount. Factors identified in costs of Nr run-off and leaching in studies in high income countries include property loss [100], and to a lesser extent the denial of freshwater resources for agricultural and industry use. Costings have not been related to hydrological models, in the same manner as chemical transport models have for air pollution, therefore there are no available test sets for statistical modelling and appropriate value transfer. The costs to ecosystems through Nr run-off and leaching to groundwater remain the most uncertain components. As a conservative estimate, we halve the amounts from [70] in Table 2.

Table 6 lists the marginal damages costs for NH3 and NOx emitted to air, and Nr run-off to surface water and leaching to groundwater, calculated from Table 2 as follows:

Marginal damage cost Nr leaching to groundwater

Global spatial datasets are available of Nr leaching to groundwater given soil application or deposition of Nr [101], [102]. There is considerable lag-time before NO3- leaches into deep groundwater [103]. The proportion of Nr leached and the time it takes relate to soil properties, mineralization sub-surface, and saturation of existing nitrogen pools [102, 104]. Factors related to impact are discounting from the time at which human health effects occur to the time of the exposure to the concentrated levels of leached NO3-. Furthermore, the time at which the NO3- leached to the groundwater has to be discounted back to the time of the previous application. Following [83], Nr leached amounts are discounted over 20 years: which we assume is 10 years for lag and 10 years for emergence of symptoms.

Concentrations of NO3- differ between surface water and aquifers [103]. Without spatially explicit modelling of marginal addition to existing concentrations and exposure of human populations between surface and groundwater sources [83], the quantity of emissions acts as a proxy for concentration and the same marginal damage cost $m_{g,Nr}$ is used, besides the discounting difference.

A national level marginal damage cost (US\$2020 PPP kg^{-1}) from a kg of Nr leached to deep groundwater somewhere within country i is

$$MDC_{i,grdw,Nr} = m_{i,g,Nr} = \rho_i \cdot m_{g,Nr} \tag{1}$$

where ρ_i is a parity term including discounting over 20 years and conversion from high income GDP PPP per capita to mean GDP PPP per capita within the World Bank income bracket of country i.

This choice of ρ_i is equivalent to the assumption that the disutility of human health loss to nitrate consumption per kg of Nr leached is constant across countries [96] at any given future time t of health effect. That is, if $DALYs(i,t) = \alpha_g \cdot n_{i,g,Nr}(t)$ disability adjusted life years are attributed to nitrate consumption from Nr leaching (where α_g, a disutility factor defining the relationship between the amount of nitrate leached and the resulting DALYs, in units of ppl kg^{-1} has been assumed constant) at time t at a cost of $CF_i(t)$ GDP ($US2020 PPP) per capita for each DALY, then

$$\frac{m_{i,g,Nr}(t)\; n_{i,g,Nr}(t)}{m_{g,Nr}\;(t)\; n_{g,Nr}(t)} = \frac{DALYs(i,t)CF_i(t)}{DALYs(EU,t)CF_{EU}(t)}$$

and

$$m_{i,g,Nr}(t) = \frac{DALYs(i,t)}{n_{i,g,Nr}(t)} \frac{n_{g,Nr}(t)}{DALYs(EU,t)} \frac{CF_i(t)}{CF_{EU}(t)} \cdot m_{g,Nr}(t) = \frac{CF_i(t)}{CF_{EU}(t)} \cdot m_{g,Nr}(t).$$

To transfer costs under the assumption of equivalent disutility, neither $DALYs(i,t)$ nor α_g needs to be calculated. If $m_{g,Nr}(t)$ and $CF_{EU}(t)$ are assumed to both appreciate with the same factor, then

$$m_{i,g,Nr}(0) = \left((1 + d_i(t))^{-t} \frac{CF_i(0)}{CF_{EU}(0)} \right) \cdot m_{g,Nr}$$

where $m_{g,Nr}$ is from Table 2, $d_i(t)$ is a discount rate described below in Section 4.3.6 and $\rho_i = (1 + d_i(t))^{-t} \frac{CF_i(0)}{CF_{EU}(0)}$. The time factor is t=10 years for surface water NO3- and t=20 years for groundwater NO3-.

The assumption that α is constant, [96], does not take into account increased concentrations, increased exposure, and increased vulnerability to nitrate ingestion across countries outside the EU [55]. DALYs from nitrate leaching have not been attributed at a global level in burden of disease studies, and therefore there is a lack of global statistical data to estimate variance in α.

Marginal damage cost NH3 to air

The damage cost of 1kg of emitted NH3 in country i comes from the impact pathway involving costs of air pollution (human health) and deposition on land and surface water:

$$MDC_{i,a,NH3} = m_{i,a,NH3} + \gamma_{i,l,NH3} \cdot m_{i,l,Nr} + \gamma_{i,w,NH3} \cdot MDC_{i,surw,Nr} \quad (2)$$

The weight factors $\gamma_{i,l/w,NH3}$ were determined from a global spatial dataset of NH3 and NOx deposition [105] and totals of NH3 and NOx from EDGAR [6]. Cross boundary costs cannot be approximated by this method, the total deposition in country i divided by the total emissions from country i are taken as an approximation of $\gamma_{i,l/w,NH3}$. The relationship between the N weight of NH3 emission, and the N weight of deposition of ammonium compounds is non-linear due to atmospheric chemistry and the presence of NOx and SOx precursors in the atmosphere [1]. However, the approximation of $\gamma_{i,l/w,NH3}$ was clearly distorted for small countries where deposition from larger neighbours far exceed domestic emissions. 13 Sub-Saharan African countries and Bhutan (on the border of China) had $\gamma_{i,l/w,NH3}$ exceeding a value of 1, and were rescaled to a value of $\gamma_{i,l/w,NH3} = 1$.

Annex A

We describe adjusting the marginal damage costs $m_{i,a,NH3}$ of the factor $m_{a,NH3}$ in Table 2 based on difference in exposure of human populations to ammonium compounds in particulate matter and differences in economic impacts. Adjustment involves two factors, comparative adjustment of current exposure, and comparative adjustment of future economic losses from human health impacts attributable to exposure:

$$m_{i,a,NH3} = \rho_i \cdot \frac{CFA_i}{CFA_{EU}} \cdot m_{a,NH3}.$$

Here $\frac{CFA_i}{CFA_{EU}}$ describes an adjustment of exposure (depending on population density, as well as background levels of NOx and SOx) in country i compared to the EU (the value of $m_{a,NH3}$ in Table 2 is based on EU exposure and health costs). To adjust economic impacts from the human health effects of exposure, we use the same parity factor $\rho_i = (1 + d_i(t))^{-t} \frac{CF_i(0)}{CF_{EU}(0)}$ (t=10) described above for nitrate human health damage to estimate the transfer of EU societal economic health costs to country i.

Attribution studies for NH3 and NOx emissions are most advanced in the EU and US – which have detailed datasets of the input factors need to run CTM or reduced CTM models to understand the atmospheric distribution of NH3 agricultural emissions, interaction with NOx and SOx to form ammonium compounds, and the exposure of human populations human health impacts of air pollution [74, 75, 78].

Examination of the sensitivity of the marginal costs of air pollution of NH3 (kg) from detailed modelling shows that population density (PopDen in ppl/km^2), background levels of NOx (kg) and SOx (kg) are precursors for ammonium particulate formation [95].

We used the EASIUR regression at US county level [95] to fit a linear model in log-axes between population density, NH3 and background levels of NOx and SOx: ($\beta_0 = 12.36, \beta_1 = 0.434, \beta_2 = -0.092, \beta_3 = -0.357, \beta_4 = 0.073$)

$$\log(CFA)\,(PopDen, n_{NH3}, n_{NOx}, n_{SOx}) = \beta_0 + \beta_1 \cdot \log(PopDen) + \beta_2 \cdot \log(n_{NH3}) + \beta_3 \cdot \log(n_{NOx}) + \beta_4 \cdot \log(n_{SOx})$$

Data was available for 3106 counties, and the counties represent a wide range of combinations of NH3, NOx and SOx emissions (NH3 and NOx between 10^3 and 6x10^7 kg) and population density between 0.015 and 3000 ppl/km^2. The fit is described in Section 4.10.3 : (1) the residuals were uniform across parameters and approximately normal (Figure 14), (2) the explanatory power was good ($r^2 = 0.67$) and temperature, humidity (the other significant variables in EASIUR) and interaction terms added slightly to the explanatory power ($r^2 = 0.7 - 0.745$), and (3) the ratio of comparative values was scale invariant, meaning that scaling county level emissions of NH3 and NOx by 2 orders of magnitude to country levels of emissions (92% of country level emissions in 2015 ranged between 10^5 and 6x10^9 kg) did not change the adjustment estimate of exposure from the county level:

$$\frac{CFA(PopDen, \alpha_2 n^1_{NH3}, \alpha_3 n^1_{NOx}, \alpha_4 n^1_{SOx})}{CFA(PopDen, \alpha_2 n^2_{NH3}, \alpha_3 n^2_{NOx}, \alpha_4 n^2_{SOx})} = \frac{CFA(PopDen, n^1_{NH3}, n^1_{NOx}, n^1_{SOx})}{CFA(PopDen, n^2_{NH3}, n^2_{NOx}, n^2_{SOx})}, \qquad \alpha_2, \alpha_3, \alpha_4 > 0\,.$$

With $n^1_{NH3}, n^1_{NOx}, n^1_{SOx}$ and $n^2_{NH3}, n^2_{NOx}, n^2_{SOx}$ referring to different levels of NH3, NOx and SOx respectively. From the chemistry of ammonium nitrate and ammonium sulphate formation, the regression for NH3 is negative for increasing n_{NH3} and n_{NOx} levels given existing concentration of NOx in the atmosphere, which is why scale variance is important and the linear regression is applied to the interpolation of country NH3, NOx and SOx within the scaled ranges. Interaction and quadratic terms ($r^2 = 0.73$) provided more potential to extrapolate from the county data, but not scale invariance of the ratio.

One way to view the scaling assumption is: (1) dividing a country into US county size cells (approximately into 30 arcmin by 30 arcmin cells), (2) assuming the US county level relationship holds on average in that cell using the national population density, (3) background emissions in the cell equal the national NH3, NOx and SOx emissions divided by the number of cells. The air pollution exposure for the country is the average across cells. Details on scaling the uncertainty for the ratio $\frac{CFA_i}{CFA_{EU}}$ is discussed in Section 4.3.6.

The mean value for the ratio $\frac{CFA_i}{CFA_{EU}}$, explicitly, under the given assumptions, is

$$\frac{CFA_i}{CFA_{EU}} = \left(\frac{1}{27}\sum_{\mathrm{k\in EU27}} \exp\left(\beta_1 \cdot (\log(PopDen_k) - \log(PopDen_i)) + \beta_2 \cdot (\log(n_{NH3,k}) - \log(n_{NH3,i})) + \beta_3 \cdot (\log(n_{NOx,k}) - \log(n_{NOx,i})) + \beta_4 \cdot (\log(n_{SOx,k}) - \log(n_{SOx,i}))\right)\right)^{-1}$$

where $PopDen_i$ is the population density of country i, $n_{NH3,i}$ is the emission in kg of NH3 of country i, $n_{NOx,i}$ is the emission in kg of NOx of country i, $n_{SOx,i}$ is the emission in kg of SOx of country i, and the summation k runs over the EU27 countries of 2008.

Marginal damage cost NOx to air

The damage cost of 1kg of emitted NH3 comes from the impact pathway involving costs of air pollution (human health) and deposition on land and surface water:

$$MDC_{i,a,NOx} = m_{i,a,NOx} + c_{i,a,NOx} + \gamma_{i,l,NOx} \cdot m_{i,l,Nr} + \gamma_{i,w,NOx} \cdot MDC_{i,surw,Nr} \quad (3)$$

$c_{i,a,NOx}$ is the attributable damage to cereal crops from ozone production due to a 1kg atmospheric emission of NOx for country i. The weight factors $\gamma_{i,l/w,NOx}$ were determined from a global spatial dataset of NH3 and NOx deposition [105] and totals from [6]. Cross boundary costs cannot be approximated by this method, the total deposition in country i divided by the total emissions from country i are taken as an approximation of $\gamma_{i,l/w,NOx}$.

We adjusted the marginal damage costs $m_{i,a,NOx}$ of the factor $m_{a,NOx}$ in Table 2 using the same procedure as for NH3. Adjustment involves two factors, comparative adjustment of current exposure, and comparative adjustment of future economic losses from human health impacts attributable to exposure:

$$m_{i,a,NOx} = \rho_i \cdot \frac{CFA'_i}{CFA'_{EU}} \cdot m_{a,NOx}.$$

Here $\frac{CFA'_i}{CFA'_{EU}}$ describes an adjustment of exposure in country i compared to the EU (the value of $m_{a,NOx}$ in Table 2 is based on EU exposure and health costs). Data was available for 3106 counties, and the counties represent a wide range of combinations of NH3, NOx and SOx emissions (NH3 and

NOx between 10^3 and 6x10^7 kg) and population density between 0.015 and 3000 ppl/km^2. The fit is described in Section 0. For NOx, the marginal human damage was most explained by NOx emissions in kg and average county temperature in degrees Kelvin: ($\beta'_0 = -99.592, \beta'_1 = 0.327, \beta'_2 = -0.188, \beta'_3 = -18.612$)

$$\log(CFA')\,(PopDen, n_{NOx}, ATemp) = \beta'_0 + \beta'_1 \cdot \log(PopDen) + \beta'_2 \cdot \log(n_{NOx}) + \beta'_3 \cdot \log(ATemp)$$

For this fit: (1) the residuals were uniform across parameters and approximately normal, (2) the explanatory power was good ($r^2 = 0.515$), and (3) the ratio of comparative values was scale invariant. Details on scaling the uncertainty for the ratio $\frac{CFA'_i}{CFA'_{EU}}$ is discussed in Section 4.3.6. Scale invariance is lost under a quadratic fit, but a quadratic fit had more explanatory power: ($r^2 = 0.651$) with the most significant terms being quadratic terms for ATemp and an interaction term between ATemp and NH3. Despite a lower value $r^2 = 0.515$ for the fit of NOx compared to the fit of NH3, the unexplained variance, and so the error term used for uncertainty modelling had the same standard deviation (~0.52 for normal residuals under log transformation).

The mean value for the ratio $\frac{CFA'_i}{CFA'_{EU}}$, explicitly, under the given assumptions, is

$$\frac{CFA'_i}{CFA'_{EU}} = \left(\frac{1}{27} \sum_{\mathrm{k \in EU27}} \exp\left(\beta'_1 \cdot (\log(PopDen_k) - \log(PopDen_i)) + \beta'_2 \cdot (\log(n_{NOx,k}) - \log(n_{NOx,i})) + \beta'_3 \cdot (\log(ATemp_k) - \log(ATemp_i))\right)\right)^{-1}$$

where $PopDen_i$ is the population density of country i, $n_{NOx,i}$ is the emission in kg of NOx of country i, $ATemp_i$ is the average temperature in Celsius of country i, and the summation k runs over the EU27 countries of 2008.

Strong correlation (r=0.8578) was found between $m_{i,a,NH3}$ and $m_{i,a,NOx}$ in the EAISUR estimates of marginal damage across US counties, arising from the chemistry of ammonium particulate formation, coinciding human population exposure sites for concentrations of emission and the same populations being exposed. Section 4.3.6 discusses joint sampling of $m_{i,a,NH3}$ and $m_{i,a,NOx}$.

In equation (3), $c_{i,a,NOx}$ is the adjustment to country i of the EU estimated attributable damage to cereal crops $c_{a,NOx}$ (Table 2) from ozone production due to a 1kg atmospheric emission of NOx. Let CFP_i denote the average farm-gate price of cereals per ton in country i over 2015-2019 from FAOSTAT production data. FAOSTAT averages national quantities and local currency prices over 3 years and converts to US$2014 PPP - US$2016 PPP. Let CFP_{EU} denote the average farm-gate price of cereals per ton in the EU27 countries of 2008 (the context of the costings in Table 2) over 2015-2019 from FAOSTAT production data in US$2014 PPP - US$2016 PPP. Then

$$c_{i,a,NOx} = c_{a,NOx} \cdot \frac{CFP_i}{CFP_{EU}}.$$

Uncertainty in farm-gate prices. and using the attribution factor implicit in $c_{a,NOx}$, is discussed in Section 4.3.6.

Marginal damage cost Nr run-off to surface water

A national level marginal damage cost (US$2020 PPP kg^{-1}) from a kg of Nr run-off to surface water somewhere within country i is

$$MDC_{i,surw,Nr} = \gamma_{i,w,ret,Nr} \cdot m_{i,w,ret,Nr} + \gamma_{i,w,ret,NO3-} \cdot m_{i,g,Nr} + (1 - \gamma_{i,w,ret,Nr}) \cdot m_{i,w,exp,Nr} \quad (4)$$

The weight factors $\gamma_{i,w,ret,Nr}$, $\gamma_{i,w,ret,NO3-}$ were determined from a global spatial dataset [106] of input to global major rivers, retention, and export to coastal zone from river mouth. $\gamma_{i,w,ret,Nr}$ is the proportion of Nr retained in the riverine system, $\gamma_{i,w,ret,NO3-}$ is the proportion of Nr retained in the riverine system that is NO3-, and $(1 - \gamma_{i,w,ret,Nr})$ is the proportion of Nr exported to coastal systems. The proportions are an average across all freshwater cells in the data set within country boundaries and approximate the "fate" of Nr run-off in country i.

Global spatial datasets are available that estimate Nr run-off with NO3- separated [107] [108] as concentration (mg/l) compared to total nitrogen (mg/l). [108] investigated linear relationships across major catchments, finding a slope between 0.5 and 0.75 in concentration of NO3- to total Nr (TN). We set $\gamma_{i,w,ret,NO3-} = u(0.5,0.75) \cdot \gamma_{i,w,ret,Nr}$ where u denotes a uniform distribution sampled independently across countries – the data points were not available to examine residuals or Bayesian regression. The estimates from [70] do not distinguish marginal damages by concentrations to exposed populations, so the total load of NO3- serves as a proxy to concentrations outside the EU.

There is a lack of compiled data outside developed countries on damages from deposition and run-off. The human damages of nitrate in surface water $m_{i,g,Nr}$ was described in the section above (equation (1)). The country adjusted marginal costs of retained Nr run-off $m_{i,w,ret,Nr}$, exported Nr run-off $m_{i,w,exp,Nr}$ are described below. Hydrological geospatial information, which allows calculation of concentrations of nitrate and retention at high spatial resolution, also includes attached data such as population levels and ecosystem information [109].

Models calculate riverine export of run-off Nr to coastal ecosystems [106], but there are no comprehensive sets of costings for coastal damages from eutrophication damages to separate riverine and coastal ecosystem service loss damages [110]. There are estimates of loss of value from coastal ecosystem services, for example from the Ecosystem Services Valuation Database (ESVD) [111] and meta-regressions based upon it [112], but still missing is the attribution of Nr run-off to a measure of "effective lost hectares" of those ecosystems and hence services. We lack a natural measure of the capital damaged in the Nr run-off case (humans and DALYs were used in the nitrate case) and the productivity of that capital in terms of consumption-based welfare to make measures of economic damage consistent (GDP/capita was used for DALYs in the nitrate). Without comparable measures of economic damage across economies it remains difficult to convert the value $m_{w,Nr}$ of $US2020 10-25 / kg for the EU to an equivalent disutility in other countries.

Our method scales damages by the different proportions of ecosystems vulnerable to Nr run-off in country i compared to the EU, and the estimated costs of losing ecosystem services compared to the EU.

In the absence of global data and a measure of "effective lost hectares", we use the same principle of equivalent disutility as in the previous section to transfer damage costs and factor out "effective lost hectares". Therefore, we assume a measure ELhaES (effective lost ha of ecosystem services) of ha in a habitat k at future time t is given by

$$ELhaES_k(i,t) = \alpha_w \cdot a_{i,k} \cdot n_{i,surf,Nr}(t) \tag{5}$$

where α_w in units of ha kg^{-1} per habitat k has been assumed constant (across all countries and habitats being considered) and $a_{i,k}$ is a weight for country i such that $\sum_{k\in ret} a_{i,k} = \gamma_{i,ret,Nr}$ and $\sum_{k\in exp} a_{i,k} = (1-\gamma_{i,ret,Nr})$ for inland and coastal habitats effected by retained or exported Nr, respectively. The weight factor provides that the total disutility from retained and exported Nr

$$\sum_k ELhaES_k(i,t) \ = \ \alpha_w \cdot n_{i,surw,Nr}(t)$$

is proportional across all countries and times to the quantity of retained or exported Nr. Thus, equation (5) is the constant proportional attribution of Nr to loss of ecosystem services equivalent to the same assumption about DALYs. As before, to transfer EU marginal damages $ELhaES_k$ and α_w do not need to be calculated, but the assumption is evidently a gross simplification of the different vulnerabilities of ecosystems across inland or coastal habitats and the spatial distribution of the load of Nr run-off. Uncertainty in the loads to each ecosystem represented by $a_{i,k}$ is discussed in the uncertainty section below.

For Nr run-off retained we take $a_{i,k}$, k=4,5, to be the proportional ha in country i of 2 biomes as defined by the Ecosystem Services Valuation Database (ESVD): inland wetlands, as well as lakes and rivers. That is, if $c_{i,4}$ is the km^2 surface area of inland wetland and $c_{i,5}$ is the km^2 surface area of rivers and lakes, then $a_{i,k}{}' = c_{i,k}/\sum_{k=4,5} c_{i,k}$ and set $a_{i,k} = a'_{i,k} \cdot \gamma_{i,ret,Nr}$. The weight factor provides a crude approximation to the proportion of loads of retained Nr received by the habitats.

For Nr run-off exported we take $a_{i,k}$, k=2,3, to be the proportional ha in the national and exclusive economic zone of country i of 2 habitats as defined by the ESVD: coastal systems, and coral reefs. That is, if $c_{i,3}$ is the km^2 surface area of coastal systems and $c_{i,2}$ is the km^2 surface area of coral reefs, then $a_{i,k}{}' = c_{i,k}/\sum_{k=2,3} c_{i,k}$ and set $a_{i,k} = \left(1-\gamma_{i,ret,Nr}\right) \cdot a_{i,k}{}'$. The weight factor provides the proportional distribution of exported Nr between the habitats.

Table 3 lists the breakdown of ecosystem included in the ESVD. Annex A - Land assigns values in \$US2020 PPP of $CF_{i,k}$ to country i per ha per yr to the ecosystem services per ha from the ESVD. Then, equating total damages from Nr retained in the denominator and numerator

$$\frac{m_{i,w,ret,Nr}(t)\gamma_{i,ret,Nr}n_{i,surf,Nr}(t)}{m_{w,Nr}\ (t)\ \gamma_{EU,ret,Nr}\ n_{EU,surf,Nr}(t)} = \frac{\sum_{k=4,5} ELhaES_k(i,t)CF_{i,k}(t)}{\sum_{k=4,5} ELhaES_k(EU,t)CF_{EU,k}(t)}$$

$$\Rightarrow m_{i,w,ret,Nr}(t) = m_{w,Nr}(0) \cdot \frac{\sum_{k=4,5} a'_{i,k}CF_{i,k}(t)}{\sum_{k=4,5} a'_{EU,k}CF_{EU,k}(0)}.$$

Similarly

$$m_{i,w,exp,Nr}(t) = m_{w,Nr}(0) \cdot \frac{\sum_{k=2,3} a'_{i,k}CF_{i,k}(t)}{\sum_{k=2,3} a'_{EU,k}CF_{EU,k}(0)}.$$

Here $a'_{EU,k}$ and $CF_{EU,k}(0)$ are averaged across the EU27 states of the original study [70], and we assumed the EU values $m_{w,Nr}(t)$ and $CF_{EU,k}(t)$ appreciate at the same rate over time.

The proportions of habitats $a'_{i,k}$ were calculated from global spatial datasets classifying biomes. River, lakes and inland wetlands from the Global Lake and Wetlands Database (GLWD) Level 3 (Table 3 of [113]) were mapped to the ESVD biomes (Table 3). The GLWD provides static information on maximum surface water extent in the habitats, is not dynamic, and similar datasets have some errors depending on satellite technique [114]. The spatial datasets are used for estimates of proportions only.

Table 3: Matching Lake and Wetland categories in the Global Lakes and Wetlands Database (Level 3) (GLWD) dataset to the categories of ecosystems in the Ecosystem Services Valuation Database (ESVD).

GLWD Level 3		**ESVD**		
Name	**GLWD-3 ID**	**ESVD ID (k)**	**Name**	**ESVD Sub-Id**
Lake	1	5	Lakes, Freshwater	5.2
Reservoir	2	5	Human made water bodies	5.4
River	3	5	Rivers	5.1
Freshwater marsh. Floodplain	4	4	Swamps, marshes. Floodplains	4.1 4.8
Swamp Forest, Flooded Forest	5	4	Wetlands, Forested	4.6 4.7
Coastal Wetland	6	3	Coastal Systems	3
Pan, Brackish/Saline Wetland	7	5	Lakes, saltwater	5.3
Bog, Fen, Mire	8	4	Peatland	4.2-4.5
Intermittent Wetland	9	4	Other (inland wetlands)	4.9
Wetland 50%, 25%, Complex	10,11,12			
UNEP-WCMC Global Distribution of Coral Reefs				
Name	**Id**			
Tropical Coral Reefs		2	Coral Reefs	2

To calculate coral reef areas in km^2 in proximity to agricultural activities of country i we intersected the Exclusive Economic Zone (EEZ) zone[3] with the UNEP-WCMC Global Distribution of Coral Reefs data set[4] and calculated the area.

Annex A - Land assigns values in $US2020 PPP of $CF_{i,k}$ per ha per year to the ecosystem services per ha per year from the ESVD. We use the uncertainty in $CF_{i,k}$ described in Annex A – Land.

[3] Flanders Marine Institute (2019). Maritime Boundaries Geodatabase, version 11. Available online at https://www.marineregions.org/. https://doi.org/10.14284/382

[4] UNEP-WCMC, WorldFish Centre, WRI, TNC (2021). Global distribution of warm-water coral reefs, compiled from multiple sources including the Millennium Coral Reef Mapping Project. Version 4.1. Includes contributions from IMaRS-USF and IRD (2005), IMaRS-USF (2005) and Spalding et al. (2001). Cambridge (UK): UN Environment World Conservation Monitoring Centre. Data DOI: https://doi.org/10.34892/t2wk-5t34

We have no information on the onset and duration of the loss of ecosystem services and how future losses may increase compared to present damages due to future scarcity of ecosystem services and/or pathways of emissions, so we chose not to discount to a net present value. The eutrophication and acidification effects of nitrogen on ecosystems are relatively fast compared to other damages. Continued emissions in the future are attributable to sustaining the damage. This is a simplification, as the effect of present emissions (1) have some attribution to the increase in marginal damage in the future, and (2) have long term effects until socio-economic systems equilibrate around ecosystem changes that are irreversible. Therefore, the values used in equation (4) are $m_{i,w,ret,Nr} = m_{i,w,ret,Nr}(0)$ and $m_{i,w,exp,Nr} = m_{i,w,exp,Nr}(0)$.

Appendix Section 4.8 discusses potential alternatives to factoring through “effective ha” of ecosystem loss to transfer marginal damages on Nr run-off.

Marginal damage cost Nr deposition on land

A national level marginal damage cost (US$2020 PPP kg^{-1}) from a kg of Nr deposited on land somewhere within country i is

$$m_{i,l,Nr} = \gamma_{i,l,ret,Nr} \cdot m_{i,l,ret,Nr} + \gamma_{i,l,g,Nr} \cdot MDC_{i,grdw,Nr} + (1 - \gamma_{i,l,ret,Nr} - \gamma_{i,l,g,Nr}) \cdot M_{i,surfw,Nr} \quad (6)$$

The weight factors $\gamma_{i,l,ret,Nr}, \gamma_{i,l,g,Nr}$ are the proportions of the deposited Nr on land that is retained in the terrestrial system and leached to groundwater, respectively. The remaining Nr is assumed to be exported as surface water run-off. Deposition datasets [105] and run-off datasets [106] do not generally describe the interaction between deposition and run-off, i.e. what proportion of run-off has come from atmospheric deposition of emitted Nr. Studies show correlations between wet Nr deposition in high emission areas and riverine Nr concentrations; regression implying a >20% contribution of deposition to total riverine export from the study catchment [50, 51]. We have no information globally on leaching from deposition. We set $\gamma_{i,l,g,Nr} = 0$ and $\gamma_{i,l,ret,NO3-} = u(0.8,1)$ where u denotes a uniform distribution (sampled independently across countries), indicating 80-100% of Nr deposition is retained and causes ecosystem losses in land systems.

There is a lack of compiled data outside developed countries on damages from deposition. We use the previous method as for surface water, and scale damages by the different proportions of ecosystems vulnerable to Nr deposition in country i compared to the EU, and the estimated costs of losing ecosystem services compared to the EU. Therefore,

$$m_{i,l,ret,Nr} = m_{l,Nr} \cdot \frac{\sum_{k=6,7,8} a'_{i,k} CF_{i,k}(0)}{\sum_{k=6,7,8} a'_{EU,k} CF_{EU,k}(0)}.$$

Here $m_{l,Nr}$ is the EU damage cost from Table 6 and $a'_{EU,k}$ and $CF_{EU,k}(0)$ are averaged across the EU27 states of the original study [70]. Damages are not discounted.

For Nr deposition retained we take $a_{i,k}$, k=6,7,8 to be the proportional ha in country i of 4 biomes as defined by the ESVD: tropical forests, temperate forests, woodland & shrubland, and grass & range-land. The area of woodland & shrubland and grass & range-land are combined in k=8 as their damage costs in ESVD are within 5% of each other and they have less studies in ESVD than other biomes. Biomes in ESVD outside of those mentioned have lower and or uncertain damages, and are generally more remote from agricultural concentrations of NH3 and food system emissions of NOx. If

$c_{i,6}$ is the km^2 surface area of tropical forests, $c_{i,7}$ is the km^2 surface area of temperate forests and $c_{i,8}$ is the km^2 surface area of woodland etc., then $a_{i,k}{}' = c_{i,k} / \sum_{k=6,7,8} c_{i,k}$.

For land deposition we used the EcoRegions dataset [115] to calculate areas and aggregated them to ESVD categories using Table 4.

Table 4: Matching Forest and Grassland categories in the Ecoregions WWF dataset to the categories of ecosystems in the Ecosystem Services Valuation Database (ESVD).

EcoRegions		**ESVD (6,7,8,9)**		
Name	**BIOME-ID**	**ESVD ID (k)**	**Name**	**ESVD Sub-Id**
Tropical & Subtropical Moist Broadleaf Forests	1	6	Tropical Rain Forest	6.1
Tropical & Subtropical Dry Broadleaf Forests	2	6	Tropical Dry Forest	6.2
Tropical & Subtropical Coniferous Forests	3	6	Other (tropical forests)	6.4
Temperate Broadleaf & Mixed Forests	4	7	Temperate deciduous forest Other (temperate forest)	7.2 7.4
Temperate Conifer Forests	5	7	Other (temperate forest)	7.4
Boreal Forests/Taiga	6	7	Boreal Forests/Taiga	7.3
Tropical & Subtropical Grasslands, Savannas & Shrublands	7	8/9	Tropical wood and shrublands Tropical grasslands Savanna	8.1 9.1 9.2
Temperate Grasslands, Savannas & Shrublands	8	8/9	Temperate wood and shrublands Temperate grasslands Savanna	8.3 9.1 9.3
Flooded Grasslands & Savannas	9	(Used GWLD)	Other (inland wetlands)	4
Montane Grasslands & Shrublands	10	8	Other (woodland and shrubland)	8.5
Tundra	11	11	Tundra	11
Mediterranean Forests, Woodlands & Scrub	12	8	Mediterranean wood-& shrubland	8.2

Deserts & Xeric Shrublands	13	10	Desert	10
Mangroves	14	(Used GWLD)	Mangroves	3.4

4.3.6 Uncertainty

No uncertainty was available for the globally modelled proportions for deposition or run-off. We used uniform distributions on the uncertainty ranges given in Table 2, as described in the last section, for uncertainty in NO3- concentrations in retained Nr run-off and in the amount of land deposited Nr land washed into waterways before reacting with land ecosystems.

Uncertainty in transfer of nitrate health losses

We used uniform distributions on the uncertainty ranges given in Table 2 and uncertainty in future GDP projections (using random choice of Shared Socioeconomic Pathways (SSPs) as described in Section 2.5.6 of Annex A – Water) in ρ_i for uncertainty in $MDC_{i,g,Nr}$ (equation (1)). No global data was available to examine variance in α. 10000 samples of ρ_i for each country are correlated up to all countries being in the same future represented by a random choice of SSP, as described in Section 2.5.6 of Annex A – Water. The value, $m_{g,Nr}$ in Table 2 is sampled 10000 times independently for each country. This represents differences in concentrations and fate of leached nitrogen ending up in drinking water, but it underestimates uncertainty as it ignores the common biology of human reaction to nitrates.

Uncertainty in transfer of ecosystem damages from deposition and run-off of Nr

Uncertainty in the fate and load of Nr deposition and Nr run-off on ecosystems, means that we also replace the weight vectors $a'_{i,k}$ by their random variable counterparts. That is, terms such as

$$\sum_{k=4,5} a'_{i,k} CF_{i,k}(0)$$

are replaced by

$$\sum_{k=4,5} A'_{i,k} \cdot CF_{i,k}(0)$$

where $A'_{i,k} = \left(A'_{i,4}, A'_{i,5}\right)$ is a discrete random variable of the simplex of weights $\{x \in [0,1]^2 : x = (a, 1-a), 0 \leq a \leq 1\}$. We take for A' distribution the mapping to the simplex of the truncated exponential distribution on a in the interval [0,1] with mean $a'_{i,4}$. The truncated exponential distribution is the maximal entropy distribution with given mean. The mean value of the sum with the random variable A' is $\sum_{k=4,5} a'_{i,k} CF_{i,k}(0)$. When k=6,7,8 (three weights), the same principle applies by mapping to the simplex of weights $\{x \in [0,1]^3 : x = (a, b, 1-a-b), 0 \leq a, b \leq 1, a + b \leq 1\}$ the truncated exponential distribution with mean $(a'_{i,6}, a'_{i,7})$ over the projection of the simplex onto two dimensions $\{(a, b) \in [0,1]^2 : a + b \leq 1\}$.

This uncertainty has the interpretation as uncertainty in the load of the Nr run-off being proportionally more to one biome or the other in country i. We include this uncertainty as, for a national level cost without spatial resolution on the location of emission, we cannot be certain which ecosystem will be affected by deposition and run-off. The samples of $A'_{i,k}$ across countries are independent.

Uncertainty in transfer of ecosystem valuation

We determined ecosystem values for countries in Annex A – Land using grouping by Human Development Index (HDI) to increase sample sizes of valuations across provisioning, regulating and cultural services.

We used the updated December 2020 version of ESVD. There were 208 valuations from studies for k=2 coral reefs across 33 countries and the three classes of services, 914 valuations from studies for k=3 coastal systems across 51 countries and the three classes of services, 365 valuations for k=4 inland wetlands across 38 countries, 169 valuations for k=5 lakes and rivers across 25 countries, 160 valuations for k=6 tropical forests across 14 countries, 379 valuations for k=7 temperate forest and 106 valuations for k=8 & 9 shrubland and grasslands across 8 countries. By considering total value using only a valuation from each of the provisioning, regulating and cultural classes the total may be underestimated.

Since the distribution of estimates of CF_k involved the Anderson-Darling test of normality and a normal best fit to $log(CF_k)$, CF_k will generally have a lognormal shape. The co-efficient of the form $\frac{\sum_{k=4,5} a'_{i,k} CF_{i,k}(0)}{\sum_{k=4,5} a'_{EU,k} CF_{EU,k}(0)}$ will then, as a division of random variables will generally follow a lognormal shape. We drew 10000 samples as above for the coefficients $a'_{i,k}$ and the distributions of $CF_{i,k}$ from Annex A – Land to represent the co-efficient. The sampling is independent across countries, to represent that variation in the local characteristics of ecosystems outweighed potential under or overestimates of damage implicit in the chemistry of Nr reactions. For the same reason, $m_{w,Nr}$ and $m_{l,Nr}$ is sampled 10000 samples from the uniform distribution between the values in Table 2 independently for each country. Multiplying the random variables provides 10000 samples for $m_{i,l,ret,Nr}$, $m_{i,w,ret,Nr}$ and $m_{i,w,exp,Nr}$

Having 10000 samples also of $M_{i,grdw,Nr}$, we can then generate 10000 samples of $MDC_{i,surw,Nr}$ per equation (4) and 10000 samples of $m_{i,l,Nr}$.

Uncertainty in transfer of crop losses from O3

For uncertainty in crop losses, assumed to be loss of an in-country farm-gate price of unknown cereal crop distribution according to the proportion of production in country of cereal crops (FAOSTAT), we varied CFP_i by the method described in Section 2.5.4 of Annex A – Water. This involved adding variation around the decadal mean of the FAO producer price index to CFP_i. The variation in Annex A – Water uses a joint sample across 182 countries – a different sample is used here to express a lack correlation between variation in losses for future water deprivation and variation in relatively immediate losses after NOx emission from tropospheric ozone. The value, $c_{a,NOx}$ in Table 2 was sampled 10000 times independently for each country, as it is unclear from the reference [70] whether the variance in the EU value is from factors that are common to impact pathways in other countries. This is likely an underestimate of the effects of price transmission from global commodity markets.

Uncertainty in transfer of air pollution damage costs from NH3 and NOx emissions

For uncertainty in air pollution human health costs for NH3 and NOx, we used the uncertainty in the statistical fit of variance of human health impact across US counties described in Section 4.6.3. The normal fit to the residuals in Figure 14 and Figure 15 are the basis of uncertainty in the ratios $\frac{CFA_i}{CFA_{EU}}$ for NH3 and $\frac{CFA'_i}{CFA'_{EU}}$ for NOx.

Annex A

The calculation of the trend in the ratios across countries was transferred from a scale invariant formula involving US counties. We must argue for how the uncertainty of human health impact at the US county level should scale. We viewed the scaling assumption by dividing a country into US county size cells (approximately into 30 arcmin by 30 arcmin cells), assuming the US county level relationship with its uncertainty held in that cell using the national population density, and emissions equal to the national NH3, NOx and SOx emissions divided by the number of cells.

The cells are therefore homogenous. Assuming a 1kg quantity of NH3 emissions occurs in one of these cells and is not being totalled across several cells for the purpose of determining the ratio, then the error random variable (assumed identically distributed by the normal distribution fitted to the residuals in Figure 14) represents error in CFA_i. The term CFA_{EU} represent the average across 27 countries. At the US County scale, the correlation between log(CFA) and the residuals (the unexplained variance) is 0.58. This likely overestimates the cross-border distribution of NH3, NOx and SOx emissions and the level of similarity of geographic distribution of human populations, transport and agriculture at the country level compared to the US county level, but it also represents commonality in human biology from exposure and commonality in the underlying atmospheric chemistry. A multivariate normal distribution across all countries was constructed and sampled 10000 times with the given correlation coefficient of 0.58. The joint error terms representing the 27 EU countries were averaged and added to the model estimate of $\log(CFA_{EU})$ for an estimate of the uncertainty in CFA_{EU}. This random variable was divided against the error term for country i added to the model estimate of $\log(CFA_i)$. This provided a representation of the uncertainty in the ratio $\frac{CFA_i}{CFA_{EU}}$. Examples of the distribution of the factor $\frac{CFA_i}{CFA_{EU}}$ for a range of countries are given in Figure 16 to Figure 18. The same procedure was used for NOx and $\frac{CFA'_i}{CFA'_{EU}}$, where the correlation between log(CFA') and residuals was 0.72. Examples of the distribution of the factor $\frac{CFA'_i}{CFA'_{EU}}$ for a range of countries are given in Figure 19 to Figure 21.

Samples for $m_{i,a,NH3}$ were obtained by multiplying the samples for ρ_i (the same samples generated for groundwater since they represent the same future for discounting) with $\frac{CFA_i}{CFA_{EU}}$. The value, $m_{a,NH3}$ in Table 2 is sampled 10000 times independently for each country, as it is unclear from the reference [70] whether the variance in the EU value is from factors that are common to impact pathways in other countries (chemistry and human biology). The same procedure provided samples for $m_{i,a,NOx}$. Correlates in cross-county variance, representing common factors in impact pathways, were reintroduced by joint sampling described in Section 4.10.5.

Pearson correlation (p=0.8578) was found between marginal damage costs from NH3 and NOx in the EAISUR estimates of across US counties, arising from the chemistry of ammonium particulate formation, coinciding human population exposure sites for concentrations of emission, and the same populations being exposed. Therefore, the individual distributions of $m_{i,a,NH3}$ and $m_{i,a,NOx}$ for each country, were fitted to lognormal distributions (Figure 22 to Figure 27) and treated as marginals of a joint lognormal distribution and jointly sampled. The differences between the original samples for of $m_{i,a,NH3}$ and $m_{i,a,NOx}$ and the outcome of joint sampling is discussed in Section 4.10.5.

Finally, the joint samples of air pollution, samples of crop losses as described above, were combined with the samples of $MDC_{i,grdw,Nr}$, $MDC_{i,surw,Nr}$ and $m_{i,l,Nr}$ in equations (1) and (4) to obtain 10000 samples of $MDC_{i,a,NH3}$ and $MDC_{i,a,NOx}$.

See Figure 8 to Figure 10 for histograms of the sampling of $MDC_{i,grdw,Nr}$, $MDC_{i,surw,Nr}$, $MDC_{i,a,NH3}$ and $MDC_{i,a,NOx}$.

4.4 Fitting the damage costs of nitrogen emissions

The components of the equations (1)-(4) were derived, with uncertainty, in the previous section. The mean value of costs of nitrogen emissions (NH3 to air, NOx to air, Nr to surface waters and Nr leaching to groundwater) in US$2020 PPP kg^{-1} emitted for 171 countries where data was available is listed in Table 6 in Section 4.10.1. All tables of results are in Section 4.10.1.

4.4.1 Joint uncertainty and parametric fit

Independent factors that result in variance in emissions, variance in distribution (atmospheric or aquatic) of nitrogen compounds, and variance in the ecosystem or human response are serial in the impact pathway in Figure 5. The sequential process of impact implies that uncertainty in the marginal damage cost per emission is the product of several random variables, which tends toward a log-normal distribution as the number of terms in the product increases. Even the product of three similarly supported and weakly correlated random variables demonstrates a distinct log-normal shape.

Log-normal is the expected shape of uncertainty in impact from a small weight/quantity of emissions from the same source, undertaking the same distribution, and affecting the same ecosystem or human population. This shape was observed for marginal damages for NH3, NOx and Nr surface run-off emissions.

When aggregating total costs from quantities of emissions across sources, then consideration needs to be given about how much the marginal damage costs are correlated between sources. Correlation is not an indication of absolute size of the damage cost, so it does not matter so much that the impact pathways vary in terms of magnitude of the marginal damage cost. Correlation is a measure of when samples of one random variable are above the mean, how many samples and by how much would samples of the other random variable expected to be above the mean. If factors in damage costs are fully independent between sources, i.e. the variation in damage costs between sources is purely due to factor related to that source, then we would expect emissions from sources to be independent.

Atmospheric and organic chemistry, and common biological processes, are shared across all nitrogen impact pathways. Human biological response on air pollution [116] and nitrate ingestion are shared to a greater degree than the greater diversity of biological responses across ecosystems in different locations. We correlated air damages between NOx and NH3 and across countries, interaction between NH3 and NOx have a known joint impact pathway through formation of ammonium nitrate [94]. We kept the degree of correlation in air pollution suggested by the comparison across US counties and through price transmissions suggested for crop losses. We did not correlate ecosystem services damages between land, surface water or direct run-off origins, nor across countries. Variation in the ecosystems impacted, the dependence on services, are assumed to outweigh the under or overestimation from acidification and eutrophication mechanisms being common.

As discussed above, we assumed that NH3 and NOx emissions within countries occurred from 'county size' sources. This may overstate the uncertainty in total damages when multiplied against larger quantities of emissions, as emissions spread amongst many sources with a degree of independent variance will tend towards a normal distribution with variance the inverse of the square root of the number of sources. This, however, requires certain knowledge (specification) of the sources, and it requires modelling that has subnational resolution of emissions sources. The marginal damage costs were derived without assuming this knowledge of sub-national location of emission, and as much as possible without assuming knowledge of the quantity of emissions, except that is small enough that deviation in the marginal costs because of larger quantity changes is within the uncertainty estimate. This is a limitation in attempting to derive marginal damage costs with the assumption only that an emission occurred somewhere in a country, and no knowledge of the specific quantity of emissions. Uncertainty in total costings should be remodelled when there is greater certainty in source of emissions.

We reject the proposition (see for example the CE Delft handbook on Environmental Prices) that marginal damages either from the same emission source, or from different nitrogen emission sources, can be safely treated as independent. A centrality argument was made in the CE Delft handbook that total costs from 10000s of kg of nitrogen emissions would be a very narrow band of uncertainty around the mean value because of the central limit theorem. The centrality argument seems unlikely to hold for nitrogen or carbon emissions.

On the independence assumption for carbon cost, it is unclear why, consistently tonnes of CO2 emissions from production in The Netherlands in 2020 get reabsorbed into the global economy in a future world where that carbon had say 2020US$ PPP 20 impact (below the mean of 2020US$ PPP 51 see Annex A – GHG), and consistently tonnes of CO2 emission from production in Germany in 2020 gets reabsorbed into the global economy in a future world where carbon had say 2020US$ PPP 200 impact. The emissions from The Netherlands and Germany in the same year face the same atmospheric chemistry and the same causal mechanism for temperature increases in the same future world. If atmospheric science has underestimated the radiative potential of CO2, this is a feature of the physics and the chemistry in the impact pathway of every CO2 emission. The impact of the CO2 emissions between the different countries is much more likely drawn from the same lottery not different lotteries for the social cost of carbon.

We would not expect marginal damages for nitrogen emissions to be as correlated as GHG emissions that have an impact pathway involving, essentially, long term residence in a global atmospheric pool, and global affect through temperature change – there are more local aspects and variance within the nitrogen pathways. However, we do not expect the influence of common systematic factors in the nitrogen pathways mentioned, including human biology and fundamental chemistry, to be swamped by local variance to such a degree that uncertainty in impact is removed by totalling of hundreds of emissions from the same source or different sources.

Correlation in economic damages is very challenging to estimate. Long causal chains from emission to impact resist the ability to trace the fate of joint emissions. Similar complex chains, without mechanisms to trace them, can be seen in securitisation of mortgages with high joint chances of failure into separate Collateralised Debt Obligations (CDOs). The correlated failure rates of CDOs was only revealed post-hoc and initiated the financial crisis [117]. It is more conservative in the low frequency and observational process of revealed environmental change to assume correlations in impact pathways and place the burden of evidence on independence.

The (joint) sampling data for $MDC_{i,grdw,Nr}$, $MDC_{i,surw,Nr}$, $MDC_{i,a,NH3}$ and $MDC_{i,a,NOx}$ are available in the full SPIQ dataset, providing a non-parametric form for risk assessment.

Parametric forms of distributions are easier to disseminate. A parametric form, using lognormal distributions given the mathematical rationale above, is informed by the mean and standard deviation from the sampling. Table 7 lists the lognormal fits. The damage costs of nitrogen are joint distributions across the quantities of emission and across countries. Table 7 therefore describes the marginals for individual countries. The correlation matrix from the sampling data can be used to generate the explicit formula and samples for multivariate lognormal distribution representing the joint distribution of marginal damage costs. The correlation matrix is available in the SPIQ dataset.

4.4.2 Box: Aggregating damage costs across countries

We emphasise that the joint distribution should be used when adding totals across countries. Studies of subsidy repurposing, dietary change, and food waste make changes to impact quantities such as water withdrawals and nitrogen emissions across countries, and when aggregating the effects the joint distribution should be used to assess risk. Correlations can increase the probability of extreme costs, and so sampling independently from marginals can underestimate, in some cases to a large degree, the economic risk of food system impacts.

4.4.3 Results

The mean value of costs of US$2020 PPP kg^{-1} of NH3 emission to air, NOx to air, Nr to groundwater and Nr to surface water for 171 countries where data was available is listed in Table 6 in Section 4.10. Table 8 indicates the potential contribution of NH3 emission to air, NOx emission to air, Nr surface water run-off and Nr leached to deep groundwater to nitrogen pollution damages using 2015 quantities of emissions from EDGAR5.0 and IMAGE-GNM modelling. At a global level (Figure 12), confirmed in other studies of air pollution, agricultural NH3 emissions represent up to 4 times greater damages than agricultural NOx emissions, mainly from the greater quantity of emissions. Surface run-off has similar damages to NH3 air emissions (though the quantities include a potential double-counting factor between run-off from deposition and direct run-off), with a greater spread of uncertainty.

4.4.4 Box: "Hidden cost" of agricultural nitrogen emissions

Table 8 includes a 'total damage cost' by multiplying the national marginal costs by quantities of agricultural emission of NH3 to air, NOx to air, Nr to surface waters, and Nr to groundwater for 2015 obtained from EDGAR5.0 (NH3 and NOx - https://edgar.jrc.ec.europa.eu/dataset_ghg50) and Nr run-off and leaching from agricultural obtained from the IMAGE-Global Nutrient Model (GNM) spatial dataset In [102]). Comparison to GVA is unreliable for small countries and countries subject to large transboundary effects (Table 10), but generally confirm findings of the EU Nitrogen Assessment that cost of nitrogen pollution may be comparable to the GVA of agriculture in many countries. The totals (Table 8 and Figure 11 to Figure 13) are presumptive figures and should be used carefully in terms of comparison to national or the global economy given lack of consideration of social costs and second order effects for large changes in emissions. They are damage estimates from present agricultural Nr pollution without accounting for the value provided to society from the use of nitrogen in agriculture. There is no comparison with a counterfactual, so it does not provide any indication of the economic value of food system transformation, i.e. the balance of value between decreasing nitrogen emissions and damage costs and what it costs to abate nitrogen emission with overall social welfare the same as present value. Reducing nitrogen pollution to very low levels will not 'save the costs' to the global economy of the amounts in Figure 11. Damage costs must be paired with abatement costs and counterfactuals to determine economic potential in reducing nitrogen emissions.

Countries facing the largest “hidden” nitrogen costs are shown in Figure 13 in Section 4.10.1.

It is less valuable to compare the marginal costs across countries, they represent primarily the externalised costs of nitrogen emission for market corrections in the economies where the costs are borne. They are therefore more usefully compared against economic indicators of the same country. Table 9 provides the amounts for Figure 13 and compares nitrogen damage costs against Gross Value Added (GVA) of agriculture for that country.

We caution on using the marginal damage costs for individual countries where large transboundary effects are suspected, meaning that the weights $\gamma_{i,w,ret,Nr}$, $\gamma_{i,w,ret,NO3-}$, $\gamma_{i,l,NOx}$, $\gamma_{i,l,NH3}$, $\gamma_{i,l,NOx}$, $\gamma_{i,w,NOx}$ and $\gamma_{i,w,NH3}$ indicating the fate of nitrogen through atmospheric deposition and retained (and hence exported) Nr in surface waters are poor estimates when most of the deposited or surface water load is due to the much larger emissions of neighbours. 46 countries in Table 10, all at lower HDI and lower production than respective high emission neighbours such as China, the EU, Russia, India, and Nigeria, have higher marginal costs for atmospheric emissions of NH3 and NOx that are likely distorted by transboundary deposition. Many low-income countries are also at the boundary of effective interpolation of air pollution costs, as they may have low population density and disproportionate or variable total NOx and SOx emissions compared to NH3 emissions. As these countries have low data for transboundary correction and few estimates for nitrogen damages, we have otherwise kept them in the dataset with a deposition correction (Table 10). Future improvements of the dataset will utilise reduced complexity geospatial modelling of nitrogen fate to remove distortion of using aggregation over national areas in the weights.

The marginal costs in Table 6 vary greatly, even across similar countries, due to the many factors represented in equations (1)-(4). Overall, the attribution of human and ecosystem damage from the nitrogen cascade of NH3 or NOx emitted to air from agricultural activities, or reactive nitrogen leached to groundwater or entering surface waters as run-off, come from a limited set of studies. The values in Table 6 and their uncertainty Table 7 were determined using basic relationships and broad assumptions for transport of figures from the EU nitrogen assessment to other countries. Transfer to other countries involves approximation of modification terms to exposure and ecosystem damages, with a large amount of uncertainty.

Large variation is due to primary factors (such as population density) and the nitrogen cascade, where the “fate” of emitted nitrogen varies greatly between countries. Spatial datasets based on modelling show large variation, for example, between nitrogen retained in inland water systems and export to coastal systems. Large uncertainties remain on the run-off from deposition, exposure to nitrate in surface drinking water, and differences in concentrations between surface water and ground water.

Table 9 lists 19 countries where the estimated total costs to ecosystem from surface water run-off outweigh by several times the costs to human health from air pollution. The largest variance between countries is in the estimate of the marginal damage cost of Nr surface run-off. This is due to order of magnitude uncertainty in the estimation of the value of coastal ecosystems. Where a country has a high proportion of riverine export of Nr to coastal systems, the valuations in the ESVD database (see Annex A – Land) for many countries has much higher values for coral reefs and coastal systems than retention in inland wetlands than the EU. Those estimates also have the greater uncertainty, introducing distinctly longer tails for Nr surface run-off than the estimates of NH3 and NOx air emissions.

4.5 Social costs to society

Costing should separate between exercises to estimate damage and mitigation costs and costing optimal economic action. The latter may use damage and mitigation costs to determine the optimal level of Nr emissions that maximise social surplus.

Cost-benefit exercises for Nr emissions reduction, or increase, compare damage and mitigation costs. A cost-effectiveness exercise examines if the mitigation costs are the least costs to reduce or increase Nr emissions by a set amount. An optimal social cost links the two, determining the amount of Nr reduction where the social surplus, that is, the difference between the damage cost reduction for reducing Nr emissions and the least cost mitigation to achieve the reduction, is maximised.

If current Nr emissions are above the socially optimal level, then, according to economic theory, paying the marginal societal damage costs of present emissions are too expensive. This does not imply, at the societal level, that the full damage costs should be paid, as the social surplus is less than the damage costs. The benefits of N application at the societal level allow some Nr emissions to be desirable and there is presently no other technology that achieves completely the same benefits for less costs without N application.

If current Nr emissions are below the socially optimal level, then, according to economic theory, the marginal societal damage costs of present emissions should be paid because they are exceeded by the marginal benefits of N application.

A cluster of Sub-Sahara African (SSA) countries apply less than 25kg/ha of N input through fertiliser, with cereal yields less than 2 t / ha (FAOSTAT, Hannah Ritchie and Max Roser (2013) - "Fertilizers". Published online at OurWorldInData.org. 'https://ourworldindata.org/fertilizers'). Analysis of maize shows that yield is N limited [118, 119] (though the determination of benefits from increased N application is complicated by other factors, see below), and optimal rates in terms of maximising private profits to farmers is between 60-100 kg/ha. Damage costs imply that the socially optimal rates will be less than this (50-80kg /ha, assuming a 20% reduction on the private optimal application rate in line with the Chinese study [82], which is closer in terms of development and smallholder farmers to the cluster of SSA countries than the 30% estimated for Europe [70]). Current N fertiliser application in SSA is therefore likely less than half the socially optimal level. Depending on nitrogen use efficiency, this roughly translates to the fact that Nr emissions are presently below the socially optimal level for a range of low-income countries.

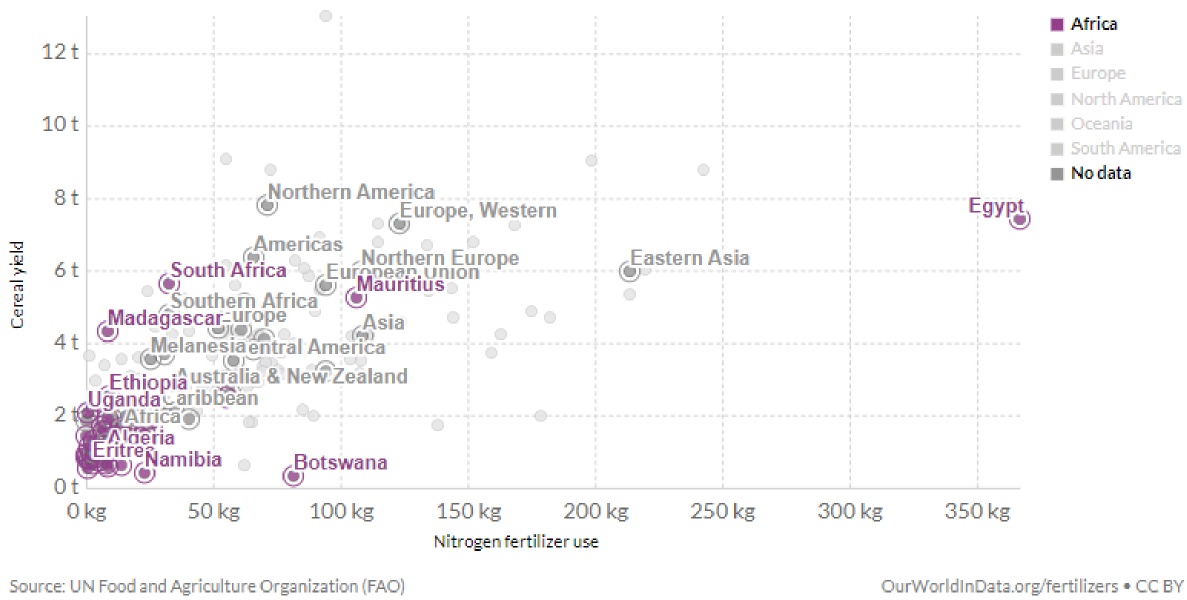

Figure 6: Source: Our World in Data. Hannah Ritchie and Max Roser (2013) - "Fertilizers". Published online at OurWorldInData.org. 'https://ourworldindata.org/fertilizers'. Average yield across the total cereal category in FAOSTAT compared to estimated use of nitrogen fertilizer in kg per ha. Fertilizers used within and across countries vary in their chemical properties, N formulation, total N-weight and conversion to N emissions.

A simple determination of socially optimal rates hides complications in the calculation of benefits for increased N application. Increasing crop yield may be limited by water availability and, increasingly, may be phosphorous (P) limited [120-122], reinforcing that optimal targets for food system emissions, across quantities such as GHG emissions, water consumption, Nr and P emissions, need joint consideration.

Some studies place the marginal profit of crop gains for a unit of Nr emission as a subtraction from the marginal damage cost of that Nr emission, and some studies consider the marginal loss of crop gains for a unit of Nr emission reduction as a marginal cost of abatement [70, 82]. However, the cost of yield reduction may not be among the least costs for N reduction. Best practice for determining the social cost of Nr emissions is to include the marginal crop loss from reduction of Nr emissions in a marginal abatement curve.

The incompleteness of abatement curves for nitrogen mitigation (or nitrogen supplementation in countries where marginal social benefits of increasing agricultural yield still outweigh the marginal damages of Nr emissions) make determining the optimal marginal social cost of nitrogen difficult in practice. For example, globally inefficient use of N means that up to 50% of Nr emissions reduction could come, not from the cost of lost yields, but for the costs of increased N efficiency [123, 124]. Uncertainty in social costs will come from the uncertainty presented here in damage costs and uncertainty in abatement. The uncertainty in different views and knowledge of abatement persists even if marginal societal damages cost of Nr emissions are represented with certainty at a spatial and contextual level.

4.5.1 The cost to whom?

The difference between damage costs and optimal social costs reinforces the need to consider the cost to whom. The damage costs to exposed populations vulnerable to respiratory disease and nitrate intake, and to polluted ecosystems, are always negative amounts. However, the “damage” to society overall is the economic distance between the present social surplus and the maximal social surplus.

The marginal damage costs of NH3, NOx and Nr to water are taken as damage to GDP (aggregate economic effects) and a proxy for social welfare and costs to society. This provides consistency when aggregating nitrogen marginal damages costs with costs from other quantities associated to impacts (GHG, dietary intake, etc.). The marginal damages are not intended to describe costs transacted between sectors nor full costs for actors. Full costs for actors should be adjusted to account for counterfactuals. In the case of cost to society, the counterfactual is the optimal social arrangement.

Consumption as a proxy for welfare is comparable across national economies through purchase price parity (PPP). The unit of marginal costing is 2020USD per kg, understood for PPP comparisons as 2020 international dollars [125] (using PPP ratios from 2017 https://www.worldbank.org/en/programs/icp#5).

In the case of many African nations, an increase in Nr application (and thereby Nr emissions) maximises outcomes to society. A negative social cost of nitrogen in SSA, in this case, sponsors the argument for increasing fertiliser use in SSA, especially if high nitrogen use efficiency is maintained through the increase in input. Fertiliser use is mostly constrained in SSA by high cost/kg of fertiliser and low income, and a negative social cost should translate into subsidisation.

In determining the optimal marginal social cost, the benefits to society may not make their way to those experiencing damages, which introduces distributional issues and inequity in cost bearing.

In the present series of food system costs, for consistency with other costings the focus is on the cost to society. It is uncorrected for potential losses to society from distributional effects.

4.6 Temporal aspects of nitrogen impact

Most of the exposure from nitrogen pollution for impacts on ecosystem and human health are within a short time frame – days for atmospheric transport of particulate matter and weeks to months for short term biotic effects in ecosystems (but not the effects of sustained pollution on ecosystems) [2, 8]. There is a delay in the emergence of nitrate into drinking water supply from leaching. Human health effects for exposure to particulate matter and nitrate have been assumed to manifest at 10 years from exposure, and discounted. More detailed modelling of groundwater flux, and the human disease pathways from exposure, could improve the temporal modelling of future impacts from present emission.

Modelling nitrogen impact of emissions at a future date requires future projections relevant to population distributions and density, spatial context of agricultural land-use, the future context of ecosystem services (increased or decreased use and value of services) and background total nitrogen and sulphur emissions [126]. Environmental and ecosystem modelling would also need to determine the potential for saturation of Nr pools and additional stress on systems (the effect of sustained pollution) that results in costs above just inflation. Socio-economic modelling might also need to consider any change in vulnerability of populations to health impacts, above increases in population exposure through proximity to particulate loading.

4.7 Corrections and quantification of correlates

Corrections and correlations are required for aggregating the total damage costs of the food system. Many studies assume a first order linear approximation with constant marginal constants, and do not correct for the joint effects and joint uncertainty across the marginal costs [127]. More costs that are summed in this way (adding more impacts such as the cost of anti-biotic resistance, pollinator losses, etc.) under the assumption that they are biophysically and economically independent, introduces more error to the sum as an approximation of mean total costs if correlations are present. Protection from large errors is not guaranteed if marginal costs have individually been modelled by sophisticated Computable General Equilibrium (CGE) models and IAM; the covariation between the models may be absent.

Similar considerations are required for marginal abatement costs due to the mutual abatement potential of measures.

To remove double counting of costs, nutrient water pollution has been excluded from the damage costing of blue water withdrawal in Annex A – Water. N2O emissions are costed under Annex A – GHG and not costed under nitrogen. Soil erosion is not currently included as an impact category as there is some double counting adjustment needed between nutrient displacement to waterways and sediment run-off.

Marginal damage costs for phosphorous emissions are not estimated in the current dataset. The impact pathway for phosphorous is mainly soluble phosphorous and through soil displacement. When both N and P are enhanced, the impact of N can be larger through increased biotic growth (both positive and negative impacts, including increased carbon sequestration and increased biodiversity loss) [128, 129].

4.7.1 Correlation between nitrogen marginal damage costs

The joint distribution of marginal damage costs for NH3 and NOx emissions to air, and Nr run-off and leaching across 171 countries (sampled or parametric) described in Section 4.3.5 considered double counting and correlation within marginal damage costs. Section 4.4.1 discussed the complexity of correlations between the marginal damage costs for nitrogen emissions. NH3 and NOx emissions to air share similar component of the impact pathway and interact through the formation of ammonium nitrate. The relationship is non-linear, excess NOx can inhibit conversion rates to ammonium. Agricultural emissions may also only be weakly interacting – burning of biomass and application of fertiliser is likely separated in time, and the bulk of NOx emission from food system energy use is likely separated in space from agricultural locations. This has been represented by moderate correlation in air pollution observed in the attribution study of US counties.

Correlations between air and groundwater and surface water impact pathways may be present in emission factors used to determine quantity of emissions – certain soils and climate conditions may induce greater volatilisation rates at the same time as greater concentrates in groundwater and rivers. For correlation in marginal costs of nitrogen emissions, ecosystems downstream stressed by nitrogen pollution may be superlinearly (double the dose of Nr induces more than double the impacts) effected by deposition, but this requires more detailed modelling and assessment of the variation in ecosystem responses and the interaction of species of nitrogen retained from surface run-off and deposited from NH3 and NOx air emissions. Vegetation changes in ecosystems can change NH3 exchange between soils and atmosphere, and there is bi-directional representation of these physical exchanges in some Chemical Transport Models (CTMs) [1].

An advantage of examining and framing nitrogen damages parametrically using normal distributions on log axes is that Pearson correlation matrices log-transformed can be used to reconstruct joint distributions. The correlation matrix determined from joint Monte-Carlo sampling of discounting and the damage components in Section 4.3 is used for correlation between the marginal damage costs of nitrogen and available in the SPIQ dataset.

4.7.2 Quantification of correlations with non-nitrogen costs

Methodology for the correlation of marginal damage costs for nitrogen with the marginal damage costs of other quantities of impact, and sensitivity analysis, is described in Annex B. We discuss the interactions of the impacts of Nr emissions with the other impact categories and estimate block cross-quantity correlation coefficients (Table 5) for Table 3 in Annex B. For the sensitivity analysis described in Annex B, weak, moderate, and strong interactions between marginal costs are described by set correlation coefficients indicating proportion of covariance (Pearson):

Correlation	**P**	
Strong negative	-0.8	
Moderate negative	-0.5	
Weak negative	-0.2	
None	0	
Weak positive	0.2	
Moderate positive	0.5	
Strong positive	0.8	

To use block correlation between country level costs, we make broad assumptions factoring in biophysical interactions between atmospheric and aquatic pathways, and the joint response of human populations and ecosystems exposed to either increased doses or mutual effects. Low correlation does not indicate independence and no interactions, it may indicate negative correlations of from some biophysical effects, e.g. changes in the CO_2 and CH_4 flux between atmosphere and land due to NH_3 deposition, but positive correlations in other components, e.g. air pollution and temperature increased cardiovascular stress, and an estimate of the overall balance between the effects.

Interactions at the level of marginal damages, that is, in the impact pathway given a joint change in a unit of GHG emissions and joint change in kg of nitrogen emission, are described in the correlation coefficients here. A later version of the dataset will consider correlates with the individual nitrogen marginal damages. Interactions between quantity change (the number of units) and joint distributions on vectors of quantities must be factored into modelling of quantities, not marginal damages.

Table 5: Block Pearson correlation coefficients between uncertain marginal damage costs

Costs of…	GHG emissions	Water withdrawal and deprivation	Land use and change	Nr Emissions	Poverty	Chronic & Hidden Hunger	NCDs

Nitrogen pollution	0	+0.2	+0.5		0	-0.2	0

Symmetry of the correlation matrix means that the interaction of marginal impacts from blue water withdrawal and land-use conversion and effective loss of ha of ecosystem services has been assessed in Annex A – Water and Annex A – Land. Briefly, nitrogen pollution of waterways and deposition can worsen the effect of water deprivation due to a unit of water withdrawal, through effective denial of water use from quality reduction and coupled stress from biodiversity loss and acidification with water scarcity. Nitrogen induced acidification damages in the nitrogen cascade are widely distributed across biomes by air to land deposition and surface water run-off, including export of Nr to coastal systems and coral reefs. Acidification and eutrophication of terrestrial and aquatic biomes generally result in damage to biodiversity and ecosystem structure and hence service provision per ha [130]. There are mitigation effects such as increased carbon sequestration (and hence more valuable services) from increased biotic growth, but this effect is predominantly counted in the GHG and nitrogen interaction to avoid double counting. Overall, greater than expected damages from a ha of lost ecosystem services are expected to coincide with greater than expected damages from nitrogen pollution.

4.7.3 Marginal damage costs of GHG emissions and nitrogen emissions

The interaction between GHG marginal damages and nitrogen marginal damages overall is informed by covariance in damages from the highly complex interactions between global carbon and methane cycle with the global nitrogen cycle.

Nr emissions effect climate impacts through changes in temperature (a reduction in radiative forcing) and co-incident (increased) stress on humans and ecosystems. Higher temperature and changes in precipitation, associated to higher climate damages can induce co-incident (increased) stress on humans and ecosystems, and produce conditions in the future for increased secondary Nr emissions.

Influence on emissions and exposure

High temperature and precipitation enhance N mineralization rates, hence enhance the N availability but also the potential for emissions. [25] estimates a 5 °C increase in global temperature would increase NH3 volatilisation from anthropogenic sources (assuming those sources stay constant) by 42%. The increase would apply to primary emissions and secondary emissions from deposition – primary NH3 emissions are the quantity for marginal damages, but a proportional increase in secondary emissions from a component in the impact pathway would increase the marginal damages. The additional NH3 emissions to atmosphere (volatilization) from the same deposition of Nr occurs in warmer and drier conditions. There would also be a coincident increase in transport distance of PM2.5 produced by NH3 and NOx in warmer and drier conditions, with a potentially greater exposure to human populations and deposition on a greater area of ecosystems [25]. Variations in humidity and temperature effect the relationship between atmospheric NH3 (from fertiliser application or untreated animal manure) and increase formation of

PM2.5 [131-133]. O3 production from the same amount of emitted NOx increases with increasing temperature [134].

The timeframe, however, of atmospheric reactions and Nr deposition from present NH3 and NOx emissions is weeks. The temperature effects of present GHG emissions, even CH4, are in the scale of decades. Timeseries of GHG and Nr atmospheric emissions would have lag terms of interactions, but for the present study the consideration is on the interaction of the impact pathways for coincident units of quantity change. Therefore, the positive lag correlation in marginal damages as very small for concurrent emissions.

Precipitation increases run-off of Nr to waterways, which increases the quantity of Nr surface run-off emissions. Wetter soil increases the volatilisation of ammonia, increasing the quantity of NH3 emitted to air [135], though soil chemistry is the more dominant effect [136]. Precipitation changes the concentration and distribution of loads from a kg of Nr surface run-off (increasing the quantity of decreased run-off was discussed above) [137]. Higher streamflow increases export to higher value ecosystem services in coastal systems [138], which would increase marginal damages from Nr emissions. Temperature increases stratification in the water, and hence increases eutrophication damages [138]. It is unclear without spatially explicit modelling of precipitation changes, which have higher uncertainty than temperature projections, the trade-off between drier conditions with increased NH3 volatilisation and decreased Nr run-off and the converse in wetter conditions. Precipitation changes from climatic change also have lag.

Aerosol and sequestration effects
Nr emissions have warming and cooling effects that influence climate impacts, summarised in [139] and [36] (Figure 7).

The formation of particulate matter from NH3 and NOx emissions has aerosol effects. The reduction of the radiative forcing from NH3 is estimated between -0.1 Wm^{-2} and -0.2 Wm^{-2} from modelling [1] [1, 140]. Site measurements confirm contribution of ammonium nitrate to aerosol formation near agricultural sources of NH3 and that NH3 has the largest aerosol effect on radiative forcing per kg of emission [1]. NH3 and NOx are estimated to be responsible for ~25% of aerosol radiative forcing reduction [1]. The timescale of impact is different, continual Nr emissions are reducing the impacts of resident CO2 emissions (the albedo radiative forcing effect is short term).

NOx emissions to atmosphere produce tropospheric O3. O3 has a positive radiative forcing and impairs C sequestration by damaging plant growth [36]. However, tropospheric O3 decreases CH4 concentration, their interaction producing the hydroxyl radical which is responsible for 88% of the atmospheric CH4 sink (Figure 7).

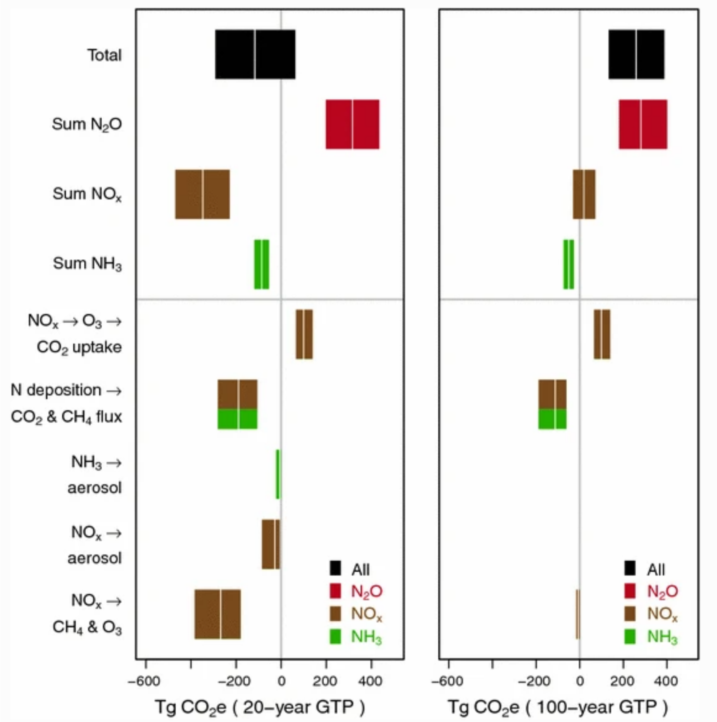

The climate change impacts of US reactive nitrogen emissions, by chemical species, in common units of equivalent Tg of CO_2 (Tg CO_{2e}) on a 20-year and 100-year GTP basis. The width of the bar denotes the uncertainty range; the *white line* is the best-estimate; and the *color shading* shows the relative contribution of NO_x and NH_3 emissions to nitrogen deposition (adapted from Pinder et al. 2012)

Figure 7: Quantification in Global Temperature Potential (GTP) from [36] of the complex interactions on radiative forcing between Nr emissions and GHG emissions. Particulate matter associated to NH3 and NOx air pollution has an aerosol effect (NH3, NOx -> aerosol), reducing radiative forcing and countering warming potential while present in the atmosphere. Deposition of nitrogen increases sequestration and acidification, resulting in net increased drawdown of CO2 and CH4 from the atmosphere (N deposition -> CO2 & CH4 flux). NOx pollution produces tropospheric O3, which has a warming potential itself and damages vegetation and hence sequestration (NOx -> O3 -> CO2 uptake). However, O3 has a larger cooling effect by increasing the hydroxyl radical and the breakdown of CH4 in the atmosphere (NOx -> CH4 & O3).

Deposition on land, surface run-off of Nr, and deposition on the open ocean, has increased CO2 sequestration from increased biological growth. This reduces the impact of GHG emissions as Nr emissions increase. Models have estimated an increase of ~3% in biological growth in the open ocean and an increase in overall ocean carbon sequestration of ~0.4% due to anthropogenic N deposition [28, 65].

Carbon (C) sequestration increases from Nr deposition on temperate and tropical forest soils [141] (an estimated 25 kg C sequestration per kg N deposited [29]). Though high Nr deposition can reduce the sequestration amount per kg due to damage from acidification [142]. Sequestration through biomass growth in forests is the clearest effect. Increased soil storage from N deposition in grasslands [143] is less certain through the influence of human activity [144, 145].

It is unclear the contribution of water vapor from excess Nr biological growth and the fate of sequestered carbon when ecosystems tip from Nr saturation to collapse (dead zones, etc).

Co-incident stress and vulnerability of humans and ecosystems
IAM damage modelling includes effects of heat stress on human cardio-vascular disease [146], which is also the primary pathway for air-pollution damages [77]. The effects of present air pollution couple more closely to extreme temperature events induced potentially by short-term warming from present CH4 emissions and from past CO2 emissions.

IAM damage modelling includes costs of changes in terrestrial ecosystem services. Riverine nitrogen from agricultural run-off and deposition degrades ecosystem services. The effects of excess nutrients from present Nr emission couple more closely to temperature change from present CH4 emissions. Positive correlations are expected in the magnitude of degradation, climatic impact will reinforce with non-GHG agricultural sources of stress [147].

Multiple climate drivers interact with eutrophication with positive and negative effects. Current modelling predicts small enhancement in eutrophication primarily from temperature increase of water and decrease solubility of oxygen (O) [148]. This is expected to vary considerably depending on local coastal (sea level rise) conditions, precipitation and loadings [148].

Nr deposits to marine and coastal environments increases CO2 sequestration and accelerates acidification. Estimates are that only a few percent of additional acidification and increase sequestration is due to the interaction between Nr deposition and C [58]. This increases is related to the exposure of ecosystem services in costal zones to acidification [58]. It is unclear whether increased acidification has the counter effect of reducing natural N2O emissions from the ocean [149, 150] or not [151, 152]. CO2 sequestration is the major source of acidification in the open ocean [28].

PM2.5 and O3 attributable mortality associated with increased temperature over the 21st century are expected to decline if NH3 and NOx emissions were reduced [153]. Factors of human vulnerability to climate change and air-pollution coincide [154, 155].

C and N global cycles share common drivers in impact pathways which also induces correlation [36].

There is a decrease in O3 damage to plants as CO2 concentration increases [156]: a concurrent effect. Over a longer timeframe, more O3 is produced from NOx emissions as temperature increases.

Coupled C and N cycle models to jointly represent the above effects are presently missing or limited [36]. Overall, coupled C and N emission modelling lacks the sophistication to consider a joint time series of emissions, where N emissions in 2020 interact jointly with the effects of 2020 GHG emissions. Given the complexity of positive and negative effects, the inability to consider quantitatively temporal differences in impact from emissions, and the lower climate forcing reduction effects of NH3 which are the primary agricultural atmospheric emission, we use a correlation coefficient of zero. The negative effect on radiative forcing is countered by positive co-impact on human populations and ecosystems.

4.7.4 Marginal damage costs of noncommunicable disease from dietary intake and nitrogen emissions

The primary factor for per kg NH3 air pollution damages is PM2.5 production. PM2.5 exposure is associated to cardiovascular risk [157]. Most Global Burden of Disease (GBD) risks from dietary consumption per unit of intake increase CVD and are increased by existing CVD conditions [158]. Health co-morbidity effects of air pollution and dietary intake (CVD is the predominate pathway for DALYs lost from dietary intake [159]) can simultaneously increase the years of life lost, but could produce double counting across cost estimates as premature death of the same vulnerable individuals may be counted twice.

Nitrate can have positive effects for CVDs but negative effects for cancers, with small increased risks jointly associated to diets high in meat and low in fibre [56]. Nitrate's highest concentrations of intake at the population level occur from vegetable and fruit consumption [56]. Overall, the mixed effects on coincident health effects from consumption, the uncertainty in nitrate's impact, and the low marginal impacts compared to marginal damage from air pollution, NO3- contributes little to correlated marginal damages between consumption and Nr emissions.

There are tertiary positive effects between CVDs, poverty alleviation, and hence nitrogen inputs [160], though most studies are from high income countries where nitrogen use and poverty alleviation are decoupled [161].

These interactions are expected to be weak, and they may be downgraded further by spatial and temporal coincidence of impacts. Cardiovascular effects of air pollution may escalate existing conditions, whereas human health aspects of dietary intake now may take a decade or more to manifest. Weak positive links between nitrogen damage to cultural and recreation ecosystem services values and health coeffects are also.

4.7.5 Poverty gap and marginal damages of nitrogen emissions

Section 4.10.6 demonstrates a strong trend between increase in Nr emissions and increase in GVA from agriculture. When the *quantity* of Nr emissions increases GVA increases. For low-income countries with large share of Gross National Income (GNI) associated to agriculture this indicates a potential for reduction in the poverty gap [162]. Historically, increased use of nitrogen is positively correlated with reduction of poverty gaps, and headcounts of poverty [163]. For more advanced economies, nitrogen use and poverty decouple. Distributional issues might also lower the effects of increased nitrogen use and poverty alleviation. It is not as clear whether and to what degree an increase in external economic damages per kg of nitrogen emitted is associated to a decrease in the poverty gap, except through the assumed tertiary relationship that increased quantity of Nr emissions increases damages per unit of emissions (the marginal damage functions for nitrogen are convex in Nr emissions). Interpolating the relationship in Section 4.10.6, there is some uncertainty whether the marginal benefit to GVA from Nr surface run-off is convex. That it is potentially linear or concave even for low-income countries could be due to poor nitrogen use efficiency and the quality of fertiliser used [163, 164]. Nitrogen use-efficiency reduces the quantity of emissions from reduction of the poverty gap.

It is not clear that higher than expected marginal damages from unit of nitrogen emissions (which are related mostly to the biophysical fate of nitrogen and the vulnerability of ecosystems and exposed human populations) equates to a lower than expected poverty gap. Poverty alleviation is associated historically to over-utilised and hence scarcer ecosystems provisioning services, which provide potentially greater value per ha [165]. Increased poverty can be associated to higher air pollution costs through greater proximity to precursors NOx and SOx of particulate formation (dirtier combustion, industrial neighbourhoods, power plants, etc.) [166, 167] and vulnerability [168]. The evidence is more limited on crowding in urban populations from poverty and for widely dispersed particulates like ammonium compounds [169]. The effects on marginal ecosystem value and costs from human health impacts are globally variable and potentially opposing.

Overall, though poverty and nitrogen use are clearly not independent [162], the correlation between the marginal damages of nitrogen emissions and poverty gaps are not clearly positive nor negative.

4.7.6 Marginal damages from chronic and hidden hunger and nitrogen emissions

Marginal damages from chronic and hidden hunger factor through the number of DALYs per person in malnutrition. Coincident health effects of water pollution, water quality and excess nitrate intake, can increase potential co-morbidity with protein-energy malnutrition [170-172]. There are opposing effects: increased DALYs per person in malnutrition is moderately correlated with absolute numbers of ppl in malnutrition itself (Annex A – Water) and weakly correlated with poverty, and hence negatively weakly correlated with the total quantity of nitrogen pollution. The role of nutrient deficiencies in exacerbating the human response to air pollution is speculated but has few studies [173]. Other potential moderating factors to the interaction of the impact pathways of undernourishment and nitrogen emissions are temporal and spatial coincidence of health impacts. Nitrate contamination of groundwater has a temporal lag of transport from topsoil to groundwater (present leaching will influence the cost of future changes in malnutrition impact more than present change sin malnutrition impact).

Overall, though malnutrition and nitrogen use are clearly not independent [162, 174], we assign a weak negative correlation. We assess, generally, countries with high levels of malnutrition, receive mitigation in the health effects per person with malnutrition from the input of a nitrogen and increased nitrogen coincides with increased marginal damages.

4.8 Consideration for use

4.8.1 Agricultural subsidy reform

As in Annex A – GHG, since subsidies are largely social welfare policies, economic arguments for subsidy reform should be framed as costs to society.

Global subsidy reform will involve potentially large changes in spatial distribution of agricultural production and volumes of commodities. Price effects change non-food consumption and/or demand change for agricultural commodities, with a secondary correction to production distribution and volumes. Competition for land-use and spatial changes in production have effects on labour and inputs. General equilibrium modelling of changes to the economy, resulting in quantities associated to impacts, are appropriate, as are comparisons with consumption/GDP outputs from the models with costs to society estimates of corrections of market failure.

The modelling of global subsidy change should take into account increased income and poverty reduction in lower income countries (i.e. the benefits of nitrogen use), to offset the potential damages from increased nitrogen use. A further factor, modelling should consider, is an explicit nitrogen use efficiency component in projections of technological improvements.

Because of their different chemical cascades through atmospheric, terrestrial, and aquatic environments, NH3, NOx and riverine Nr should be costed as joint marginals. It would be useful to improve widespread availability and use in costings of nitrogen emissions factors. Attribution using formulas from N application or livestock production to NH3, N3O and riverine Nr emission such as those available in FAO's Livestock Environmental Assessment and Performance (FAO LEAP) are not widely implemented in models or nitrogen accounting.

Implicit in exogenous scenarios are emission trajectories. If setting exogenous scenarios, there should be some consideration whether the marginal social costs need adjustment for Nr future pooling and saturation effects in ecosystems, or more exposed and more vulnerable human populations downwind and downstream of N emissions.

4.9 References

1. Zhu, L., et al., *Sources and Impacts of Atmospheric NH3: Current Understanding and Frontiers for Modeling, Measurements, and Remote Sensing in North America.* Current Pollution Reports, 2015. **1**(2): p. 95-116.
2. Fowler, D., et al., *The global nitrogen cycle in the twenty-first century.* Philosophical Transactions of the Royal Society B: Biological Sciences, 2013. **368**(1621): p. 20130164.
3. Olivier, J.G.J., et al., *Global air emission inventories for anthropogenic sources of NOx, NH3 and N2O in 1990.* Environmental Pollution, 1998. **102**(1, Supplement 1): p. 135-148.
4. McDuffie, E.E., et al., *A global anthropogenic emission inventory of atmospheric pollutants from sector- and fuel-specific sources (1970–2017): an application of the Community Emissions Data System (CEDS).* Earth Syst. Sci. Data, 2020. **12**(4): p. 3413-3442.
5. Paulot, F., et al., *Ammonia emissions in the United States, European Union, and China derived by high-resolution inversion of ammonium wet deposition data: Interpretation with a new agricultural emissions inventory (MASAGE_NH3).* Journal of Geophysical Research: Atmospheres, 2014. **119**(7): p. 4343-4364.
6. Crippa, M., et al., *Gridded emissions of air pollutants for the period 1970–2012 within EDGAR v4.3.2.* Earth Syst. Sci. Data, 2018. **10**(4): p. 1987-2013.
7. de Vries, W., *Impacts of nitrogen emissions on ecosystems and human health: A mini review.* Current Opinion in Environmental Science & Health, 2021. **21**: p. 100249.
8. Erisman, J.W., et al., *Consequences of human modification of the global nitrogen cycle.* Philosophical transactions of the Royal Society of London. Series B, Biological sciences, 2013. **368**(1621): p. 20130116-20130116.
9. Billen, G., J. Garnier, and L. Lassaletta, *The nitrogen cascade from agricultural soils to the sea: modelling nitrogen transfers at regional watershed and global scales.* Philosophical Transactions of the Royal Society B: Biological Sciences, 2013. **368**(1621): p. 20130123.
10. Usubiaga-Liaño, A., P. Behrens, and V. Daioglou, *Energy use in the global food system.* Journal of Industrial Ecology, 2020. **24**(4): p. 830-840.
11. Seitzinger, S.P., *Denitrification in freshwater and coastal marine ecosystems: Ecological and geochemical significance.* Limnology and Oceanography, 1988. **33**(4part2): p. 702-724.
12. Tian, H., et al., *A comprehensive quantification of global nitrous oxide sources and sinks.* Nature, 2020. **586**(7828): p. 248-256.
13. Uwizeye, A., et al., *Nitrogen emissions along global livestock supply chains.* Nature Food, 2020. **1**(7): p. 437-446.
14. Henchion, M., et al., *Future Protein Supply and Demand: Strategies and Factors Influencing a Sustainable Equilibrium.* Foods (Basel, Switzerland), 2017. **6**(7): p. 53.
15. Luo, Z., S. Hu, and D. Chen, *The trends of aquacultural nitrogen budget and its environmental implications in China.* Scientific Reports, 2018. **8**(1): p. 10877.
16. Liu, J., et al., *Reducing human nitrogen use for food production.* Scientific Reports, 2016. **6**(1): p. 30104.
17. Zhang, X., et al., *Quantification of global and national nitrogen budgets for crop production.* Nature Food, 2021. **2**(7): p. 529-540.
18. Strokal, M. and C. Kroeze, *Nitrous oxide (N2O) emissions from human waste in 1970–2050.* Current Opinion in Environmental Sustainability, 2014. **9-10**: p. 108-121.
19. Van Drecht, G., et al., *Global nitrogen and phosphate in urban wastewater for the period 1970 to 2050.* Global Biogeochemical Cycles, 2009. **23**(4).

20. Bouwman, A.F., L.J.M. Boumans, and N.H. Batjes, *Estimation of global NH3 volatilization loss from synthetic fertilizers and animal manure applied to arable lands and grasslands.* Global Biogeochemical Cycles, 2002. **16**(2): p. 8-1-8-14.
21. Oita, A., et al., *Substantial nitrogen pollution embedded in international trade.* Nature Geoscience, 2016. **9**(2): p. 111-115.
22. Schlesinger, W.H., *On the fate of anthropogenic nitrogen.* Proceedings of the National Academy of Sciences, 2009. **106**(1): p. 203.
23. Crippa, M., et al., *Food systems are responsible for a third of global anthropogenic GHG emissions.* Nature Food, 2021. **2**(3): p. 198-209.
24. Van Damme, M., et al., *Industrial and agricultural ammonia point sources exposed.* Nature, 2018. **564**(7734): p. 99-103.
25. Sutton, M.A., et al., *Towards a climate-dependent paradigm of ammonia emission and deposition.* Philosophical Transactions of the Royal Society B: Biological Sciences, 2013. **368**(1621): p. 20130166.
26. Galloway, J.N., et al., *Transformation of the Nitrogen Cycle: Recent Trends, Questions, and Potential Solutions.* Science, 2008. **320**(5878): p. 889.
27. Seitzinger, S., et al., *DENITRIFICATION ACROSS LANDSCAPES AND WATERSCAPES: A SYNTHESIS.* Ecological Applications, 2006. **16**(6): p. 2064-2090.
28. Duce, R.A., et al., *Impacts of Atmospheric Anthropogenic Nitrogen on the Open Ocean.* Science, 2008. **320**(5878): p. 893.
29. *The European Nitrogen Assessment: Sources, Effects and Policy Perspectives*. 2011, Cambridge: Cambridge University Press.
30. Galperin, M.V. and M.A. Sofiev, *The long-range transport of ammonia and ammonium in the Northern Hemisphere.* Atmospheric Environment, 1998. **32**(3): p. 373-380.
31. Philip, S., et al., *Global Chemical Composition of Ambient Fine Particulate Matter for Exposure Assessment.* Environmental Science & Technology, 2014. **48**(22): p. 13060-13068.
32. Domingo, N.G.G., et al., *Air quality–related health damages of food.* Proceedings of the National Academy of Sciences, 2021. **118**(20): p. e2013637118.
33. Fann, N., et al., *Estimating the National Public Health Burden Associated with Exposure to Ambient PM2.5 and Ozone.* Risk Analysis, 2012. **32**(1): p. 81-95.
34. Gu, B., et al., *Atmospheric Reactive Nitrogen in China: Sources, Recent Trends, and Damage Costs.* Environmental Science & Technology, 2012. **46**(17): p. 9420-9427.
35. Krupa, S.V., *Effects of atmospheric ammonia (NH3) on terrestrial vegetation: a review.* Environmental Pollution, 2003. **124**(2): p. 179-221.
36. Pinder, R.W., et al., *Impacts of human alteration of the nitrogen cycle in the US on radiative forcing.* Biogeochemistry, 2013. **114**(1): p. 25-40.
37. Feng, Z., et al., *Economic losses due to ozone impacts on human health, forest productivity and crop yield across China.* Environment International, 2019. **131**: p. 104966.
38. Avnery, S., et al., *Global crop yield reductions due to surface ozone exposure: 2. Year 2030 potential crop production losses and economic damage under two scenarios of O3 pollution.* Atmospheric Environment, 2011. **45**(13): p. 2297-2309.
39. Jarvis, D.J., G. Adamkiewicz, and M.E. Heroux, *Nitrogen dioxide*, in *WHO Guidelines for Indoor Air Quality: Selected Pollutants*. 2010, World Health Organization: Geneva.
40. Bruce, N., et al., *Does household use of biomass fuel cause lung cancer? A systematic review and evaluation of the evidence for the GBD 2010 study.* Thorax, 2015. **70**(5): p. 433.
41. Hesterberg, R., et al., *Deposition of nitrogen-containing compounds to an extensively managed grassland in central Switzerland.* Environmental Pollution, 1996. **91**(1): p. 21-34.
42. Xu, W., et al., *Quantifying atmospheric nitrogen deposition through a nationwide monitoring network across China.* Atmos. Chem. Phys., 2015. **15**(21): p. 12345-12360.

43. Tian, D. and S. Niu, *A global analysis of soil acidification caused by nitrogen addition.* Environmental Research Letters, 2015. **10**(2): p. 024019.
44. Bobbink, R., et al., *Global assessment of nitrogen deposition effects on terrestrial plant diversity: a synthesis.* Ecological Applications, 2010. **20**(1): p. 30-59.
45. Bowman, W.D., et al., *Negative impact of nitrogen deposition on soil buffering capacity.* Nature Geoscience, 2008. **1**(11): p. 767-770.
46. Stevens, C.J., T.I. David, and J. Storkey, *Atmospheric nitrogen deposition in terrestrial ecosystems: Its impact on plant communities and consequences across trophic levels.* Functional Ecology, 2018. **32**(7): p. 1757-1769.
47. Zhu, Q., et al., *Enhanced acidification in Chinese croplands as derived from element budgets in the period 1980–2010.* Science of The Total Environment, 2018. **618**: p. 1497-1505.
48. Zhu, Q., et al., *Cropland acidification increases risk of yield losses and food insecurity in China.* Environmental Pollution, 2020. **256**: p. 113145.
49. Bijay, S. and E. Craswell, *Fertilizers and nitrate pollution of surface and ground water: an increasingly pervasive global problem.* SN Applied Sciences, 2021. **3**(4): p. 518.
50. Shen, J., et al., *Contribution of atmospheric nitrogen deposition to diffuse pollution in a typical hilly red soil catchment in southern China.* Journal of Environmental Sciences, 2014. **26**(9): p. 1797-1805.
51. Zhan, X., et al., *Evidence for the Importance of Atmospheric Nitrogen Deposition to Eutrophic Lake Dianchi, China.* Environmental Science & Technology, 2017. **51**(12): p. 6699-6708.
52. Durand, P., et al., *Nitrogen processes in aquatic ecosystems*, in *The European Nitrogen Assessment: Sources, Effects and Policy Perspectives*, A. Bleeker, et al., Editors. 2011, Cambridge University Press: Cambridge. p. 126-146.
53. Ward, M.H., et al., *Drinking Water Nitrate and Human Health: An Updated Review.* International journal of environmental research and public health, 2018. **15**(7): p. 1557.
54. Rahman, A., N.C. Mondal, and K.K. Tiwari, *Anthropogenic nitrate in groundwater and its health risks in the view of background concentration in a semi arid area of Rajasthan, India.* Scientific reports, 2021. **11**(1): p. 9279-9279.
55. Damania, R., et al., *Quality Unknown : The Invisible Water Crisis*. 2019, World Bank: Washington, DC.
56. Bryan, N.S. and H. van Grinsven, *Chapter Three - The Role of Nitrate in Human Health*, in *Advances in Agronomy*, D.L. Sparks, Editor. 2013, Academic Press. p. 153-182.
57. Camargo, J.A. and Á. Alonso, *Ecological and toxicological effects of inorganic nitrogen pollution in aquatic ecosystems: A global assessment.* Environment International, 2006. **32**(6): p. 831-849.
58. Doney, S.C., et al., *Impact of anthropogenic atmospheric nitrogen and sulfur deposition on ocean acidification and the inorganic carbon system.* Proceedings of the National Academy of Sciences, 2007. **104**(37): p. 14580.
59. Anthony, K.R.N., et al., *Ocean acidification causes bleaching and productivity loss in coral reef builders.* Proceedings of the National Academy of Sciences, 2008. **105**(45): p. 17442.
60. Nancy, N.R., *Nitrogen in Aquatic Ecosystems.* AMBIO: A Journal of the Human Environment, 2002. **31**(2): p. 102-112.
61. BergstrÖM, A.-K. and M. Jansson, *Atmospheric nitrogen deposition has caused nitrogen enrichment and eutrophication of lakes in the northern hemisphere.* Global Change Biology, 2006. **12**(4): p. 635-643.
62. Altieri, A.H., et al., *Tropical dead zones and mass mortalities on coral reefs.* Proceedings of the National Academy of Sciences of the United States of America, 2017. **114**(14): p. 3660-3665.

63. Selman, M., Z. Sugg, and S. Greenhalgh, *Eutrophication and Hypoxia in Coastal Areas: A Global Assessment of the State of Knowledge*. 2008, World Resources Institute: Washington, DC.
64. Diaz, R.J. and R. Rosenberg, *Spreading Dead Zones and Consequences for Marine Ecosystems.* Science, 2008. **321**(5891): p. 926.
65. Jickells, T.D., et al., *A reevaluation of the magnitude and impacts of anthropogenic atmospheric nitrogen inputs on the ocean.* Global Biogeochemical Cycles, 2017. **31**(2): p. 289-305.
66. Elser, J.J., et al., *Shifts in Lake N:P Stoichiometry and Nutrient Limitation Driven by Atmospheric Nitrogen Deposition.* Science, 2009. **326**(5954): p. 835.
67. Moon, J.-Y., et al., *Anthropogenic nitrogen is changing the East China and Yellow seas from being N deficient to being P deficient.* Limnology and Oceanography, 2021. **66**(3): p. 914-924.
68. Zhu, L., et al., *Algal Accumulation Decreases Sediment Nitrogen Removal by Uncoupling Nitrification-Denitrification in Shallow Eutrophic Lakes.* Environmental Science & Technology, 2020. **54**(10): p. 6194-6201.
69. Birch, M.B.L., et al., *Why Metrics Matter: Evaluating Policy Choices for Reactive Nitrogen in the Chesapeake Bay Watershed.* Environmental Science & Technology, 2011. **45**(1): p. 168-174.
70. van Grinsven, H.J.M., et al., *Costs and Benefits of Nitrogen for Europe and Implications for Mitigation.* Environmental Science & Technology, 2013. **47**(8): p. 3571-3579.
71. Sutton, M.A., et al., *Too much of a good thing.* Nature, 2011. **472**(7342): p. 159-161.
72. Sobota, D.J., et al., *Cost of reactive nitrogen release from human activities to the environment in the United States.* Environmental Research Letters, 2015. **10**(2): p. 025006.
73. Xia, L., et al., *Greenhouse gas emissions and reactive nitrogen releases during the life-cycles of staple food production in China and their mitigation potential.* Science of The Total Environment, 2016. **556**: p. 116-125.
74. Matthias, V., et al., *Modeling emissions for three-dimensional atmospheric chemistry transport models.* Journal of the Air & Waste Management Association, 2018. **68**(8): p. 763-800.
75. Dore, A.J., et al., *Evaluation of the performance of different atmospheric chemical transport models and inter-comparison of nitrogen and sulphur deposition estimates for the UK.* Atmospheric Environment, 2015. **119**: p. 131-143.
76. Evangelopoulos, D., et al., *The role of burden of disease assessment in tracking progress towards achieving WHO global air quality guidelines.* International Journal of Public Health, 2020. **65**(8): p. 1455-1465.
77. Dockery, D.W., *Health Effects of Particulate Air Pollution.* Annals of Epidemiology, 2009. **19**(4): p. 257-263.
78. Gilmore, E.A., et al., *An inter-comparison of the social costs of air quality from reduced-complexity models.* Environmental Research Letters, 2019. **14**(7): p. 074016.
79. Wang, Z.-H. and S.-X. Li, *Chapter Three - Nitrate N loss by leaching and surface runoff in agricultural land: A global issue (a review)*, in *Advances in Agronomy*, D.L. Sparks, Editor. 2019, Academic Press. p. 159-217.
80. Holland, M., et al., *Damages per tonne emission of PM2.5, NH3, SO2, NOx and VOCs from each EU25 member State (excluding Cyprus) and surrounding seas*. 2005, AEA Technology Environment: Didcot, UK.
81. Compton, J.E., et al., *Ecosystem services altered by human changes in the nitrogen cycle: a new perspective for US decision making.* Ecology Letters, 2011. **14**(8): p. 804-815.
82. Yin, Y., et al., *Calculating socially optimal nitrogen (N) fertilization rates for sustainable N management in China.* Science of The Total Environment, 2019. **688**: p. 1162-1171.
83. Keeler, B.L., et al., *The social costs of nitrogen.* Science Advances, 2016. **2**(10): p. e1600219.

84. Von Blottnitz, H., et al., *Damage costs of nitrogen fertilizer in Europe and their internalization.* Journal of Environmental Planning and Management, 2006. **49**(3): p. 413-433.
85. Adenuga, A.H., et al., *Environmental Efficiency and Pollution Costs of Nitrogen Surplus in Dairy Farms: A Parametric Hyperbolic Technology Distance Function Approach.* Environmental and Resource Economics, 2019. **74**(3): p. 1273-1298.
86. Schmidt, A., et al., *Reduction of nitrogen pollution in agriculture through nitrogen surplus quotas: an analysis of individual marginal abatement cost and different quota allocation schemes using an agent-based model.* Journal of Environmental Planning and Management, 2021. **64**(8): p. 1375-1391.
87. Quan, Z., et al., *Different quantification approaches for nitrogen use efficiency lead to divergent estimates with varying advantages.* Nature Food, 2021. **2**(4): p. 241-245.
88. Quemada, M., et al., *Exploring nitrogen indicators of farm performance among farm types across several European case studies.* Agricultural Systems, 2020. **177**: p. 102689.
89. EEA, *EMEP/EEA air pollutant emission inventory guidebook 2019: Technical guidance to prepare national emission inventories*, in *EEA Report*. 2019, European Environment Agency: Copenhagen.
90. WHO, *Health riaks of particulate matter from long-range transboundary air pollution*. 2006, World Health Organization Europe: Copenhagen, Denmark.
91. Boakes, E.H., et al., *Extreme contagion in global habitat clearance.* Proceedings of the Royal Society B: Biological Sciences, 2010. **277**(1684): p. 1081-1085.
92. Moriasi, D.N., et al., *Modeling the impact of nitrogen fertilizer application and tile drain configuration on nitrate leaching using SWAT.* Agricultural Water Management, 2013. **130**: p. 36-43.
93. Nelson, E., et al., *Modeling multiple ecosystem services, biodiversity conservation, commodity production, and tradeoffs at landscape scales.* Frontiers in Ecology and the Environment, 2009. **7**(1): p. 4-11.
94. Buonocore, J.J., et al., *Using the Community Multiscale Air Quality (CMAQ) model to estimate public health impacts of PM2.5 from individual power plants.* Environment International, 2014. **68**: p. 200-208.
95. Heo, J., P.J. Adams, and H.O. Gao, *Reduced-form modeling of public health impacts of inorganic PM2.5 and precursor emissions.* Atmospheric Environment, 2016. **137**: p. 80-89.
96. van Grinsven, H.J.M., A. Rabl, and T.M. de Kok, *Estimation of incidence and social cost of colon cancer due to nitrate in drinking water in the EU: a tentative cost-benefit assessment.* Environmental health : a global access science source, 2010. **9**: p. 58-58.
97. Pretty, J.N., et al., *Environmental Costs of Freshwater Eutrophication in England and Wales.* Environmental Science & Technology, 2003. **37**(2): p. 201-208.
98. Dodds, W.K., et al., *Eutrophication of U.S. Freshwaters: Analysis of Potential Economic Damages.* Environmental Science & Technology, 2009. **43**(1): p. 12-19.
99. Moxey, A., *Agriculture and Water Quality: Monetary Costs and Benefits across OECD Countries*. 2012, OECD: Paris.
100. Azevedo, L.B., et al., *Assessing the Importance of Spatial Variability versus Model Choices in Life Cycle Impact Assessment: The Case of Freshwater Eutrophication in Europe.* Environmental Science & Technology, 2013. **47**(23): p. 13565-13570.
101. Ascott, M.J., et al., *Global patterns of nitrate storage in the vadose zone.* Nature Communications, 2017. **8**(1): p. 1416.
102. Beusen, A.H.W., et al., *Coupling global models for hydrology and nutrient loading to simulate nitrogen and phosphorus retention in surface water – description of IMAGE–GNM and analysis of performance.* Geosci. Model Dev., 2015. **8**(12): p. 4045-4067.

103. Matiatos, I., et al., *Global patterns of nitrate isotope composition in rivers and adjacent aquifers reveal reactive nitrogen cascading.* Communications Earth & Environment, 2021. **2**(1): p. 52.
104. Bouwman, A.F., et al., *Lessons from temporal and spatial patterns in global use of N and P fertilizer on cropland.* Scientific Reports, 2017. **7**(1): p. 40366.
105. Ackerman, D., D.B. Millet, and X. Chen, *Global Estimates of Inorganic Nitrogen Deposition Across Four Decades.* Global Biogeochemical Cycles, 2019. **33**(1): p. 100-107.
106. Beusen, A.H.W., et al., *Global riverine N and P transport to ocean increased during the 20th century despite increased retention along the aquatic continuum.* Biogeosciences, 2016. **13**(8): p. 2441-2451.
107. McDowell, R.W., et al., *Global database of diffuse riverine nitrogen and phosphorus loads and yields.* Geoscience Data Journal, 2020. **n/a**(n/a).
108. Turner, R.E., et al., *Global Patterns of Dissolved N, P and Si in Large Rivers.* Biogeochemistry, 2003. **64**(3): p. 297-317.
109. Linke, S., et al., *Global hydro-environmental sub-basin and river reach characteristics at high spatial resolution.* Scientific Data, 2019. **6**(1): p. 283.
110. Seitzinger, S.P., et al., *Global river nutrient export: A scenario analysis of past and future trends.* Global Biogeochemical Cycles, 2010. **24**(4).
111. de Groot, R., et al., *Global estimates of the value of ecosystems and their services in monetary units.* Ecosystem Services, 2012. **1**(1): p. 50-61.
112. Magalhães Filho, L., et al., *A Global Meta-Analysis for Estimating Local Ecosystem Service Value Functions.* Environments, 2021. **8**(8).
113. Lehner, B. and P. Döll, *Development and validation of a global database of lakes, reservoirs and wetlands.* Journal of Hydrology, 2004. **296**(1): p. 1-22.
114. Pham-Duc, B., et al., *Comparisons of Global Terrestrial Surface Water Datasets over 15 Years.* Journal of Hydrometeorology, 2017. **18**(4): p. 993-1007.
115. Dinerstein, E., et al., *An Ecoregion-Based Approach to Protecting Half the Terrestrial Realm.* BioScience, 2017. **67**(6): p. 534-545.
116. Kushta, J., A. Pozzer, and J. Lelieveld, *Uncertainties in estimates of mortality attributable to ambient PM 2.5 in Europe.* Environmental Research Letters, 2018. **13**(6): p. 064029.
117. United States. Congress. Senate. Committee on Homeland Security and Governmental Affairs. Permanent Subcommittee on Investigations., *Wall Street and the financial crisis : anatomy of a financial collapse : majority and minority staff report*. 2011, Washington, DC: US Senate. Permanent Subcommittee on Investigations.
118. Matsumoto, T. and T. Yamano, *Optimal Fertilizer Use on Maize Production in East Africa*, in *Emerging Development of Agriculture in East Africa: Markets, Soil, and Innovations*, T. Yamano, K. Otsuka, and F. Place, Editors. 2011, Springer Netherlands: Dordrecht. p. 117-132.
119. Essel, B., et al., *Economically Optimal Rate for Nutrient Application to Maize in the Semi-deciduous Forest Zone of Ghana.* Journal of Soil Science and Plant Nutrition, 2020. **20**(4): p. 1703-1713.
120. Pasley, H.R., et al., *Nitrogen fertilizer rate increases plant uptake and soil availability of essential nutrients in continuous maize production in Kenya and Zimbabwe.* Nutrient Cycling in Agroecosystems, 2019. **115**(3): p. 373-389.
121. van der Velde, M., et al., *African crop yield reductions due to increasingly unbalanced Nitrogen and Phosphorus consumption.* Global Change Biology, 2014. **20**(4): p. 1278-1288.
122. Penuelas, J., et al., *Anthropogenic global shifts in biospheric N and P concentrations and ratios and their impacts on biodiversity, ecosystem productivity, food security, and human health.* Global Change Biology, 2020. **26**(4): p. 1962-1985.
123. Mueller, N.D., et al., *A tradeoff frontier for global nitrogen use and cereal production.* Environmental Research Letters, 2014. **9**(5): p. 054002.

124. Folberth, C., et al., *The global cropland-sparing potential of high-yield farming.* Nature Sustainability, 2020. **3**(4): p. 281-289.
125. Silver, M., *IMF Applications of Purchasing Power Parity Estimates*. 2010, International Monetary Fund: Washington DC.
126. Kanter, D.R., et al., *A framework for nitrogen futures in the shared socioeconomic pathways.* Global Environmental Change, 2020. **61**: p. 102029.
127. Lord, S., *Valuing the impact of food: Towards practical and comparable monetary valuation of food system impacts*. 2020: Oxford. p. 224.
128. Elser, J.J., et al., *Global analysis of nitrogen and phosphorus limitation of primary producers in freshwater, marine and terrestrial ecosystems.* Ecology Letters, 2007. **10**(12): p. 1135-1142.
129. Harpole, W.S., et al., *Nutrient co-limitation of primary producer communities.* Ecology Letters, 2011. **14**(9): p. 852-862.
130. Cardinale, B.J., et al., *Biodiversity loss and its impact on humanity.* Nature, 2012. **486**(7401): p. 59-67.
131. Behera, S.N. and M. Sharma, *Investigating the potential role of ammonia in ion chemistry of fine particulate matter formation for an urban environment.* Science of The Total Environment, 2010. **408**(17): p. 3569-3575.
132. Wang, S., et al., *Atmospheric ammonia and its impacts on regional air quality over the megacity of Shanghai, China.* Scientific Reports, 2015. **5**(1): p. 15842.
133. Plautz, J., *Piercing the haze.* Science, 2018. **361**(6407): p. 1060.
134. Wu, S., et al., *Effects of 2000–2050 global change on ozone air quality in the United States.* Journal of Geophysical Research: Atmospheres, 2008. **113**(D6).
135. Milchunas, D.G., et al., *Factors influencing ammonia volatilization from urea in soils of the shortgrass steppe.* Journal of Atmospheric Chemistry, 1988. **6**(4): p. 323-340.
136. McGarry, S.J., P. O'Toole, and M.A. Morgan, *Effects of Soil Temperature and Moisture Content on Ammonia Volatilization from Urea-Treated Pasture and Tillage Soils.* Irish Journal of Agricultural Research, 1987. **26**(2/3): p. 173-182.
137. Altieri, A.H. and K.B. Gedan, *Climate change and dead zones.* Global Change Biology, 2015. **21**(4): p. 1395-1406.
138. Rabalais, N.N., et al., *Global change and eutrophication of coastal waters.* ICES Journal of Marine Science, 2009. **66**(7): p. 1528-1537.
139. Erisman, J.W., et al., *Reactive nitrogen in the environment and its effect on climate change.* Current Opinion in Environmental Sustainability, 2011. **3**(5): p. 281-290.
140. Skjøth, C.A. and C. Geels, *The effect of climate and climate change on ammonia emissions in Europe.* Atmos. Chem. Phys., 2013. **13**(1): p. 117-128.
141. Lu, X., et al., *Nitrogen deposition accelerates soil carbon sequestration in tropical forests.* Proceedings of the National Academy of Sciences, 2021. **118**(16): p. e2020790118.
142. Aber, J., et al., *Nitrogen Saturation in Temperate Forest Ecosystems: Hypotheses revisited.* BioScience, 1998. **48**(11): p. 921-934.
143. Reid, J.P., et al., *Biodiversity, Nitrogen Deposition, and CO_2 Affect Grassland Soil Carbon Cycling but not Storage.* Ecosystems, 2012. **15**(4): p. 580-590.
144. Chang, J., et al., *Climate warming from managed grasslands cancels the cooling effect of carbon sinks in sparsely grazed and natural grasslands.* Nature Communications, 2021. **12**(1): p. 118.
145. Conant, R.T., et al., *Nitrogen pools and fluxes in grassland soils sequestering carbon.* Nutrient Cycling in Agroecosystems, 2005. **71**(3): p. 239-248.
146. McMichael, A.J., R.E. Woodruff, and S. Hales, *Climate change and human health: present and future risks.* The Lancet, 2006. **367**(9513): p. 859-869.

147. Watson, L., et al., *Global ecosystem service values in climate class transitions.* Environmental Research Letters, 2020. **15**(2): p. 024008.
148. Irby, I.D., et al., *The competing impacts of climate change and nutrient reductions on dissolved oxygen in Chesapeake Bay.* Biogeosciences, 2018. **15**(9): p. 2649-2668.
149. Beman, J.M., et al., *Global declines in oceanic nitrification rates as a consequence of ocean acidification.* Proceedings of the National Academy of Sciences, 2011. **108**(1): p. 208.
150. Rees, A.P., et al., *The inhibition of N2O production by ocean acidification in cold temperate and polar waters.* Deep Sea Research Part II: Topical Studies in Oceanography, 2016. **127**: p. 93-101.
151. Breider, F., et al., *Response of N2O production rate to ocean acidification in the western North Pacific.* Nature Climate Change, 2019. **9**(12): p. 954-958.
152. Codispoti, L.A., *Interesting Times for Marine N_2O.* Science (American Association for the Advancement of Science), 2010. **327**(5971): p. 1339-1340.
153. Fann, N.L., et al., *Associations Between Simulated Future Changes in Climate, Air Quality, and Human Health.* JAMA Network Open, 2021. **4**(1): p. e2032064-e2032064.
154. Suddick, E.C., et al., *The role of nitrogen in climate change and the impacts of nitrogen–climate interactions in the United States: foreword to thematic issue.* Biogeochemistry, 2013. **114**(1): p. 1-10.
155. Morello-Frosch, R., et al., *Understanding The Cumulative Impacts Of Inequalities In Environmental Health: Implications For Policy.* Health Affairs, 2011. **30**(5): p. 879-887.
156. Tai, A.P.K., et al., *Impacts of Surface Ozone Pollution on Global Crop Yields: Comparing Different Ozone Exposure Metrics and Incorporating Co-effects of CO2.* Frontiers in Sustainable Food Systems, 2021. **5**(63).
157. Lepeule, J., et al., *Chronic Exposure to Fine Particles and Mortality: An Extended Follow-up of the Harvard Six Cities Study from 1974 to 2009.* Environmental Health Perspectives, 2012. **120**(7): p. 965-970.
158. Afshin, A., et al., *Health effects of dietary risks in 195 countries, 1990–2017: a systematic analysis for the Global Burden of Disease Study 2017.* The Lancet, 2019. **393**(10184): p. 1958-1972.
159. Davis, J., et al., *Generic strategy LCA and LCC : Guidance for LCA and LCC focused on prevention, valorisation and treatment of side flows from the food supply chain*, in *SP Rapport*. 2017. p. 111.
160. Rosengren, A., et al., *Socioeconomic status and risk of cardiovascular disease in 20 low-income, middle-income, and high-income countries: the Prospective Urban Rural Epidemiologic (PURE) study.* The Lancet Global Health, 2019. **7**(6): p. e748-e760.
161. Abdalla, S.M., S. Yu, and S. Galea, *Trends in Cardiovascular Disease Prevalence by Income Level in the United States.* JAMA Network Open, 2020. **3**(9): p. e2018150-e2018150.
162. Cervantes-Godoy, D. and J. Dewbre, *Economic Importance of Agriculture for Poverty Reduction*, in *OECD Food, Agriculture and Fisheries Papers*. 2010, OECD Publishing: Paris.
163. Sánchez, P.A., *Tripling crop yields in tropical Africa.* Nature Geoscience, 2010. **3**(5): p. 299-300.
164. Ladha, J.K., et al., *Chapter Two - Achieving the sustainable development goals in agriculture: The crucial role of nitrogen in cereal-based systems*, in *Advances in Agronomy*, D.L. Sparks, Editor. 2020, Academic Press. p. 39-116.
165. Day, J.W., Jr., et al., *Ecology in Times of Scarcity.* BioScience, 2009. **59**(4): p. 321-331.
166. Miranda, M.L., et al., *Making the Environmental Justice Grade: The Relative Burden of Air Pollution Exposure in the United States.* International Journal of Environmental Research and Public Health, 2011. **8**(6).
167. Hajat, A., C. Hsia, and M.S. O'Neill, *Socioeconomic Disparities and Air Pollution Exposure: a Global Review.* Current Environmental Health Reports, 2015. **2**(4): p. 440-450.

168. Morello-Frosch, R. and M. Jesdale Bill, *Separate and Unequal: Residential Segregation and Estimated Cancer Risks Associated with Ambient Air Toxics in U.S. Metropolitan Areas.* Environmental Health Perspectives, 2006. **114**(3): p. 386-393.
169. Lipfert, F.W., *Air pollution and poverty: Does the sword cut both ways?* Journal of Epidemiology and Community Health, 2004. **58**(1): p. 2.
170. Talbert, A., et al., *Diarrhoea Complicating Severe Acute Malnutrition in Kenyan Children: A Prospective Descriptive Study of Risk Factors and Outcome.* PLOS ONE, 2012. **7**(6): p. e38321.
171. Lindgren, E. and T. Elmqvist, *Ecosystem Services and Human Health*. 2017, Oxford University Press.
172. Prüss-Ustün, A., et al., *Burden of disease from inadequate water, sanitation and hygiene for selected adverse health outcomes: An updated analysis with a focus on low- and middle-income countries.* International Journal of Hygiene and Environmental Health, 2019. **222**(5): p. 765-777.
173. Miller, C.N. and S. Rayalam, *The role of micronutrients in the response to ambient air pollutants: Potential mechanisms and suggestions for research design.* Journal of toxicology and environmental health. Part B, Critical reviews, 2017. **20**(1): p. 38-53.
174. Sanchez, P.A. and M.S. Swaminathan, *Hunger in Africa: the link between unhealthy people and unhealthy soils.* The Lancet, 2005. **365**(9457): p. 442-444.

4.10 Appendix

4.10.1 Tables of results

Caveats from the main text: attribution of human and ecosystem damage from the nitrogen cascade of NH3 or NOx emitted to air from agricultural activities, or reactive nitrogen leached to groundwater or entering surface waters as run-off, come from a limited set of studies. Most marginal estimates are based on calculations for the EU nitrogen assessment. Transfer to other countries involves approximation of modification terms to exposure and ecosystem damages, with a large amount of uncertainty.

Large variation is due to primary factors (such as population density) and the nitrogen cascade, where the "fate" of emitted nitrogen varies greatly between countries. Spatial datasets based on modelling show large variation, for example, between nitrogen retained in inland water systems and export to coastal systems. Large uncertainties remain on the run-off from deposition, exposure to nitrate in surface drinking water, and differences in concentrations between surface water and ground water.

The largest variance between countries is in the estimate of the marginal damage cost of Nr surface run-off. This is due to order of magnitude uncertainty in the estimation of the value of coastal ecosystems. Where a country has a high proportion of riverine export of Nr to coastal systems, the valuations in the ESVD database (see Annex A – Land) for many countries has much higher values for coral reefs and coastal systems than retention in inland wetlands than the EU. Those estimates also have the greater uncertainty, introducing distinctly longer tails for Nr surface run-off than the estimates of NH3 and NOx air emissions.

The values in Table 6 and their uncertainty Table 7 were determined using basic relationships and broad assumptions for transport of figures from the EU nitrogen assessment to other countries. Transboundary effects of run-off and deposition for smaller countries within proximity to large nitrogen emitters may be large. Detailed spatial modelling of the fate of nitrogen, and the connection to surrounding socio-economic systems is recommended to improve the estimates and reduce uncertainty, though, even with this modelling, attribution between services lost and the load of nitrogen to human and natural systems is still a challenge.

Some mean values for health damages from NH3 and NOx are lower than other studies based on value of a statistical life – part of this arises from lower population density compared to the EU and the requirement to obtain an average marginal damage cost to be used at a country level. Despite having lower mean values, the uncertainty represented in Table 7 spans an order of magnitude. It is not recommended to use the mean values in Table 6 separate from the uncertainty estimates in Table 7 .

Table 6: Valuation of 171 countries based on country level adjustment to economic costs from human and natural capital impacts, the fate of emitted nitrogen, and exposure. Measured in US$2020 purchasing power parity (international dollars) per kg (N-weight). It is not recommended to use the mean values in this table separate from the uncertainty estimates in ***Error! Reference source not found.****. The column of values (bold) provide the mean of the log-normal distributed value in U S$2020 PPP, per kg of Nr leached to groundwater for $MDC_{i,grdw,Nr}$, per kg of Nr run-off to surface water for $MDC_{i,surw,Nr}$, per kg of NH3 emission to air for $MDC_{i,a,NH3}$, and per kg of NOx emission to air for $MDC_{i,a,NOx}$. Estimates for low emission countries in proximity to large emitting neighbours may be unreliable due to transboundary effects (Table 10).*

Country	ISO3166 -1	UN M49	HDI	MDC Nr leached US$2020 PPP per kg	MDC Nr run-off US$2020 PPP per kg	MDC NH3 air US$2020 PPP per kg	MDC NOx air US$2020 PPP per kg
Afghanistan	AFG	4	0.511	**0.15**	**1.56**	**5.35**	**10.02**
Angola	AGO	24	0.581	**0.43**	**7.13**	**5.16**	**10.23**
Albania	ALB	8	0.795	**0.78**	**1.27**	**7.67**	**15.92**
United Arab Emirates	ARE	784	0.89	**3.84**	**53.18**	**14.21**	**32.17**
Argentina	ARG	32	0.845	**0.78**	**5.34**	**3.51**	**9.57**
Armenia	ARM	51	0.776	**0.79**	**3.35**	**8.33**	**17.17**
Australia	AUS	36	0.944	**3.86**	**25.32**	**5.5**	**15.06**
Austria	AUT	40	0.922	**3.87**	**1.2**	**24.88**	**46.7**
Azerbaijan	AZE	31	0.756	**0.79**	**1.14**	**8.09**	**16.39**
Burundi	BDI	108	0.433	**0.15**	**0.38**	**3.93**	**8.46**
Belgium	BEL	56	0.931	**3.8**	**22.93**	**25.27**	**53.68**
Benin	BEN	204	0.545	**0.46**	**7.34**	**8.93**	**15.37**
Burkina Faso	BFA	854	0.452	**0.15**	**6**	**1.37**	**6.16**
Bangladesh	BGD	50	0.632	**0.42**	**84.17**	**14.88**	**25.45**
Bulgaria	BGR	100	0.816	**0.79**	**4.02**	**7.48**	**14.63**
Bahamas, The	BHS	44	0.814	**3.84**	**96.67**	**28.29**	**37.43**
Bosnia and Herzegovina	BIH	70	0.78	**0.78**	**1.76**	**21.26**	**28.04**
Belarus	BLR	112	0.823	**0.79**	**4.17**	**2.91**	**10.57**
Belize	BLZ	84	0.716	**0.42**	**130.15**	**31.64**	**36.22**
Bolivia	BOL	68	0.718	**0.42**	**17.28**	**9.72**	**15.79**
Brazil	BRA	76	0.765	**0.78**	**115.49**	**17.54**	**23.66**
Brunei Darussalam	BRN	96	0.838	**3.81**	**150.47**	**37.02**	**53.63**
Bhutan	BTN	64	0.654	**0.42**	**5.76**	**13.04**	**19.11**
Botswana	BWA	72	0.735	**0.78**	**37.2**	**8.37**	**13.97**
Central African Republic	CAF	140	0.397	**0.15**	**0.87**	**14.68**	**18.87**
Canada	CAN	124	0.929	**3.82**	**6.39**	**9.46**	**19.64**
Switzerland	CHE	756	0.955	**3.85**	**1.31**	**27.88**	**53.06**
Chile	CHL	152	0.851	**3.87**	**8.23**	**8.12**	**23.14**
China	CHN	156	0.761	**0.79**	**97.89**	**6.68**	**14.42**
Cote d'Ivoire	CIV	384	0.538	**0.46**	**7.65**	**16.59**	**24.37**
Cameroon	CMR	120	0.563	**0.42**	**7.25**	**9.66**	**15.58**

Congo, Dem. Rep.	COD	180	0.48	**0.15**	**6.81**	**8.16**	**13.23**
Congo, Rep.	COG	178	0.574	**0.46**	**7.2**	**2.99**	**9.03**
Colombia	COL	170	0.767	**0.79**	**120.34**	**21.67**	**30.72**
Comoros	COM	174	0.554	**0.46**	**5.59**	**26.5**	**23.79**
Cabo Verde	CPV	132	0.665	**0.47**	**0.41**	**9.1**	**12.34**
Costa Rica	CRI	188	0.81	**0.78**	**117.19**	**8.38**	**19.04**
Cuba	CUB	192	0.783	**0.79**	**100.2**	**9.59**	**18.28**
Cyprus	CYP	196	0.887	**3.84**	**0.67**	**45.99**	**57.53**
Czech Republic	CZE	203	0.9	**3.81**	**2.53**	**21.26**	**43.01**
Germany	DEU	276	0.947	**3.8**	**21.87**	**15.32**	**39.92**
Djibouti	DJI	262	0.524	**0.47**	**7.16**	**5.02**	**9.43**
Denmark	DNK	208	0.94	**3.8**	**21.5**	**22.25**	**48.02**
Dominican Republic	DOM	214	0.756	**0.79**	**115.76**	**8.87**	**19.88**
Algeria	DZA	12	0.748	**0.42**	**50.03**	**6.55**	**11.63**
Ecuador	ECU	218	0.759	**0.79**	**111.21**	**17.24**	**25.93**
Egypt, Arab Rep.	EGY	818	0.707	**0.42**	**48.04**	**3.6**	**9.93**
Eritrea	ERI	232	0.459	**0.15**	**7.07**	**9.36**	**13.57**
Spain	ESP	724	0.904	**3.85**	**21.48**	**9.88**	**30.02**
Estonia	EST	233	0.892	**3.84**	**21.26**	**29.23**	**46.9**
Ethiopia	ETH	231	0.485	**0.16**	**2.15**	**6.68**	**11.36**
Finland	FIN	246	0.938	**3.8**	**4.74**	**16.27**	**31.05**
Fiji	FJI	242	0.743	**0.79**	**134.74**	**8.19**	**16.66**
France	FRA	250	0.901	**3.83**	**17.91**	**11.79**	**34**
Gabon	GAB	266	0.703	**0.78**	**112.87**	**17.75**	**23.68**
United Kingdom	GBR	826	0.932	**3.86**	**20.17**	**15.08**	**40.84**
Georgia	GEO	268	0.812	**0.79**	**0.65**	**14.82**	**22.51**
Ghana	GHA	288	0.611	**0.42**	**7.45**	**13.68**	**20.29**
Guinea	GIN	324	0.477	**0.15**	**6.57**	**8.9**	**15.88**
Gambia, The	GMB	270	0.496	**0.15**	**7.22**	**3.95**	**8.58**
Guinea-Bissau	GNB	624	0.48	**0.15**	**6.71**	**2.25**	**8.63**
Equatorial Guinea	GNQ	226	0.592	**0.79**	**7.51**	**24.18**	**28.37**
Greece	GRC	300	0.888	**3.81**	**42.43**	**16.1**	**35.34**
Guatemala	GTM	320	0.663	**0.78**	**119.08**	**9**	**17.46**
Guyana	GUY	328	0.682	**0.79**	**87.27**	**17.93**	**26.28**
Honduras	HND	340	0.634	**0.46**	**97.11**	**19.5**	**25.35**
Croatia	HRV	191	0.851	**3.84**	**1.02**	**25.07**	**44.8**
Haiti	HTI	332	0.51	**0.46**	**7.09**	**6.22**	**13.7**
Hungary	HUN	348	0.854	**3.83**	**1.86**	**19.01**	**40.6**
Indonesia	IDN	360	0.718	**0.42**	**107.19**	**6.53**	**14.19**
India	IND	356	0.645	**0.42**	**88.43**	**6.59**	**14.48**
Ireland	IRL	372	0.955	**3.84**	**21.14**	**18.28**	**39.55**

Iran, Islamic Rep.	IRN	364	0.783	**0.71**	**85.15**	**4.33**	**10.52**
Iraq	IRQ	368	0.674	**0.78**	**65.66**	**4.5**	**11.77**
Iceland	ISL	352	0.949	**3.84**	**36.01**	**29.02**	**38.85**
Israel	ISR	376	0.919	**3.89**	**16.48**	**29.29**	**53.09**
Italy	ITA	380	0.892	**3.83**	**21.81**	**13.22**	**37.77**
Jamaica	JAM	388	0.734	**0.78**	**122.44**	**10.99**	**17.45**
Jordan	JOR	400	0.729	**0.79**	**67.82**	**9.87**	**16.29**
Japan	JPN	392	0.919	**3.83**	**33.03**	**13.25**	**40.35**
Kazakhstan	KAZ	398	0.825	**0.79**	**7.18**	**4.35**	**10.07**
Kenya	KEN	404	0.601	**0.47**	**7.26**	**6.65**	**12.76**
Kyrgyz Republic	KGZ	417	0.697	**0.42**	**0.5**	**8.57**	**13.84**
Cambodia	KHM	116	0.594	**0.46**	**6.92**	**11.28**	**19.97**
Korea, Rep.	KOR	410	0.916	**3.83**	**41.97**	**17.77**	**46.23**
Kuwait	KWT	414	0.806	**3.84**	**40.26**	**30.26**	**45.7**
Lao PDR	LAO	418	0.613	**0.42**	**0.44**	**17.91**	**25.41**
Lebanon	LBN	422	0.744	**0.79**	**0.3**	**12.6**	**20.57**
Liberia	LBR	430	0.48	**0.15**	**7.19**	**14.18**	**21.09**
Libya	LBY	434	0.724	**0.79**	**72.89**	**7.33**	**12.68**
Sri Lanka	LKA	144	0.782	**0.42**	**91.64**	**6.88**	**15.77**
Lesotho	LSO	426	0.527	**0.46**	**0.85**	**8.63**	**13.83**
Lithuania	LTU	440	0.882	**3.79**	**43.45**	**18.11**	**38.2**
Luxembourg	LUX	442	0.916	**3.83**	**0.16**	**43.15**	**64.34**
Latvia	LVA	428	0.866	**3.78**	**2.22**	**16.26**	**35.07**
Morocco	MAR	504	0.686	**0.42**	**72.41**	**5.43**	**11.21**
Moldova	MDA	498	0.75	**0.8**	**105.42**	**28.76**	**36.95**
Madagascar	MDG	450	0.528	**0.15**	**6.72**	**8.76**	**15.56**
Mexico	MEX	484	0.779	**0.79**	**83.31**	**6.32**	**13.15**
North Macedonia	MKD	807	0.774	**0.79**	**5.9**	**22.21**	**28.28**
Mali	MLI	466	0.434	**0.15**	**6.47**	**1.29**	**6.48**
Myanmar	MMR	104	0.583	**0.42**	**7.03**	**10.95**	**19.62**
Montenegro	MNE	499	0.829	**0.79**	**5.72**	**9.95**	**15.44**
Mongolia	MNG	496	0.737	**0.42**	**18.38**	**10.26**	**15.06**
Mozambique	MOZ	508	0.456	**0.15**	**6.9**	**6.38**	**10.67**
Mauritania	MRT	478	0.546	**0.42**	**9.04**	**2.01**	**8.84**
Malawi	MWI	454	0.483	**0.15**	**1.05**	**3.76**	**8.01**
Malaysia	MYS	458	0.81	**0.79**	**113.78**	**6.21**	**16.43**
Namibia	NAM	516	0.646	**0.79**	**54.63**	**8.69**	**14.75**
New Caledonia	NCL	540	0.813	**3.81**	**1.1**	**20.9**	**29.29**
Niger	NER	562	0.394	**0.15**	**7.64**	**4.5**	**9.55**
Nigeria	NGA	566	0.539	**0.42**	**7.21**	**4.76**	**12.06**
Nicaragua	NIC	558	0.66	**0.43**	**84.74**	**14.8**	**21.61**
Netherlands	NLD	528	0.944	**3.84**	**20.55**	**26.48**	**57.57**
Norway	NOR	578	0.957	**3.84**	**34.39**	**10.51**	**25.1**

Nepal	NPL	524	0.602	**0.47**	**0.48**	**12.91**	**21.21**
New Zealand	NZL	554	0.931	**3.83**	**27**	**9.08**	**25.66**
Oman	OMN	512	0.813	**3.85**	**75.35**	**17.23**	**30.74**
Pakistan	PAK	586	0.557	**0.46**	**7.37**	**3.37**	**10.88**
Panama	PAN	591	0.815	**0.79**	**117.76**	**15.26**	**23.99**
Peru	PER	604	0.777	**0.79**	**110.44**	**21.1**	**29.76**
Philippines	PHL	608	0.718	**0.43**	**114.82**	**6.86**	**15.34**
Papua New Guinea	PNG	598	0.555	**0.43**	**7.03**	**10.49**	**15.45**
Poland	POL	616	0.88	**3.84**	**4.16**	**15.65**	**36.68**
Puerto Rico	PRI	630	0.845	**3.82**	**1.79**	**88.01**	**97.4**
Korea, Dem. People's Rep.	PRK	408	0.733	**0.15**	**109.05**	**14.76**	**20.32**
Portugal	PRT	620	0.864	**3.83**	**40.6**	**18.46**	**39.82**
Paraguay	PRY	600	0.728	**0.79**	**8.1**	**6.28**	**13.4**
West Bank and Gaza	PSE	275	0.708	**0.42**	**0.17**	**15.72**	**18.79**
Qatar	QAT	634	0.848	**3.85**	**54.61**	**26.38**	**47.58**
Romania	ROU	642	0.828	**0.79**	**42.99**	**8.79**	**16.65**
Russian Federation	RUS	643	0.824	**0.78**	**102.03**	**15.61**	**21.18**
Rwanda	RWA	646	0.543	**0.15**	**1.3**	**6.76**	**11.25**
Saudi Arabia	SAU	682	0.854	**3.83**	**46.88**	**4.9**	**16.51**
Sudan	SDN	729	0.51	**0.15**	**8.16**	**2.87**	**7.29**
Senegal	SEN	686	0.512	**0.47**	**8.14**	**7**	**14.4**
Solomon Islands	SLB	90	0.567	**0.46**	**6.04**	**8.1**	**13.72**
Sierra Leone	SLE	694	0.452	**0.15**	**7**	**16.25**	**22.95**
El Salvador	SLV	222	0.673	**0.42**	**62.32**	**7.11**	**12.76**
Somalia	SOM	706	0.285	**0.15**	**7.91**	**5.54**	**9.65**
Serbia	SRB	688	0.806	**0.79**	**2.79**	**11.24**	**18.85**
South Sudan	SSD	728	0.433	**0.15**	**2.03**	**4.71**	**8.7**
Suriname	SUR	740	0.738	**0.8**	**88.25**	**21.29**	**29.28**
Slovak Republic	SVK	703	0.86	**3.81**	**1.79**	**23.83**	**44.15**
Slovenia	SVN	705	0.917	**3.86**	**0.62**	**30.71**	**49.63**
Sweden	SWE	752	0.945	**3.87**	**2.92**	**19.47**	**35.33**
Eswatini	SWZ	748	0.611	**0.42**	**0.69**	**5.24**	**9.88**
Syrian Arab Republic	SYR	760	0.567	**0.15**	**2.87**	**2.07**	**6.29**
Chad	TCD	148	0.398	**0.15**	**6.51**	**4.89**	**9.77**
Togo	TGO	768	0.515	**0.15**	**1.14**	**14.28**	**18.89**
Thailand	THA	764	0.777	**0.78**	**95.38**	**11.09**	**21.46**
Tajikistan	TJK	762	0.668	**0.42**	**0.93**	**6.59**	**12.89**
Turkmenistan	TKM	795	0.715	**0.79**	**21**	**4.57**	**11.56**
Timor-Leste	TLS	626	0.606	**0.42**	**7.39**	**8.68**	**13.41**
Trinidad and Tobago	TTO	780	0.796	**3.81**	**148.42**	**38.02**	**61.05**

Tunisia	TUN	788	0.74	**0.47**	**83.14**	**5.36**	**11.31**
Turkey	TUR	792	0.82	**0.78**	**107.26**	**8.74**	**16.71**
Tanzania	TZA	834	0.529	**0.46**	**7.01**	**6.62**	**13.29**
Uganda	UGA	800	0.544	**0.15**	**2.81**	**9.03**	**13.68**
Ukraine	UKR	804	0.779	**0.43**	**86.18**	**7.33**	**12.9**
Uruguay	URY	858	0.817	**3.84**	**1.65**	**13.46**	**30.75**
United States	USA	840	0.926	**3.78**	**28.85**	**4.88**	**17.72**
Uzbekistan	UZB	860	0.72	**0.42**	**14.17**	**3.66**	**10.09**
St. Vincent and the Grenadines	VCT	670	0.738	**0.78**	**125.33**	**37.54**	**28.2**
Venezuela, RB	VEN	862	0.711	**0.42**	**80.49**	**13.76**	**19.59**
Vietnam	VNM	704	0.704	**0.43**	**107.51**	**8.29**	**17.27**
Vanuatu	VUT	548	0.609	**0.46**	**5.9**	**8.29**	**11.16**
Yemen, Rep.	YEM	887	0.47	**0.15**	**7.68**	**1.4**	**5.73**
South Africa	ZAF	710	0.709	**0.8**	**90.02**	**3.47**	**9.82**
Zambia	ZMB	894	0.584	**0.42**	**1.06**	**7.16**	**12.22**
Zimbabwe	ZWE	716	0.571	**0.46**	**2.81**	**3.81**	**9.21**

Table 7: Shape of uncertainty in the valuation of 171 countries based on country level adjustment to economic costs from human and natural capital impacts, the fate of emitted nitrogen, and exposure. Measured in US$2020 purchasing power parity (international dollars) per kg (N-weight). The parameters mu and sigma refer to the lognormal fit of marginal damage costs (MDC) as an uncertain value: log(MDC)~N(mu,sigma), for Nr leached to groundwater for $MDC_{i,grdw,Nr}$*, Nr run-off to surface water for* $MDC_{i,surw,Nr}$*, NH3 emission to air for* $MDC_{i,a,NH3}$*, and NOx emission to air for* $MDC_{i,a,NOx}$*.*

Country	ISO 3166-1	MDC Nr leached	MDC Nr run-off	MDC NH3 air	MDC NOx air	MDC Nr leached	MDC Nr run-off	MDC NH3 air	MDC NOx air
		mu				sigma			
Afghanistan	AFG	-2.184	-0.92	1.223	2.165	1.006	1.517	0.879	0.461
Angola	AGO	-1.157	0.885	1.161	2.179	1	1.379	0.847	0.445
Albania	ALB	-0.554	-1.175	1.769	2.701	0.998	1.509	0.731	0.359
United Arab Emirates	ARE	1.043	2.815	2.397	3.389	0.988	1.295	0.714	0.401
Argentina	ARG	-0.566	0.491	0.889	2.179	1.027	1.332	0.763	0.357
Armenia	ARM	-0.545	-0.231	1.867	2.776	0.997	1.5	0.706	0.359
Australia	AUS	1.052	2.262	1.409	2.637	0.992	1.201	0.706	0.361
Austria	AUT	1.055	-0.524	3.027	3.77	0.978	1.087	0.61	0.381
Azerbaijan	AZE	-0.549	-1.11	1.826	2.718	0.986	1.362	0.69	0.367
Burundi	BDI	-2.192	-2.398	1.109	2.1	0.991	1.561	0.719	0.264
Belgium	BEL	1.023	1.539	2.972	3.898	1.017	1.874	0.714	0.411
Benin	BEN	-1.087	0.757	1.62	2.522	1.021	1.476	0.904	0.515
Burkina Faso	BFA	-2.202	0.408	-0.029	1.776	1.021	1.538	0.759	0.268
Bangladesh	BGD	-1.19	2.226	2.04	2.99	1.007	1.997	0.938	0.534
Bulgaria	BGR	-0.553	0.413	1.808	2.625	1.007	1.295	0.64	0.334
Bahamas, The	BHS	1.04	3.106	3.094	3.54	0.997	1.499	0.705	0.401

Bosnia and Herzegovina	BIH	-0.552	-0.884	2.734	3.156	0.996	1.518	0.764	0.543
Belarus	BLR	-0.55	0.188	0.816	2.307	1.013	1.325	0.709	0.317
Belize	BLZ	-1.175	2.789	2.526	2.951	1.019	2.017	1.132	0.858
Bolivia	BOL	-1.174	0.44	1.396	2.425	0.997	1.646	1.062	0.585
Brazil	BRA	-0.556	2.65	1.803	2.644	1.016	1.881	1.214	0.752
Brunei Darussalam	BRN	1.03	2.877	3.352	3.904	0.989	2.002	0.715	0.393
Bhutan	BTN	-1.158	-0.465	2.22	2.792	0.974	1.698	0.769	0.489
Botswana	BWA	-0.564	1.678	1.518	2.401	1.019	1.593	0.911	0.53
Central African Republic	CAF	-2.185	-1.508	1.302	2.265	1.012	1.517	1.426	0.853
Canada	CAN	1.029	0.865	1.892	2.87	1.007	1.172	0.797	0.433
Switzerland	CHE	1.043	-0.796	3.064	3.885	0.99	1.175	0.727	0.413
Chile	CHL	1.047	1.018	1.88	3.074	1.008	1.241	0.648	0.365
China	CHN	-0.532	2.76	1.29	2.5	0.98	1.729	0.904	0.45
Cote d'Ivoire	CIV	-1.09	0.904	1.971	2.818	1.027	1.406	1.056	0.648
Cameroon	CMR	-1.174	0.779	1.714	2.519	0.991	1.456	0.894	0.54
Congo, Dem. Rep.	COD	-2.188	0.716	1.395	2.32	1	1.503	1.045	0.585
Congo, Rep.	COG	-1.097	0.754	0.757	2.14	1.032	1.479	0.75	0.318
Colombia	COL	-0.556	2.99	2.218	3.021	1.015	1.801	1.085	0.676
Comoros	COM	-1.079	0.362	3.014	3.109	0.997	1.661	0.726	0.342
Cabo Verde	CPV	-1.08	-1.213	1.946	2.457	1.007	1.01	0.724	0.331
Costa Rica	CRI	-0.546	2.859	1.831	2.881	0.977	1.774	0.728	0.335
Cuba	CUB	-0.544	2.939	1.884	2.784	1	1.635	0.761	0.41
Cyprus	CYP	1.037	-1.154	3.576	3.966	1.004	1.125	0.709	0.411
Czech Republic	CZE	1.028	0.263	2.865	3.689	1	1.059	0.615	0.379
Germany	DEU	1.018	1.798	2.543	3.616	1.024	1.605	0.606	0.373
Djibouti	DJI	-1.076	1.101	1.357	2.197	1.009	1.226	0.711	0.302
Denmark	DNK	1.031	1.802	2.907	3.796	0.99	1.598	0.62	0.387
Dominican Republic	DOM	-0.542	3.111	1.891	2.918	0.975	1.645	0.719	0.347
Algeria	DZA	-1.157	2.343	1.245	2.231	0.982	1.597	0.934	0.516
Ecuador	ECU	-0.541	2.771	2.114	2.923	0.995	1.846	0.979	0.613
Egypt, Arab Rep.	EGY	-1.163	2.461	0.888	2.212	0.993	1.493	0.762	0.348
Eritrea	ERI	-2.189	1.084	1.517	2.269	1.011	1.281	0.974	0.613
Spain	ESP	1.04	2.041	2.076	3.329	1.01	1.409	0.649	0.377
Estonia	EST	1.038	1.827	3.201	3.773	1.001	1.554	0.593	0.385
Ethiopia	ETH	-2.162	-0.653	1.065	2.141	0.988	1.537	1.078	0.577
Finland	FIN	1.028	0.755	2.598	3.36	0.996	1.169	0.615	0.385
Fiji	FJI	-0.545	2.908	1.844	2.767	1.001	1.93	0.718	0.301
France	FRA	1.04	1.867	2.274	3.457	0.989	1.428	0.619	0.37
Gabon	GAB	-0.557	2.264	1.889	2.633	1.006	1.988	1.034	0.683
United Kingdom	GBR	1.042	1.843	2.503	3.631	1.009	1.523	0.644	0.392

Georgia	GEO	-0.544	-1.603	2.424	2.996	0.987	1.344	0.717	0.457
Ghana	GHA	-1.165	0.965	1.854	2.664	0.999	1.369	0.993	0.614
Guinea	GIN	-2.209	0.675	1.406	2.508	1.042	1.488	1.037	0.545
Gambia, The	GMB	-2.2	0.614	1.12	2.118	1.011	1.568	0.705	0.252
Guinea-Bissau	GNB	-2.171	0.638	0.576	2.128	1.002	1.548	0.672	0.234
Equatorial Guinea	GNQ	-0.544	0.798	2.763	3.097	1.005	1.473	0.827	0.579
Greece	GRC	1.031	2.67	2.549	3.49	0.989	1.549	0.673	0.384
Guatemala	GTM	-0.557	2.234	1.825	2.732	1.01	1.977	0.748	0.415
Guyana	GUY	-0.547	2.251	2.084	2.91	1.006	2.018	1.059	0.65
Honduras	HND	-1.08	2.834	2.087	2.75	1.005	1.71	1.095	0.734
Croatia	HRV	1.04	-1.092	3.007	3.721	0.999	1.251	0.652	0.4
Haiti	HTI	-1.082	0.961	1.559	2.566	1.005	1.352	0.727	0.317
Hungary	HUN	1.039	-0.176	2.684	3.62	0.988	1.17	0.724	0.406
Indonesia	IDN	-1.173	2.751	1.126	2.457	1.002	1.808	0.987	0.474
India	IND	-1.169	2.718	1.186	2.488	1.004	1.712	0.946	0.457
Ireland	IRL	1.045	1.724	2.695	3.602	0.977	1.62	0.641	0.385
Iran, Islamic Rep.	IRN	-0.659	2.698	0.976	2.236	1.014	1.706	0.834	0.398
Iraq	IRQ	-0.551	2.485	1.179	2.387	0.985	1.622	0.714	0.347
Iceland	ISL	1.038	1.693	3.134	3.538	1.005	1.788	0.66	0.462
Israel	ISR	1.057	2.057	3.122	3.883	0.987	1.086	0.711	0.419
Italy	ITA	1.034	1.935	2.359	3.556	0.992	1.499	0.66	0.386
Jamaica	JAM	-0.565	2.823	2.13	2.791	1.015	1.85	0.727	0.365
Jordan	JOR	-0.554	2.739	1.999	2.691	1.013	1.544	0.712	0.397
Japan	JPN	1.039	1.922	2.366	3.626	0.994	1.526	0.654	0.374
Kazakhstan	KAZ	-0.558	0.775	1.058	2.207	1.02	1.342	0.809	0.395
Kenya	KEN	-1.076	1.123	1.404	2.381	0.993	1.241	0.82	0.452
Kyrgyz Republic	KGZ	-1.174	-1.92	1.811	2.496	1.002	1.363	0.773	0.46
Cambodia	KHM	-1.101	0.87	1.694	2.744	1.021	1.39	0.99	0.538
Korea, Rep.	KOR	1.021	1.746	2.626	3.758	1.05	1.768	0.701	0.381
Kuwait	KWT	1.044	2.391	3.152	3.736	0.983	1.294	0.716	0.412
Lao PDR	LAO	-1.17	-1.976	1.783	2.737	1.015	1.368	1.171	0.696
Lebanon	LBN	-0.53	-2.304	2.27	2.952	0.977	1.263	0.723	0.374
Liberia	LBR	-2.182	0.764	1.667	2.646	0.993	1.484	1.198	0.69
Libya	LBY	-0.554	2.375	1.061	2.19	1.023	1.552	0.933	0.487
Sri Lanka	LKA	-1.173	2.671	1.543	2.662	1.013	1.581	0.755	0.351
Lesotho	LSO	-1.08	-1.33	1.865	2.525	0.994	1.358	0.713	0.398
Lithuania	LTU	1.022	2.585	2.661	3.564	0.988	1.657	0.687	0.393
Luxembourg	LUX	1.035	-2.684	3.519	4.078	1.005	1.204	0.704	0.414
Latvia	LVA	1.012	-0.004	2.53	3.479	1.02	1.183	0.718	0.393
Morocco	MAR	-1.167	2.472	1.224	2.275	1.006	1.733	0.798	0.418
Moldova	MDA	-0.529	2.668	2.969	3.375	0.987	1.817	0.764	0.561
Madagascar	MDG	-2.206	0.909	1.31	2.458	1.02	1.354	1.054	0.549
Mexico	MEX	-0.547	2.919	1.252	2.401	0.997	1.578	0.904	0.476

North Macedonia	MKD	-0.545	0.316	2.864	3.216	1.013	1.538	0.668	0.471
Mali	MLI	-2.179	0.529	-0.247	1.815	0.984	1.516	0.855	0.292
Myanmar	MMR	-1.191	0.739	1.695	2.73	1.036	1.466	0.935	0.514
Montenegro	MNE	-0.552	0.256	2.045	2.67	1.016	1.534	0.706	0.355
Mongolia	MNG	-1.18	0.876	1.746	2.456	1.018	1.676	0.99	0.599
Mozambique	MOZ	-2.2	0.957	1.252	2.147	1.032	1.322	0.964	0.543
Mauritania	MRT	-1.172	1.207	0.318	2.132	1.01	1.271	0.781	0.281
Malawi	MWI	-2.188	-1.325	1.007	2	1.011	1.552	0.737	0.359
Malaysia	MYS	-0.549	2.956	1.388	2.702	0.996	1.802	0.8	0.374
Namibia	NAM	-0.544	2.383	1.281	2.367	0.991	1.596	1.022	0.565
New Caledonia	NCL	1.02	-0.752	2.778	3.299	1.024	1.092	0.725	0.391
Niger	NER	-2.179	0.649	0.871	2.099	0.996	1.531	0.99	0.464
Nigeria	NGA	-1.188	0.942	1.137	2.39	1.004	1.353	0.793	0.382
Nicaragua	NIC	-1.167	2.613	1.903	2.712	1.012	1.766	1.031	0.637
Netherlands	NLD	1.034	1.765	3.04	3.971	1.008	1.608	0.683	0.403
Norway	NOR	1.034	1.535	2.003	3.116	1.026	1.778	0.767	0.422
Nepal	NPL	-1.072	-1.899	2.146	2.89	1.001	1.361	0.8	0.478
New Zealand	NZL	1.039	1.974	1.984	3.172	0.994	1.461	0.658	0.377
Oman	OMN	1.052	2.846	2.442	3.258	0.974	1.458	0.756	0.476
Pakistan	PAK	-1.086	1.043	0.961	2.336	0.997	1.31	0.659	0.296
Panama	PAN	-0.558	3.019	2.146	2.935	1.018	1.78	0.893	0.532
Peru	PER	-0.552	2.548	2.142	2.966	1	1.976	1.11	0.692
Philippines	PHL	-1.155	2.957	1.409	2.595	0.997	1.746	0.865	0.426
Papua New Guinea	PNG	-1.167	0.865	1.714	2.438	1.005	1.407	0.91	0.574
Poland	POL	1.042	0.704	2.556	3.533	0.992	1.091	0.62	0.371
Puerto Rico	PRI	1.026	-0.549	4.222	4.488	1.02	1.267	0.712	0.425
Korea, Dem. People's Rep.	PRK	-2.181	2.069	2.133	2.724	1.009	2.179	0.913	0.603
Portugal	PRT	1.032	2.714	2.673	3.61	1.016	1.471	0.694	0.384
Paraguay	PRY	-0.551	0.16	1.401	2.468	1.001	1.596	0.813	0.423
West Bank and Gaza	PSE	-1.168	-3.049	2.493	2.867	1	1.381	0.723	0.359
Qatar	QAT	1.039	2.842	3.013	3.774	1.011	1.322	0.719	0.416
Romania	ROU	-0.532	2.537	1.951	2.738	0.979	1.699	0.666	0.376
Russian Federation	RUS	-0.566	2.524	1.96	2.655	1.013	1.92	1.083	0.69
Rwanda	RWA	-2.194	-1.12	1.567	2.3	1.009	1.544	0.744	0.412
Saudi Arabia	SAU	1.038	2.773	1.286	2.727	0.988	1.243	0.718	0.367
Sudan	SDN	-2.18	1.155	0.506	1.874	1.003	1.278	0.913	0.398
Senegal	SEN	-1.069	1.125	1.615	2.572	0.997	1.296	0.729	0.377
Solomon Islands	SLB	-1.08	0.654	1.843	2.582	1.005	1.462	0.705	0.269
Sierra Leone	SLE	-2.182	0.671	1.743	2.659	1.002	1.552	1.173	0.7
El Salvador	SLV	-1.174	2.072	1.7	2.479	1.014	1.844	0.704	0.349
Somalia	SOM	-2.179	1.149	1.009	2.02	0.99	1.264	0.978	0.533

Serbia	SRB	-0.538	-0.453	2.183	2.846	0.992	1.538	0.67	0.403
South Sudan	SSD	-2.19	-0.682	1.061	2.006	1.005	1.522	0.872	0.469
Suriname	SUR	-0.533	2.313	2.194	2.942	0.995	1.931	1.053	0.681
Slovak Republic	SVK	1.026	-0.218	2.918	3.704	1.007	1.162	0.709	0.405
Slovenia	SVN	1.045	-1.299	3.176	3.823	0.996	1.199	0.702	0.402
Sweden	SWE	1.049	0.361	2.757	3.481	1.001	1.085	0.647	0.402
Eswatini	SWZ	-1.181	-1.631	1.398	2.239	1.018	1.486	0.717	0.317
Syrian Arab Republic	SYR	-2.195	-0.342	0.42	1.79	1.032	1.537	0.731	0.292
Chad	TCD	-2.198	0.483	0.952	2.102	1.023	1.544	0.98	0.483
Togo	TGO	-2.197	-1.211	1.606	2.405	1.027	1.531	1.198	0.763
Thailand	THA	-0.564	2.739	1.712	2.854	1.017	1.784	0.984	0.513
Tajikistan	TJK	-1.183	-1.482	1.537	2.45	1.052	1.426	0.757	0.399
Turkmenistan	TKM	-0.536	1.145	1.066	2.338	0.99	1.601	0.801	0.386
Timor-Leste	TLS	-1.169	1.063	1.89	2.547	0.992	1.307	0.737	0.31
Trinidad and Tobago	TTO	1.025	2.965	3.372	4.024	1.002	1.906	0.729	0.416
Tunisia	TUN	-1.079	2.259	1.281	2.303	1.012	1.881	0.728	0.374
Turkey	TUR	-0.56	2.624	1.681	2.645	1.015	1.885	0.818	0.47
Tanzania	TZA	-1.077	1.053	1.51	2.473	0.988	1.275	0.787	0.417
Uganda	UGA	-2.175	-0.362	1.472	2.299	0.98	1.552	0.995	0.601
Ukraine	UKR	-1.157	2.622	1.478	2.37	0.984	1.761	0.862	0.491
Uruguay	URY	1.037	-0.64	2.357	3.346	1.003	1.246	0.673	0.382
United States	USA	1.005	2.203	1.337	2.807	1.037	1.306	0.658	0.355
Uzbekistan	UZB	-1.171	0.681	0.911	2.223	1.008	1.564	0.735	0.337
St. Vincent and the Grenadines	VCT	-0.566	2.722	3.356	3.259	1.018	2.092	0.73	0.396
Venezuela, RB	VEN	-1.177	2.651	1.718	2.56	1.019	1.775	1.127	0.691
Vietnam	VNM	-1.157	2.926	1.466	2.67	0.984	1.761	0.955	0.473
Vanuatu	VUT	-1.082	0.662	1.858	2.358	0.993	1.441	0.716	0.325
Yemen, Rep.	YEM	-2.201	1.11	0.059	1.711	1.031	1.304	0.715	0.257
South Africa	ZAF	-0.534	2.47	0.771	2.173	1.007	1.755	0.773	0.369
Zambia	ZMB	-1.171	-1.135	1.437	2.303	0.994	1.379	0.884	0.512
Zimbabwe	ZWE	-1.085	-0.232	1.027	2.145	1.011	1.449	0.724	0.352

Table 8: Comparisons of contribution of emission source (NH3 to air, NOx to air, Nr to surface waters, Nr to groundwater) to total damage costs from agricultural nitrogen pollution. Total damage costs obtained by multiplying against agricultural emissions for 2015 obtained from EDGAR5.0 (NH3 and NOx - https://edgar.jrc.ec.europa.eu/dataset_ghg50) and Nr run-off and leaching from agricultural obtained from the IMAGE-Global Nutrient Model (GNM) spatial dataset In [102]. Comparison to GVA unreliable for small countries and countries subject to large transboundary effects (Table 10), but generally confirm findings of the EU Nitrogen Assessment that nitrogen pollution may be comparable to the GVA of agriculture in many countries.

Country	ISO 3166-1	Damage cost using total Nr emissions	Percent mean damage cost from NH3	Percent mean damage cost from NOx	Percent mean damage cost from Nr run-off	Percent mean damage cost from Nr leaching	Percent of damage costs against GVA ag

Annex A

		US$2020 billions	emission air	emission air			
Afghanistan	AFG	**0.99**	73.7%	15.1%	10.5%	0.6%	23.1%
Angola	AGO	**0.864**	62.1%	17.9%	18.5%	1.5%	10.6%
Albania	ALB	**0.342**	80.6%	11.9%	3.8%	3.6%	13.9%
United Arab Emirates	ARE	**0.227**	82.9%	17.0%	0.1%	0.0%	9.4%
Argentina	ARG	**3.846**	46.7%	35.4%	16.4%	1.5%	12.1%
Armenia	ARM	**0.225**	52.5%	8.2%	37.0%	2.2%	
Australia	AUS	**8.038**	37.6%	17.9%	41.1%	3.4%	30.0%
Austria	AUT	**2.642**	84.8%	12.1%	1.3%	1.8%	49.3%
Azerbaijan	AZE	**0.584**	78.3%	14.3%	6.2%	1.2%	16.2%
Burundi	BDI	**0.055**	71.8%	25.2%	2.7%	0.4%	6.9%
Belgium	BEL	**3.814**	80.7%	12.8%	3.3%	3.2%	99.2%
Benin	BEN	**0.274**	67.2%	22.3%	9.4%	1.1%	9.1%
Burkina Faso	BFA	**0.222**	50.2%	33.0%	16.6%	0.1%	8.0%
Bangladesh	BGD	**7.938**	71.5%	15.7%	11.1%	1.7%	34.1%
Bulgaria	BGR	**0.808**	60.0%	19.9%	18.3%	1.7%	41.6%
Bahamas, The	BHS	**0.027**	92.3%	7.7%	0.0%	0.0%	33.3%
Bosnia and Herzegovina	BIH	**0.702**	87.0%	9.4%	2.8%	0.8%	61.6%
Belarus	BLR	**0.901**	70.7%	21.8%	4.6%	2.9%	16.2%
Belize	BLZ	**0.126**	68.6%	31.4%	0.0%	0.0%	80.1%
Bolivia	BOL	**3.32**	64.3%	11.6%	23.9%	0.2%	132.6%
Brazil	BRA	**144.708**	32.5%	10.7%	56.3%	0.5%	135.1%
Brunei Darussalam	BRN	**0.183**	94.6%	5.4%	0.0%	0.0%	157.2%
Bhutan	BTN	**0.053**	76.2%	14.4%	8.7%	0.7%	20.1%
Botswana	BWA	**0.222**	66.5%	12.7%	18.9%	1.8%	75.2%
Central African Republic	CAF	**1.195**	88.0%	11.2%	0.5%	0.3%	256.7%
Canada	CAN	**8.919**	62.3%	14.8%	13.2%	9.6%	30.7%
Switzerland	CHE	**1.957**	84.0%	10.4%	1.1%	4.5%	49.5%
Chile	CHL	**2.593**	54.5%	11.1%	23.4%	11.0%	28.9%
China	CHN	**439.7**	12.3%	2.2%	84.3%	1.2%	63.4%
Cote d'Ivoire	CIV	**1.435**	71.2%	19.3%	8.5%	1.0%	18.1%
Cameroon	CMR	**1.472**	70.7%	13.8%	14.2%	1.3%	31.4%
Congo, Dem. Rep.	COD	**1.035**	34.5%	16.3%	48.3%	0.9%	18.3%
Congo, Rep.	COG	**0.066**	18.2%	9.6%	64.0%	8.2%	10.2%
Colombia	COL	**34.782**	23.4%	3.8%	72.3%	0.5%	159.3%
Comoros	COM	**0.018**	70.3%	17.9%	10.8%	1.0%	6.4%
Cabo Verde	CPV	**0.012**	86.4%	13.6%	0.0%	0.0%	7.5%
Costa Rica	CRI	**2.438**	12.6%	3.5%	83.2%	0.7%	95.5%
Cuba	CUB	**1.63**	33.1%	13.5%	52.2%	1.3%	60.8%
Cyprus	CYP	**0.289**	91.6%	8.4%	0.0%	0.0%	65.4%
Czech Republic	CZE	**2.946**	72.0%	19.6%	3.0%	5.4%	82.6%
Germany	DEU	**17.064**	66.9%	15.3%	13.5%	4.3%	65.6%

Djibouti	DJI	**0.02**	58.5%	13.4%	27.5%	0.6%	
Denmark	DNK	**4.442**	77.0%	14.0%	3.3%	5.7%	118.1%
Dominican Republic	DOM	**2.144**	30.4%	6.1%	62.9%	0.7%	55.3%
Algeria	DZA	**3.187**	16.6%	3.0%	80.1%	0.3%	16.6%
Ecuador	ECU	**5.83**	34.2%	5.5%	60.0%	0.3%	67.0%
Egypt, Arab Rep.	EGY	**2.129**	49.7%	10.9%	39.3%	0.0%	6.3%
Eritrea	ERI	**0.264**	57.3%	12.2%	30.5%	0.1%	
Spain	ESP	**9.576**	51.0%	12.9%	32.3%	3.8%	24.8%
Estonia	EST	**0.552**	74.4%	17.6%	5.0%	3.0%	73.9%
Ethiopia	ETH	**3.829**	71.8%	18.2%	9.3%	0.6%	22.5%
Finland	FIN	**1.26**	60.5%	13.0%	2.6%	23.9%	19.2%
Fiji	FJI	**0.095**	50.2%	9.6%	40.1%	0.2%	27.0%
France	FRA	**16.365**	58.8%	18.1%	15.1%	8.0%	36.0%
Gabon	GAB	**0.385**	18.6%	3.0%	77.2%	1.2%	51.5%
United Kingdom	GBR	**11.82**	60.6%	16.3%	19.6%	3.5%	66.9%
Georgia	GEO	**0.422**	73.9%	8.5%	11.9%	5.7%	35.3%
Ghana	GHA	**0.854**	72.7%	18.8%	8.2%	0.3%	8.4%
Guinea	GIN	**1.185**	74.0%	19.8%	5.9%	0.3%	75.0%
Gambia, The	GMB	**0.022**	52.8%	20.1%	26.5%	0.7%	6.0%
Guinea-Bissau	GNB	**0.033**	56.0%	27.7%	12.6%	3.7%	7.8%
Equatorial Guinea	GNQ	**0.021**	41.8%	25.0%	27.7%	5.4%	7.8%
Greece	GRC	**3.258**	35.7%	8.6%	54.0%	1.6%	35.4%
Guatemala	GTM	**3.994**	19.0%	8.3%	71.9%	0.7%	72.6%
Guyana	GUY	**0.687**	70.5%	18.1%	10.7%	0.7%	55.3%
Honduras	HND	**4.538**	15.3%	2.6%	81.8%	0.3%	192.1%
Croatia	HRV	**1.241**	81.0%	14.2%	0.8%	4.0%	76.3%
Haiti	HTI	**0.311**	45.1%	15.0%	37.6%	2.2%	14.2%
Hungary	HUN	**2.563**	72.6%	22.7%	1.6%	3.1%	53.5%
Indonesia	IDN	**55.277**	14.8%	6.1%	78.7%	0.3%	42.9%
India	IND	**83.736**	30.4%	9.5%	59.1%	1.0%	25.6%
Ireland	IRL	**4.563**	72.1%	13.6%	6.7%	7.6%	165.9%
Iran, Islamic Rep.	IRN	**22.305**	7.9%	1.4%	90.2%	0.4%	55.8%
Iraq	IRQ	**2.053**	15.7%	4.3%	79.3%	0.6%	34.6%
Iceland	ISL	**0.211**	53.5%	7.0%	36.7%	2.8%	22.0%
Israel	ISR	**0.755**	71.8%	13.8%	10.5%	4.0%	22.4%
Italy	ITA	**12.292**	52.3%	10.5%	33.4%	3.9%	31.3%
Jamaica	JAM	**0.387**	19.6%	4.6%	74.9%	0.9%	49.9%
Jordan	JOR	**0.354**	24.0%	4.4%	70.9%	0.7%	35.5%
Japan	JPN	**6.617**	48.9%	9.5%	29.2%	12.4%	11.2%
Kazakhstan	KAZ	**1.71**	40.8%	13.5%	43.2%	2.4%	21.0%
Kenya	KEN	**1.832**	69.3%	15.7%	13.9%	1.1%	15.1%
Kyrgyz Republic	KGZ	**0.391**	77.5%	13.4%	7.4%	1.8%	41.9%
Cambodia	KHM	**1.499**	55.4%	41.2%	2.3%	1.1%	35.9%
Korea, Rep.	KOR	**5.079**	50.9%	8.2%	23.9%	17.0%	19.2%

Kuwait	KWT	**0.328**	93.6%	6.3%	0.0%	0.0%	56.0%
Lao PDR	LAO	**2.418**	75.6%	23.7%	0.2%	0.4%	131.1%
Lebanon	LBN	**0.23**	87.2%	9.6%	0.4%	2.8%	14.2%
Liberia	LBR	**0.192**	72.2%	16.7%	10.2%	0.9%	19.8%
Libya	LBY	**0.292**	29.5%	6.5%	61.2%	2.8%	
Sri Lanka	LKA	**1.047**	30.5%	4.5%	63.4%	1.6%	17.7%
Lesotho	LSO	**0.064**	70.5%	17.5%	9.8%	2.1%	60.5%
Lithuania	LTU	**1.54**	62.9%	19.2%	13.5%	4.5%	108.6%
Luxembourg	LUX	**0.248**	89.0%	8.7%	0.1%	2.2%	202.9%
Latvia	LVA	**0.529**	72.9%	25.6%	0.9%	0.6%	47.1%
Morocco	MAR	**8.295**	8.0%	1.7%	90.1%	0.2%	54.5%
Moldova	MDA	**2.726**	32.7%	3.8%	63.5%	0.0%	302.9%
Madagascar	MDG	**1.009**	53.7%	13.6%	31.6%	1.0%	35.2%
Mexico	MEX	**39.012**	11.6%	3.3%	84.6%	0.5%	103.3%
North Macedonia	MKD	**0.32**	75.5%	9.1%	14.6%	0.8%	34.4%
Mali	MLI	**0.447**	54.7%	28.5%	16.0%	0.8%	10.6%
Myanmar	MMR	**7.59**	72.2%	20.5%	6.5%	0.7%	35.9%
Montenegro	MNE	**0.1**	88.2%	11.8%	0.0%	0.0%	27.4%
Mongolia	MNG	**4.907**	62.1%	7.6%	30.0%	0.3%	321.4%
Mozambique	MOZ	**0.594**	69.7%	13.3%	16.5%	0.6%	17.2%
Mauritania	MRT	**0.138**	55.0%	27.4%	17.3%	0.3%	13.2%
Malawi	MWI	**0.213**	75.3%	20.6%	3.5%	0.6%	9.0%
Malaysia	MYS	**5.935**	18.8%	4.7%	76.4%	0.1%	20.3%
Namibia	NAM	**0.676**	50.9%	10.8%	38.2%	0.1%	84.2%
New Caledonia	NCL	**0.023**	90.4%	9.6%	0.0%	0.0%	
Niger	NER	**0.896**	72.1%	24.0%	3.8%	0.0%	26.0%
Nigeria	NGA	**3.09**	52.9%	29.3%	16.8%	1.1%	2.9%
Nicaragua	NIC	**2.286**	32.6%	6.6%	60.6%	0.2%	147.9%
Netherlands	NLD	**7.316**	83.1%	11.9%	0.7%	4.3%	45.8%
Norway	NOR	**0.987**	47.8%	10.4%	12.7%	29.1%	13.9%
Nepal	NPL	**2.21**	81.5%	16.0%	1.5%	1.0%	35.3%
New Zealand	NZL	**5.567**	28.2%	8.0%	54.0%	9.8%	45.9%
Oman	OMN	**0.142**	82.1%	17.9%	0.0%	0.1%	11.1%
Pakistan	PAK	**5.451**	63.9%	22.1%	13.4%	0.7%	11.6%
Panama	PAN	**0.972**	29.3%	6.0%	64.1%	0.6%	84.4%
Peru	PER	**22.796**	23.7%	3.5%	72.7%	0.2%	194.9%
Philippines	PHL	**11.804**	16.4%	10.4%	72.8%	0.5%	36.6%
Papua New Guinea	PNG	**0.21**	75.0%	9.4%	15.4%	0.2%	6.7%
Poland	POL	**8.669**	78.5%	17.0%	2.4%	2.1%	70.6%
Puerto Rico	PRI	**0.673**	91.1%	5.5%	0.6%	2.9%	
Korea, Dem. People's Rep.	PRK	**4.445**	16.6%	2.5%	80.6%	0.3%	
Portugal	PRT	**2.201**	57.7%	9.3%	30.0%	2.9%	43.9%
Paraguay	PRY	**1.203**	63.3%	31.0%	4.8%	0.9%	29.4%

West Bank and Gaza	PSE	**0.084**	96.9%	1.8%	0.2%	1.1%	9.2%
Qatar	QAT	**0.079**	85.3%	14.7%	0.0%	0.0%	34.2%
Romania	ROU	**5.147**	35.3%	8.1%	56.4%	0.3%	53.8%
Russian Federation	RUS	**64.202**	26.7%	4.4%	68.6%	0.4%	101.7%
Rwanda	RWA	**0.217**	75.0%	16.2%	8.6%	0.2%	11.3%
Saudi Arabia	SAU	**1.606**	24.4%	6.6%	65.3%	3.7%	10.1%
Sudan	SDN	**1.415**	67.5%	24.2%	8.2%	0.0%	5.7%
Senegal	SEN	**0.399**	72.2%	21.6%	5.5%	0.8%	14.6%
Solomon Islands	SLB	**0.008**	51.9%	7.1%	34.0%	6.9%	
Sierra Leone	SLE	**0.397**	71.0%	23.4%	5.1%	0.5%	24.6%
El Salvador	SLV	**0.721**	23.7%	8.6%	67.2%	0.6%	63.3%
Somalia	SOM	**0.477**	74.8%	16.8%	8.4%	0.0%	
Serbia	SRB	**1.151**	76.2%	15.4%	8.0%	0.4%	39.5%
South Sudan	SSD	**0.182**	66.3%	14.2%	16.8%	2.6%	20.8%
Suriname	SUR	**0.088**	84.6%	15.4%	0.0%	0.0%	18.5%
Slovak Republic	SVK	**1.194**	77.2%	18.2%	2.1%	2.5%	44.3%
Slovenia	SVN	**0.672**	83.2%	10.9%	0.4%	5.5%	66.1%
Sweden	SWE	**1.878**	68.5%	14.4%	1.3%	15.7%	20.4%
Eswatini	SWZ	**0.057**	58.3%	35.8%	4.5%	1.5%	10.3%
Syrian Arab Republic	SYR	**0.158**	34.4%	24.9%	37.6%	3.1%	
Chad	TCD	**0.703**	74.9%	18.1%	6.9%	0.1%	10.7%
Togo	TGO	**0.554**	80.8%	18.0%	0.9%	0.3%	43.2%
Thailand	THA	**12.401**	32.9%	17.2%	48.5%	1.4%	33.7%
Tajikistan	TJK	**0.387**	82.2%	13.5%	3.2%	1.1%	25.3%
Turkmenistan	TKM	**0.73**	62.6%	15.3%	21.9%	0.2%	
Timor-Leste	TLS	**0.103**	41.2%	8.1%	50.7%	0.1%	51.0%
Trinidad and Tobago	TTO	**0.444**	94.1%	5.9%	0.0%	0.0%	316.7%
Tunisia	TUN	**1.586**	13.2%	2.6%	84.0%	0.2%	36.1%
Turkey	TUR	**43.485**	15.0%	3.4%	81.1%	0.5%	52.5%
Tanzania	TZA	**1.968**	60.4%	18.1%	19.6%	1.9%	19.6%
Uganda	UGA	**1.506**	79.3%	14.1%	6.5%	0.1%	15.7%
Ukraine	UKR	**14.634**	19.6%	5.3%	75.0%	0.2%	114.0%
Uruguay	URY	**2.101**	61.8%	21.9%	1.0%	15.3%	63.8%
United States	USA	**65.822**	26.6%	11.8%	50.0%	11.7%	36.9%
Uzbekistan	UZB	**1.739**	52.7%	15.7%	29.5%	2.1%	9.6%
St. Vincent and the Grenadines	VCT	**0.007**	88.0%	12.0%	0.0%	0.0%	16.6%
Venezuela, RB	VEN	**5.465**	50.9%	6.5%	42.2%	0.5%	
Vietnam	VNM	**14.711**	32.6%	14.1%	52.4%	0.9%	59.2%
Vanuatu	VUT	**0.021**	87.8%	10.0%	1.7%	0.5%	12.5%
Yemen, Rep.	YEM	**0.192**	29.6%	15.8%	53.5%	1.0%	9.1%
South Africa	ZAF	**7.391**	9.2%	5.1%	84.8%	0.9%	75.7%

Zambia	ZMB	**1.065**	80.8%	17.2%	1.3%	0.7%	55.9%
Zimbabwe	ZWE	**0.296**	59.0%	23.2%	11.2%	6.6%	20.6%

Table 9: Selected countries sorted by run-off total damage costs (to ecosystems) larger than total air pollution damage costs (to humans), total damage costs yr^{-1} in millions US$2020 PPP using annual (2015) nitrogen emissions for agriculture (Table 8), and the size of total damage costs yr^{-1} compared to annual (2015) GVA of agriculture

Country	Times larger mean ecosystem costs than mean air pollution costs		Country	Mean damage costs (billions US$2020 PPP)		Country	Percent mean damage costs against GVA
Russian Federation	49.6		China	389.2		Ireland	165%
Iran, Islamic Rep.	45.4		Brazil	133.1		Colombia	159%
Gabon	43.0		India	100.7		Peru	158%
Peru	33.6		Russian Federation	63.5		Nicaragua	156%
Honduras	32.6		United States	58.8		Costa Rica	131%
China	30.8		Indonesia	56.9		Brazil	124%
Korea, Dem. People's Rep.	30.0		Turkey	35.0		Denmark	118%
Algeria	28.6		Mexico	34.7		Ukraine	113%
Colombia	27.5		Colombia	34.7		Guatemala	108%
Morocco	22.7		Iran, Islamic Rep.	24.5		Bolivia	107%
Congo, Dem. Rep.	22.1		Peru	18.5		Russian Federation	101%
Indonesia	19.5		Germany	17.5		Belgium	100%
Mexico	19.3		France	16.5		Mexico	92%
Mongolia	19.0		Vietnam	15.6		El Salvador	90%
Brazil	16.9		Ukraine	14.5		South Africa	88%
South Africa	14.3		Thailand	12.5		Lao PDR	83%
Ukraine	13.8		Italy	12.5		Czech Republic	83%
Turkey	12.4		United Kingdom	11.5		Croatia	78%

Table 10: Countries suspected of transboundary distortion. All have lower HDI and lower production than respective high emission neighbours such as China, the EU, Russia, India, and Nigeria, that distorts weighting for anthropogenic atmospheric deposition of nitrogen. As these countries have low data for transboundary correction and few estimates for nitrogen damages, we have otherwise kept them in Table 6 and Table 7 and adjusted the factor $\gamma_{l}, ret, NH3/NOx$ (column 3) to a maximum value of 1. Deposition on land is from a global spatial dataset of inorganic nitrogen deposition [105] and MH3 and NOx emissions totals from [6]

Country	Factor by which N-weight of deposition on land exceeds N-weight of total NH3 and NOx emissions before correction

Afghanistan	1.9
Angola	4.5
Armenia	2.1
Bhutan	13.1
Bolivia	3.3
Bosnia and Herzegovina	1.2
Botswana	1.9
Belize	5.9
Myanmar	1.2
Burundi	1.7
Cameroon	3.1
Central African Republic	13.5
Chad	3.3
Colombia	1.1
Congo, Rep.	7.6
Congo, Dem. Rep.	9.0
Equatorial Guinea	13.0
Eritrea	1.2
Gabon	3.9
Guinea	2.7
Guyana	2.7
Cote d'Ivoire	2.0
Kyrgyz Republic	1.0
Lao PDR	2.9
Lesotho	1.1
Liberia	4.9
Mali	2.6
Mauritania	1.9
Mongolia	2.7
Montenegro	1.6
Mozambique	1.7
Namibia	1.8
Nepal	1.5
Niger	1.8
Papua New Guinea	2.2
Paraguay	1.6
Peru	1.4
Rwanda	1.7
Sierra Leone	2.0
South Sudan	12.8
Suriname	1.9
Eswatini	1.6
Tajikistan	1.4
Togo	2.3

Uganda	1.2
Zambia	2.3

4.10.2 Distributions of marginal and total damage costs

The tables in Section 4.10.1 describe mean values and lognormal fits of the samples for the marginal damage costs in the dataset. The following figures provide examples of the samples

Annex A

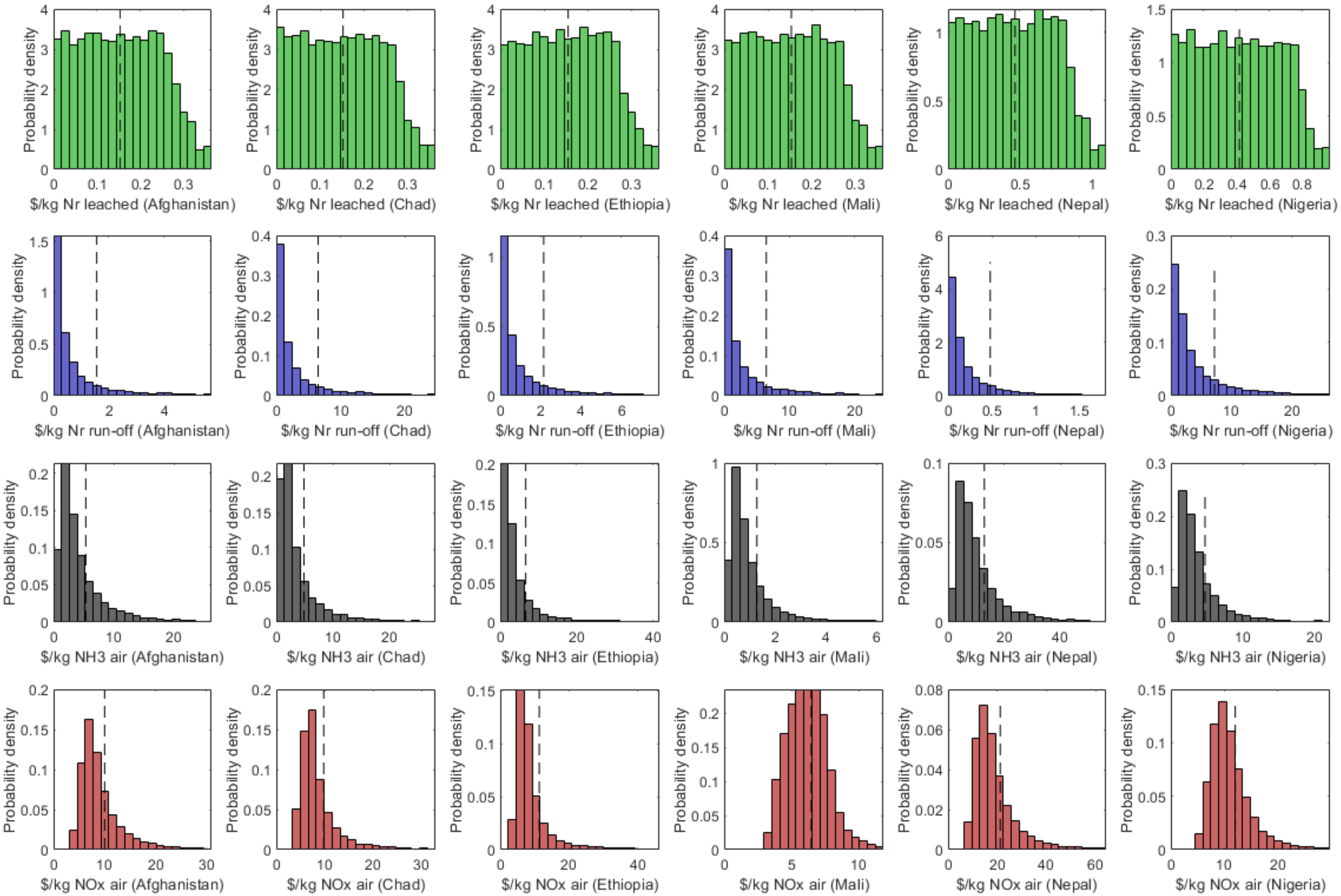

Figure 8: Examples of the distributions of marginal damage costs for nitrogen emissions for selected countries. All values in US$2020 PPP, per kg of Nr leached to groundwater for $MDC_{i,grdw,Nr}$ (green), per kg of Nr run-off to surface water for $MDC_{i,surw,Nr}$ (blue), per kg of NH3 emission to air for $MDC_{i,a,NH3}$ (black), and per kg of NOx emission to air for $MDC_{i,a,NOx}$ (red).

Annex A

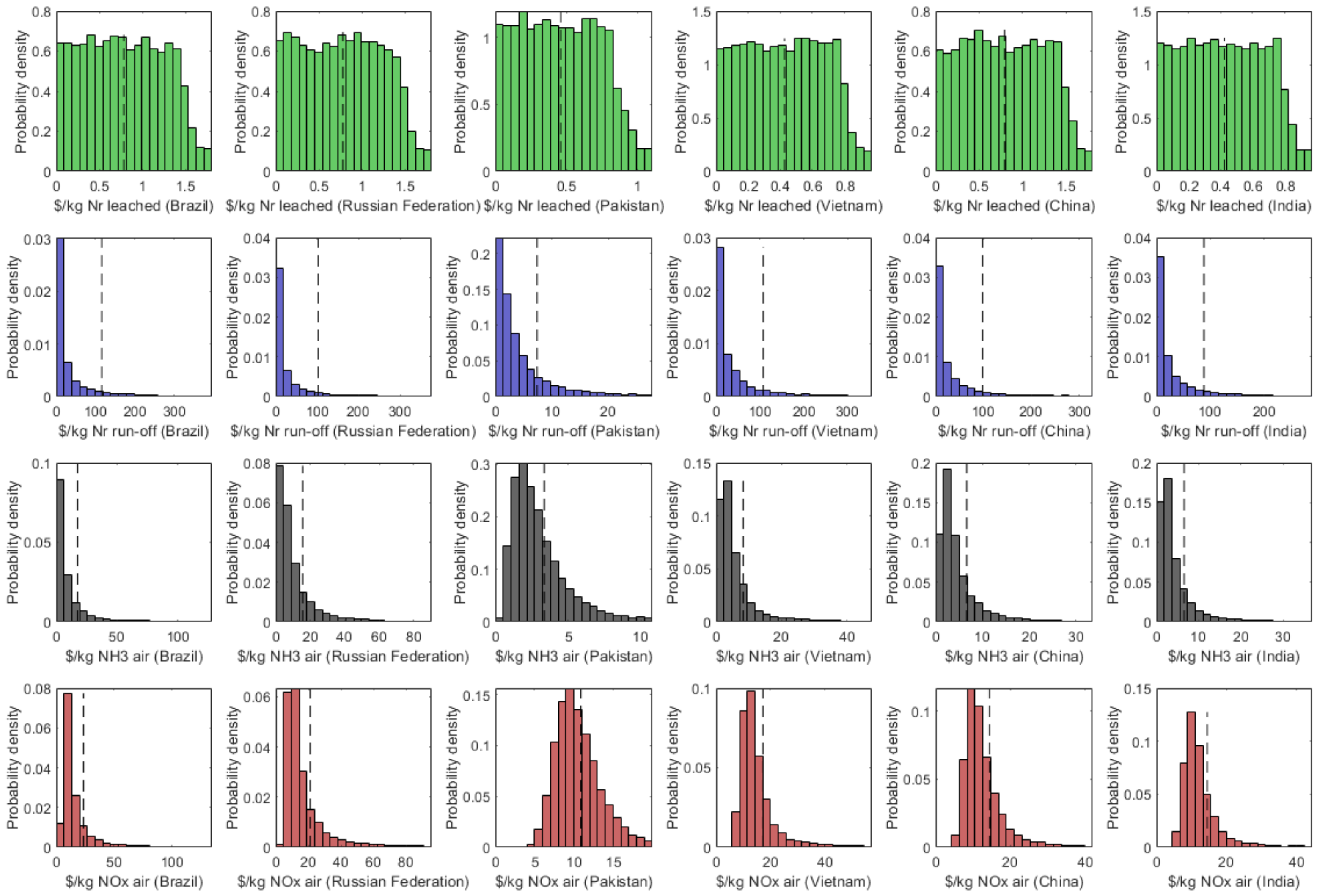

Figure 9: Examples of the distributions of marginal damage costs for nitrogen emissions for selected countries. All values in US$2020 PPP, per kg of Nr leached to groundwater for $MDC_{i,grdw,Nr}$ (green), per kg of Nr run-off to surface water for $MDC_{i,surw,Nr}$ (blue), per kg of NH3 emission to air for $MDC_{i,a,NH3}$ (black), and per kg of NOx emission to air for $MDC_{i,a,NOx}$ (red).

Annex A

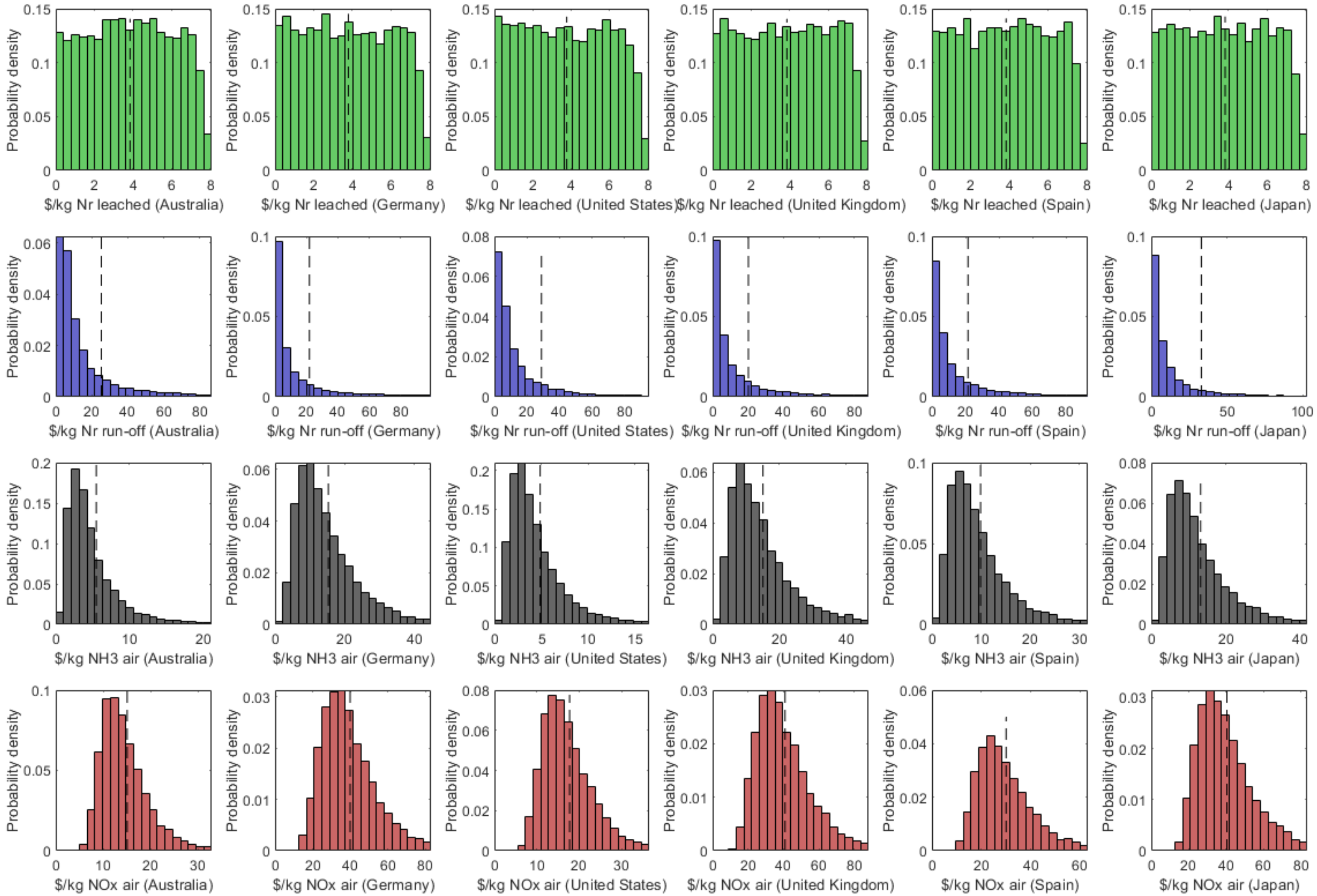

Figure 10: Examples of the distributions of marginal damage costs for nitrogen emissions for selected countries. All values in US$2020 PPP, per kg of Nr leached to groundwater for $MDC_{i,grdw,Nr}$ *(green), per kg of Nr run-off to surface water for* $MDC_{i,surw,Nr}$ *(blue), per kg of NH3 emission to air for* $MDC_{i,a,NH3}$ *(black), and per kg of NOx emission to air for* $MDC_{i,a,NOx}$ *(red).*

Annex A

The following figure (Figure 11), indicating the total costs of nitrogen pollution, should not be referred to without caveats. It is purely a damage estimate from present Nr pollution without accounting for the value provided to society from the use of nitrogen in agriculture. There is no comparison with a counterfactual, so it does not provide any indication of the economic value of food system transformation, i.e. the balance of value between decreasing nitrogen emissions and damage costs and what it costs to abate nitrogen emission with overall social welfare the same as present value.

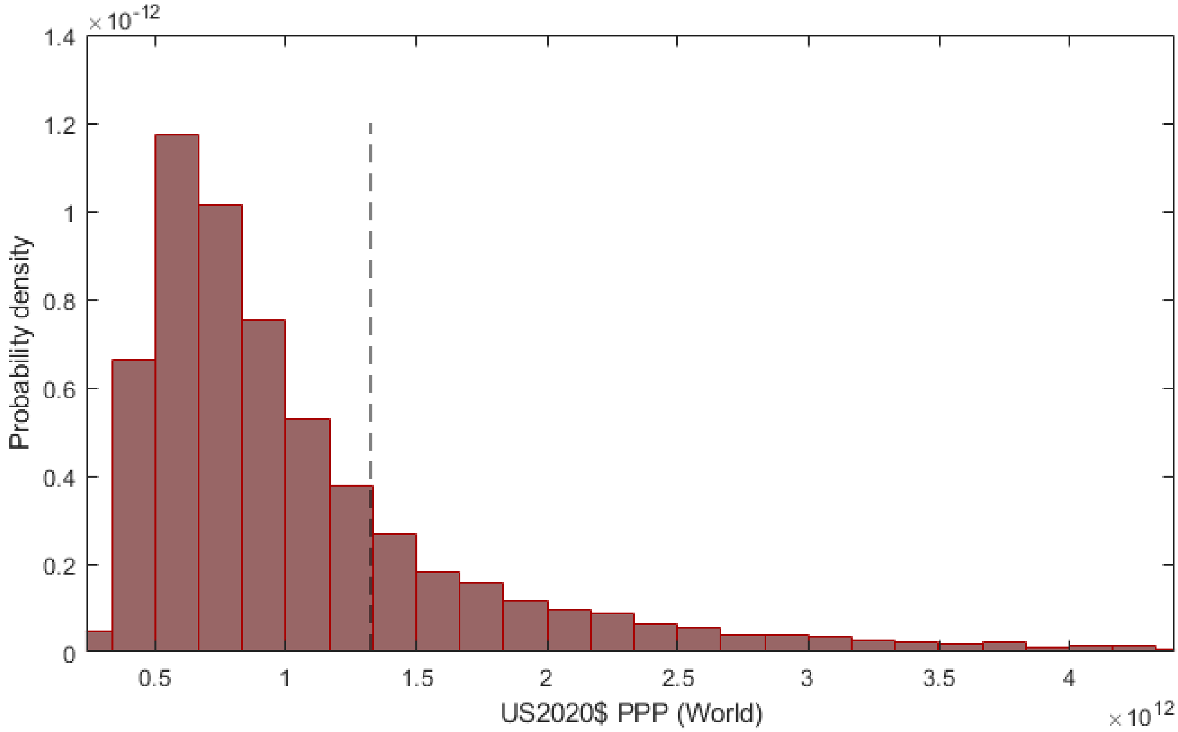

Figure 11: "hidden" cost of present nitrogen emissions from agriculture, obtained by summing marginal costs and total agricultural emissions of NH3, NOx, Nr to surface waters and Nr to groundwater across the 171 countries in Table 6. The joint distribution of marginal damage costs for individual countries are strongly correlated for air pollution damages, and several countries dominate costs, resulting in a skewed distribution shape for the addition of many correlated random variables. Total costs of ~1.4 trillion US$2020 PPP. The most likely cost is in the order of ~600 billion US$2020 PPP. Uncertainty in damage estimates indicate a 5% chance that damages could exceed ~3 trillion US$2020 PPP.

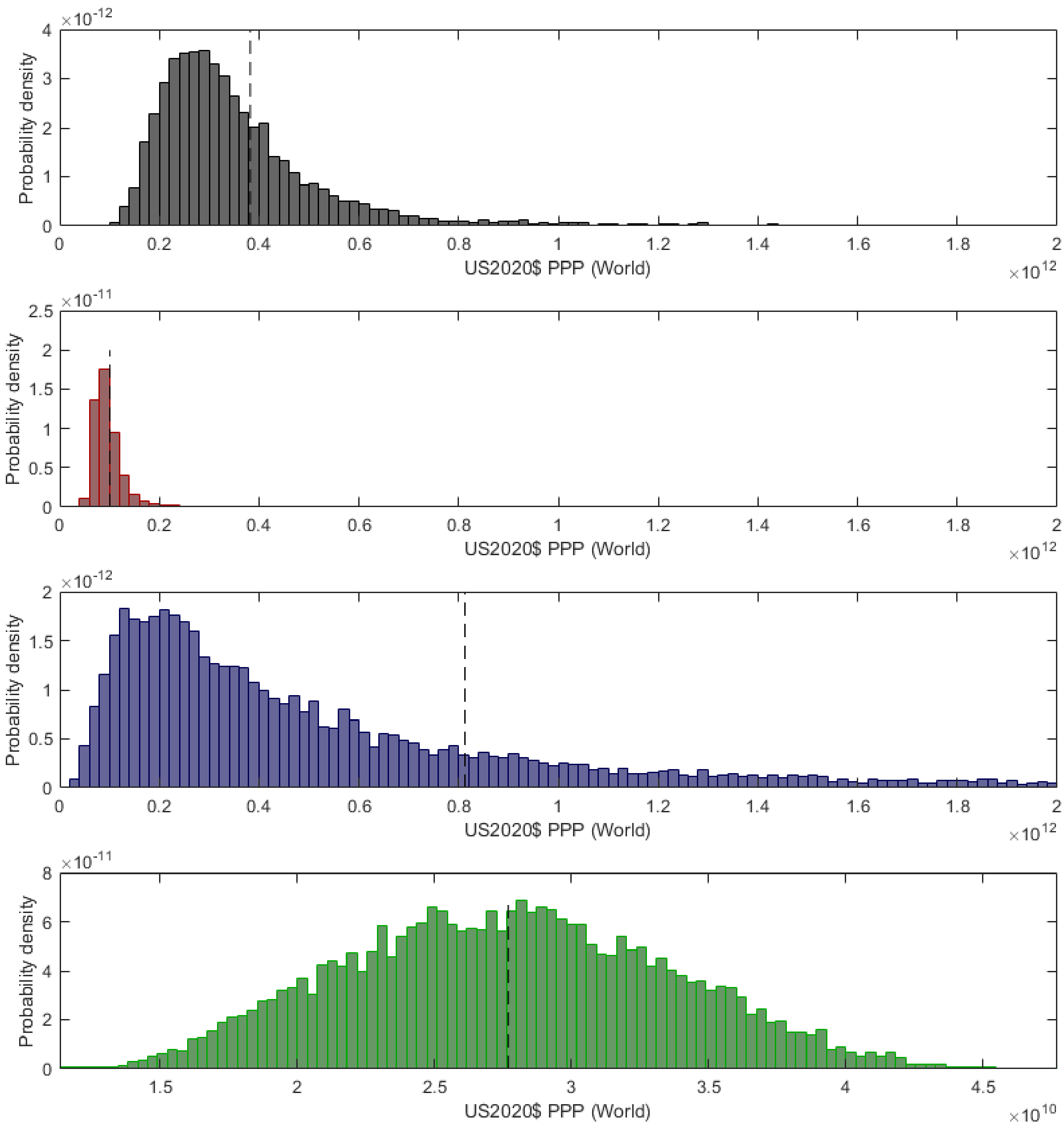

Figure 12: Disaggregation of "hidden" cost of present nitrogen emissions of NH3, NOx, Nr to surface waters and Nr to groundwater across the 171 countries in Table 6. Total in Figure 11 disaggregated into total costs NH3 (black), total costs NOx (red), total costs Nr run-off (blue) and total costs Nr groundwater (green). NH3, NOx and Nr run-off total costs are on the same scale (trillions US$2020 PPP, or 10^{12}). Nr groundwater costs in the scale of tens of billions (US$2020 PPP, 10^{10}). The considerable uncertainty into the cost of loss of ecosystem services from Nr run-off (even when ecosystem services losses from Nr pollution are treated as uncorrelated across countries) introduce a long-tail for the total costs of Nr run-off. On the same scale, total costs of Nr leaching to groundwater would appear as a green line at $0.03*10^{12}$.

Annex A

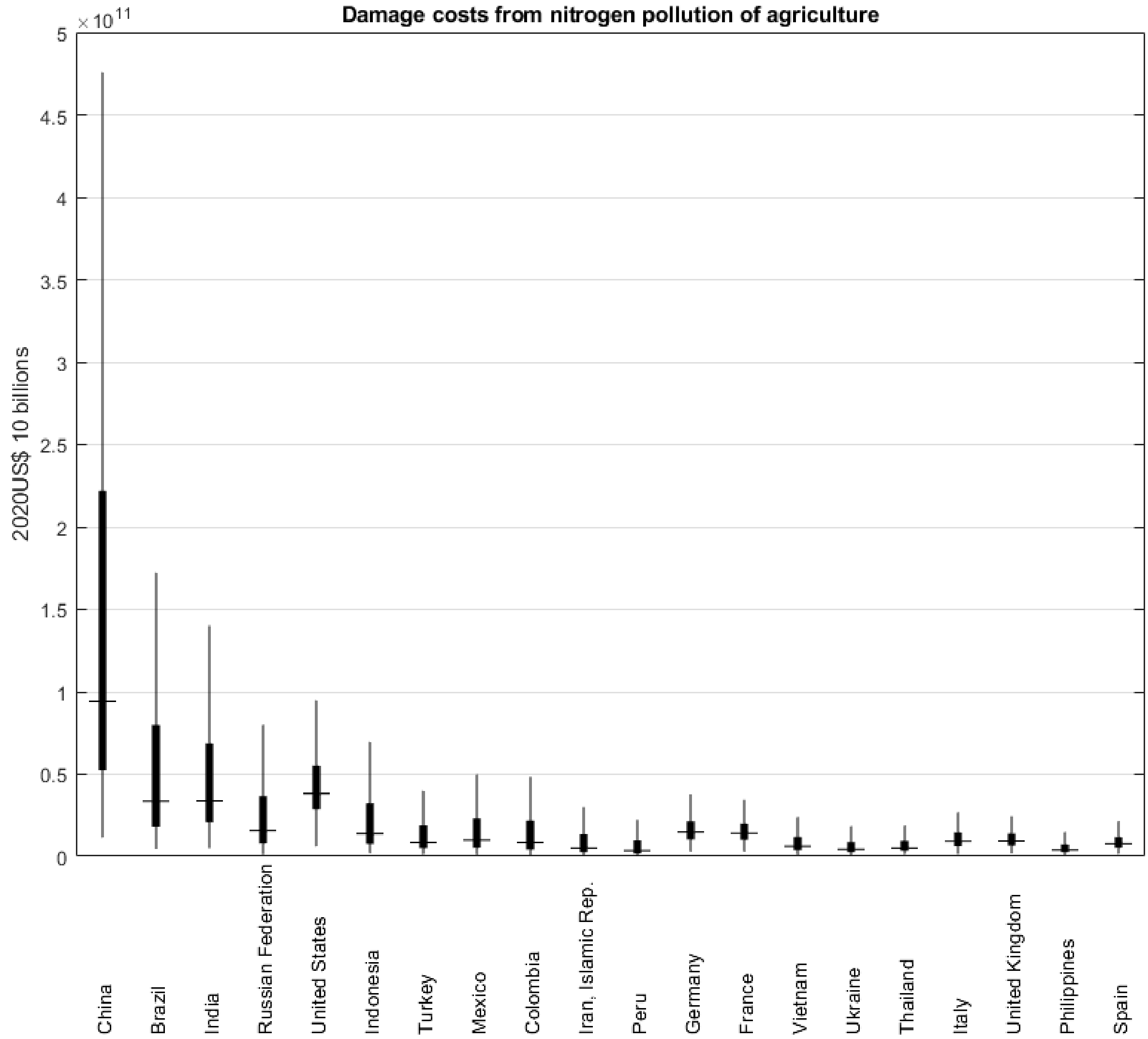

Figure 13: Boxplots for the highest damage costs using the quantity of Nr emissions for 2015. Boxplot shows the median as the largest cross line, and thick black lines show the interquartile range (25th to 75th percentiles). Note the large uncertainty in ecosystem service losses for countries with high amounts of nitrogen run-off to surface water results in fat tails. The mean is above the interquartile range for China, Brazil, and India. Measured by the median, Germany has the fourth largest damage costs, and the United States is second after China. For aggregating costs the mean is the appropriate measure (the mode and median are not additive), while risk assessment of uncertainty in systems with low frequency should examine the tail and the mode.

4.10.3 Statistical fits for value transfer of air pollution damages

We describing fitting the EASIUR regression for conterminous US counties [95] to a reduced set of variables. EASIUR uses a regression model fitted to CTM modelling of creation of ammonium particulate matter given NH3, NOx and SOx concentrations. Data on 2016 social costs per county j (NH3: CFA_j and NOx: CFA'_j) from EASIUR represent (in ppl lost yr^{-1} per US ton after dividing by the constant US$2016 8 million value of a statistical life used for all US counties) represents attributable human health damage of emission of 1 kg of NH3 or NOx per year, as a combination of air pollution exposure and vulnerability of US individuals [95]. Data on population density ($PopDen_j$ in ppl km^{-2}) and land area (in km^2) at the US county level was obtained from the 2017 US census (https://www.census.gov/acs/www/data/data-tables-and-tools/data-profiles/2017/) and data on emissions ($n_{NH3,j}, n_{NOx,j}, n_{SOx,j}$ in kg yr^{-1}) at the county level was available from the 2017 US national emissions inventory https://www.epa.gov/air-emissions-inventories/2017-national-emissions-inventory-nei-data.

Data was available for 3106 counties ($j = 1, \dots, 3106$) and the counties represent a wide range of combinations of NH3, NOx and SOx emissions between 10^4 and 10^7 kg yr^{-1} and population density between 0.05 and 3000 ppl km^{-2}. A linear model for log(CFA) involving log of emissions NOx kg per km^2 of area, NH3 kg per km^2 of area, NH3, NOx, SOx kg emissions and average temperate (in Celsius) was examined. All variables were significant (p<0.01) with $r^2 = 0.679$. Statistics for the model keeping population density and absolute emissions, still with $r^2 = 0.67$,

$$\log(CFA) = \beta_0 + \beta_1 \cdot \log(PopDen) + \beta_2 \cdot \log(n_{NH3}) + \beta_3 \cdot \log(n_{NOx}) + \beta_4 \cdot \log(n_{SOx}) + \epsilon$$

are in Table 11.

Table 11: Statistics from linear model in log-axes fitting the marginal social cost estimates for NH3 across 3106 US counties to population density (β_1), NH3 emissions (β_2), NOx emissions (β_3) and SOX emissions (β_4).

$r^2 = 0.67$	**Estimate**	**SE**	**tStat**	**pValue**
β_0	-0.97039	0.096604	-5.5254	3.5585e-08
β_1	0.43408	0.0064559	67.238	< 1e-300
β_2	-0.091959	0.010199	-9.0165	3.3224e-19
β_3	-0.35697	0.016811	-21.234	1.5533e-93
β_4	0.072888	0.0073995	9.8504	1.4584e-22

The most important statistic from Table 11 is not p-value. The p-values are artificial for so many data points from an existing model, but the r-squared value of 0.67 indicating 2/3 of variation across counties is explained by the parameters and explanatory factors for the remaining variation is unknown.

The objective of our regression is to interpolate from variation across US counties the variation of other countries from the EU marginal damage cost of air pollution in Table 2. The linear model is results in scale invariant ratios, as described in the main text. The residuals for the error term ϵ, and a visualisation of the fit using only the PopDen and NH3 emissions parameters, are in Figure 14.

The model can only be used for interpolation, it is not physically representative across all ranges of NH3, NOx and SOx emissions (marginal damages increase as NH3 emissions reduce for the same population density). A full quadratic model for the full set of parameters, which is more physical and involves interactions terms improves explanation of variation to r-squared of 0.745.

Annex A

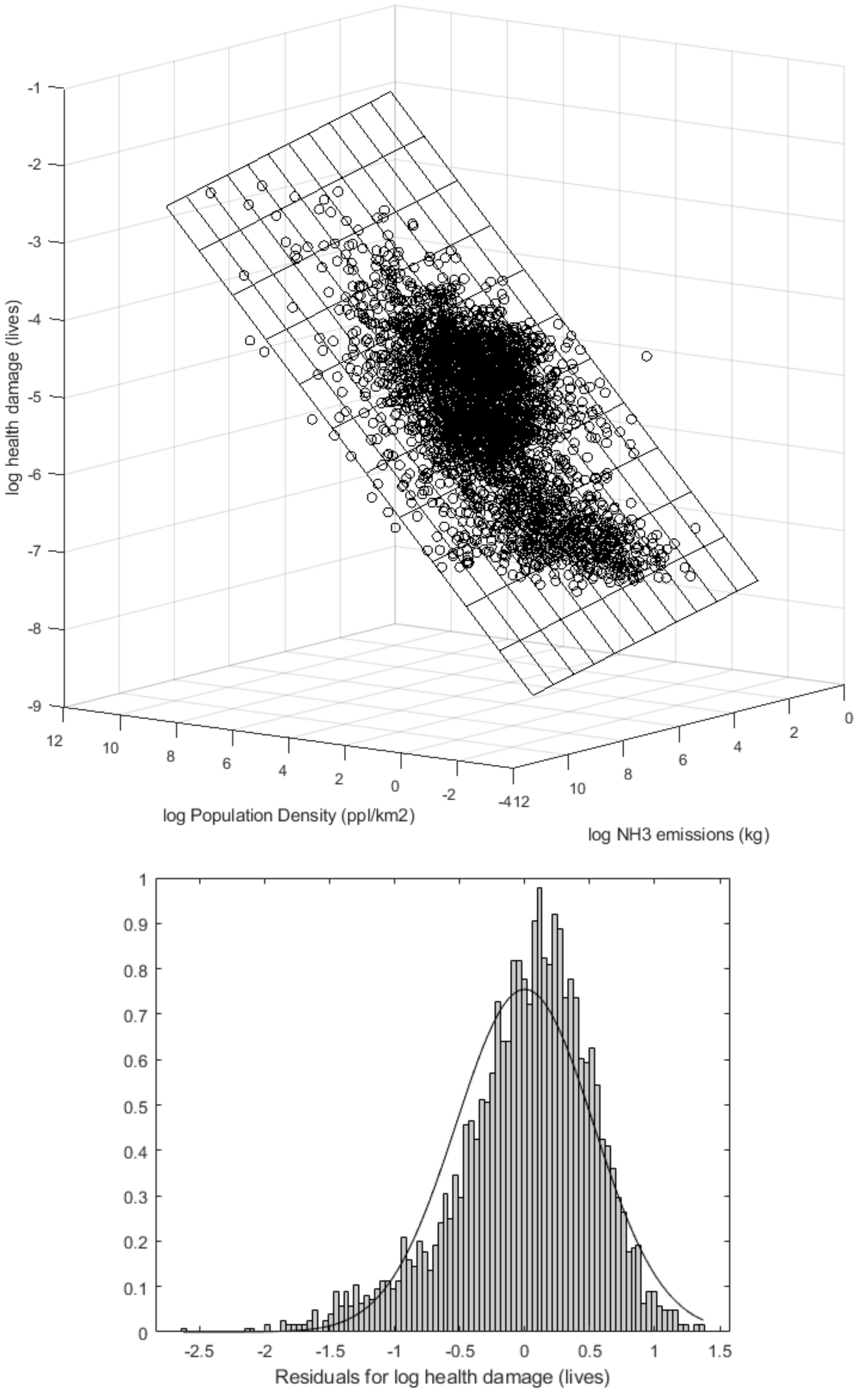

Figure 14: fit from Table 11 in 2 parameters (top panel) and residuals (bottom panel) for interpolation of attributable human health damage from NH3 emissions across US counties. PopDen is a more explanatory variable than NH3 emissions within the range of emissions for US counties (top panel), and residuals from the fit are approximately normally distributed in log-log axes. The residuals are positive skewed, indicating that a sub-log-transform would have a better representation of a standard error term.

The probability that the error term introduces an order of magnitude error is small, $Prob(\epsilon > \log(10)) < 0.001\%$.

A linear model for log(CFA') involving population density, emissions NOx kg per km^2 of area, NH3 kg per km^2 of area, NH3, NOx, SOx kg emissions and average temperate was examined. All variables were significant (p<0.01) with $r^2 = 0.563$. Statistics from linear model for NOx in log-axes involving the three factors with the most explanatory power, population density, NOx emissions and average temperature ($r^2 = 0.515$):

$$\log(CFA') = \beta'_0 + \beta'_1 \cdot \log(PopDen) + \beta'_2 \cdot \log(n_{NOx}) + \beta'_3 \cdot \log(ATemp) + \epsilon$$

are in Table 12

Table 12: Statistics from linear model in log-axes fitting the marginal social cost estimates for NOx across 3106 US counties to population density (β'_1), NH3 emissions (β'_2), NOx emissions (β'_3) and SOX emissions (β'_4).

$r^2 = 0.515$	**Estimate**	**SE**	**tStat**	**pValue**
β'_0	99.592	3.4321	29.018	9.4631e-164
β'_1	0.320	0.00603	53.033	< 1e-300
β'_2	-0.1709	0.010823	-15.792	4.5447e-54
β'_3	-18.612	0.60791	-30.617	8.2331e-180

The most important statistic from Table 12 is not p-value. P values are artificial for so many data points from an existing regression model, but the r-squared value of 0.515 indicates half of the variation across counties is explained by the parameters and explanatory factors for the remaining variation is unknown.

The objective of our regression is to interpolate from variation across US counties the variation of other countries from the EU marginal damage cost of air pollution in Table 2. The linear model is scale invariant for ratios, as described in the main text.

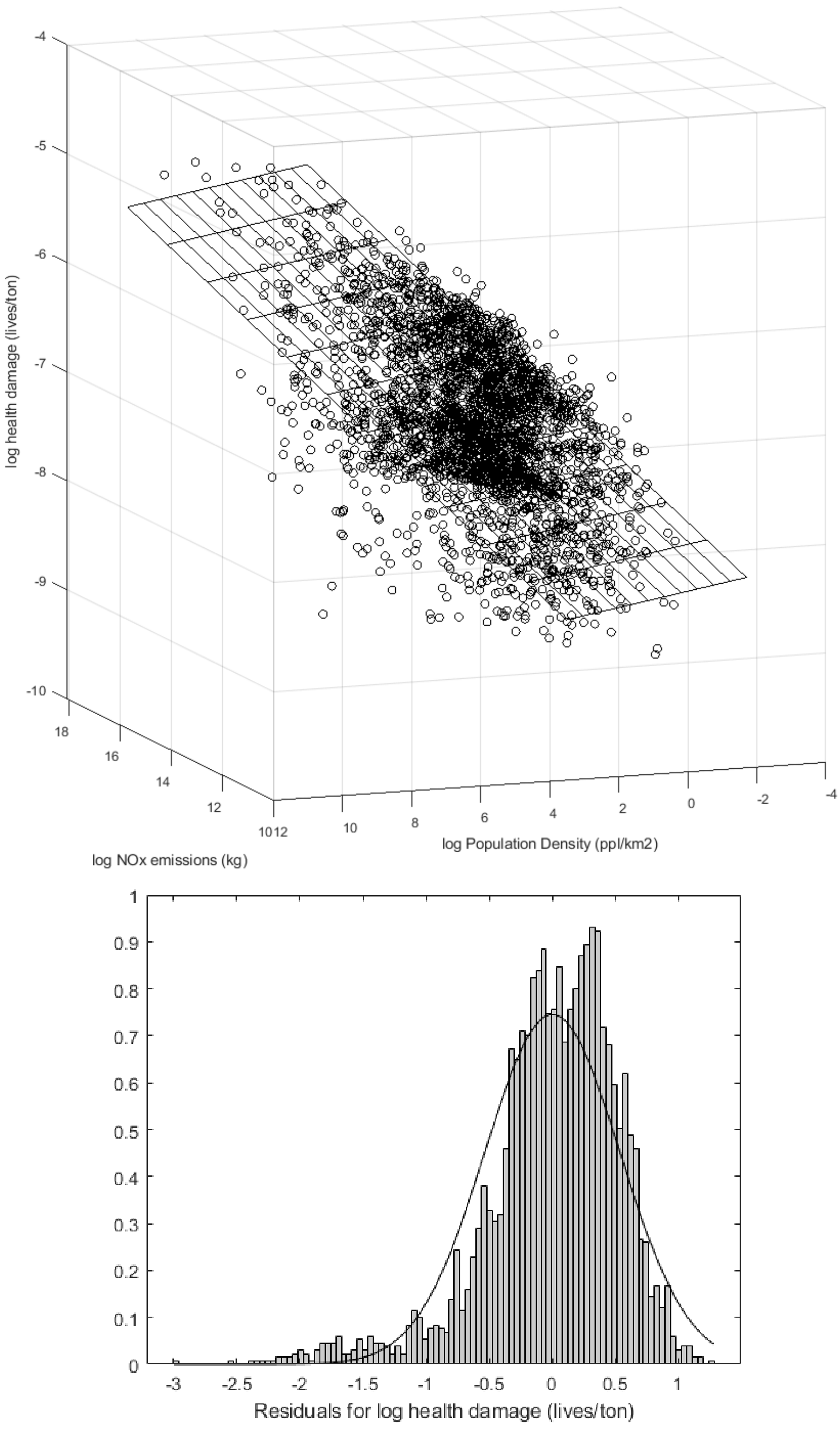

Figure 15: fit from Table 12 in 2 parameters (top panel) and residuals (bottom panel) for interpolation of attributable human health damage from NOx emissions across US counties. PopDen is a more explanatory variable than NOx emissions within the range of emissions for US counties (top panel). As expected PopDen and NOx emissions, predominantly from combustion, are correlated. Residuals from the fit (bottom panel) are approximately normally distributed in log-log axes. The residuals are positive skewed, indicating that a sub-log-transform would have a better representation of a standard error term. From examination of the data, and residuals, there was moderate evidence of mixture. Meaning that there was an additional explanatory factor creating subpopulations of counties with higher and lower marginal damages costs from NOx – the difference between the means of the group being about 30%. Examination the counties in the lower subcluster were more representative of agricultural NOx emissions.

Annex A

The probability that the error term introduces an order of magnitude error is very small, $Prob(\epsilon > \log(10)) < 0.001\%$.

4.10.4 Examples of factors in the value transfer of air pollution damages

Residuals from Figure 14 were used as uncertainty (error terms) for the transfer factors $\frac{CFA_i}{CFA_{EU}}$ for NH3 air pollution damages from the EU to country i as described in the text. Examples of the transfer factor random variables, given correlated sampling of the error terms, using the NH3, NOx and SOx totals for 2015 for each country from the EDGAR5.0, and population density and average temperature data for 2015 from the UN are shown in Figure 16 to Figure 18.

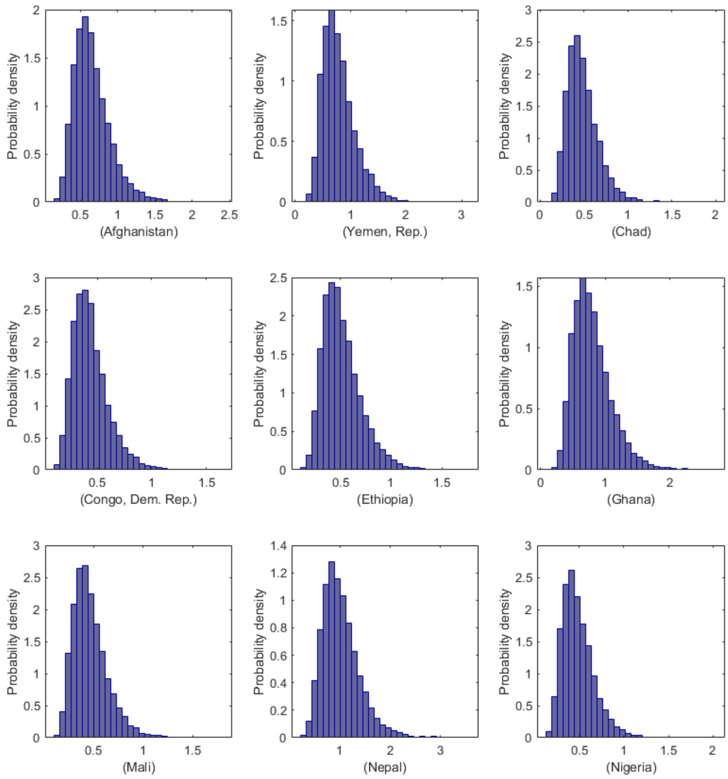

Figure 16: probable values of the ratio $\frac{CFA_i}{CFA_{EU}}$ estimating fraction of NH3 attributable marginal exposure and human health damage compared to the EU average. 1 represents the same attribution of human health damage from 1kg emission of NH3 as the EU27 average, 0.5, 50% less, 1.5 50% greater, etc.

Population density and very large NOx emissions play a large role in estimates of the differences in exposure.

Annex A

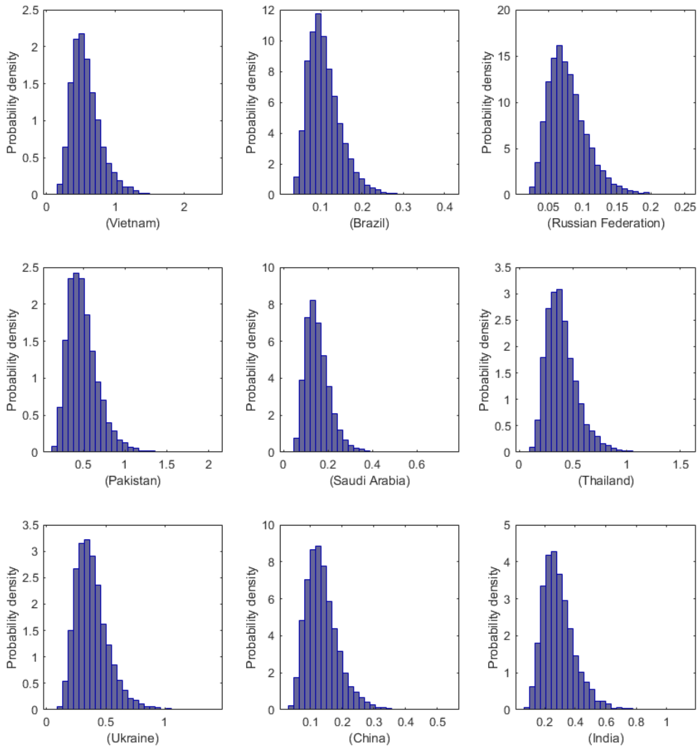

Figure 17: probable values of the ratio $\frac{CFA_i}{CFA_{EU}}$ *estimating fraction of NH3 attributable marginal exposure and human health damage compared to the EU average. 1 represents the same attribution of human health damage from 1kg emission of NH3 as the EU27 average, 0.5, 50% less, 1.5 50% greater, etc.*

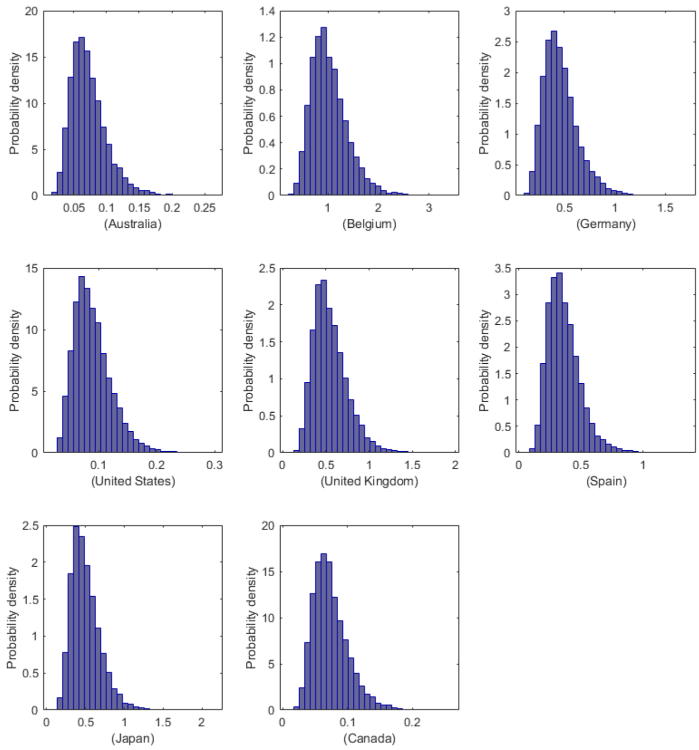

Figure 18: probable values of the ratio $\frac{CFA_i}{CFA_{EU}}$ *estimating fraction of NH3 attributable marginal exposure and human health damage compared to the EU average. 1 represents the same attribution of human health damage from 1kg emission of NH3 as the EU27 average, 0.5, 50% less, 1.5 50% greater, etc.*

Annex A

Residuals from Figure 15 were used as uncertainty (error terms) for the transfer factors $\frac{CFA'_i}{CFA'_{EU}}$ for NOx air pollution damages from the EU to country i, as described in the text. Examples of the transfer factor random variables, given correlated sampling of the error terms, using the NH3, NOx and SOx totals for 2015 for each country from the EDGAR5.0, and population density and average temperature data for 2015 from the UN are shown in Figure 19 to Figure 21.

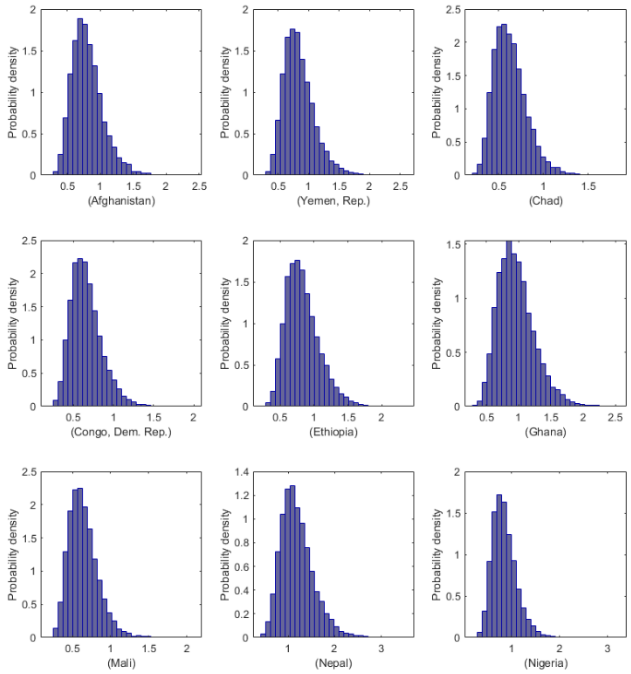

Figure 19 probable values of the ratio $\frac{CFA'_i}{CFA'_{EU}}$ estimating fraction of NOx attributable marginal exposure and human health damage compared to the EU average. 1 represents the same attribution of human health damage from 1kg emission of NOx as the EU27 average, 0.5, 50% less, 1.5 50% greater, etc.

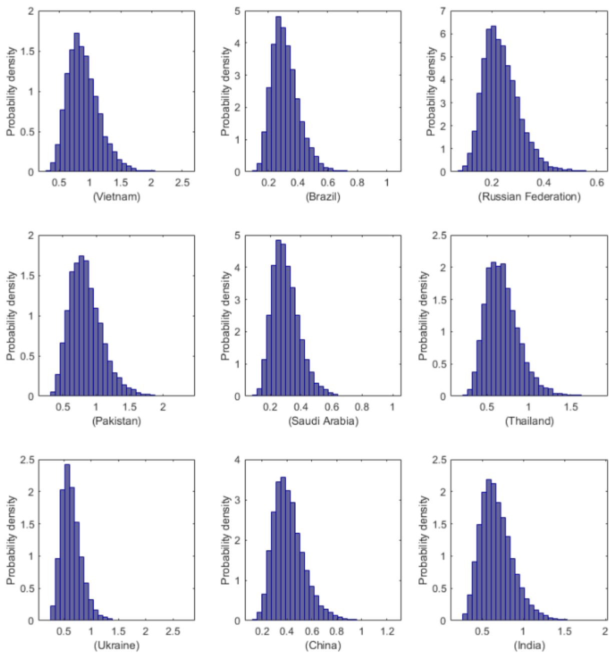

Figure 20: probable values of the ratio $\frac{CFA'_i}{CFA'_{EU}}$ estimating fraction of NOx attributable marginal exposure and human health damage compared to the EU average. 1 represents the same attribution of human health damage from 1kg emission of NOx as the EU27 average, 0.5, 50% less, 1.5 50% greater, etc.

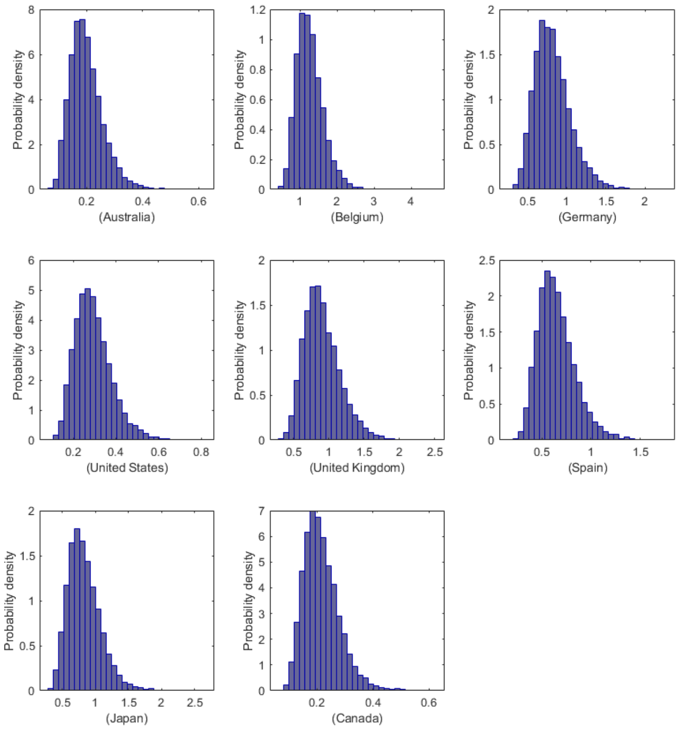

Figure 21: probable values of the ratio $\frac{CFA'_i}{CFA'_{EU}}$ estimating fraction of NOx attributable marginal exposure and human health damage compared to the EU average. 1 represents the same attribution of human health damage from 1kg emission of NOx as the EU27 average, 0.5, 50% less, 1.5 50% greater, etc.

4.10.5 Joint sampling marginal air pollution damages for NH3 and NOx

The samples of marginal damages costs $m_{i,a,NH3}$ and $m_{i,a,NOx}$, described in Section 4.3.6, across countries and between NH3 and NOx, were only weakly correlated by sampling from the terms $m_{a,NH3}$ and $m_{a,NOx}$ in Table 2, respectively, uniformly and independently.

Significant correlation between the residuals and the marginal damage costs were found in approximating the EAISUR regression across US counties. This indicates that the unexplained variance in marginal damages has common factors such as atmospheric chemistry and human biology across counties. At the US County scale, the correlation between log(CFA) and the residuals (the unexplained variance) for NH3 is 0.58. where the correlation between log(CFA') and residuals for NOx was 0.72. We assume that the common factors remain important, at the same significance level for cross-country comparison of uncertainty in NH3 and NOx marginal damage costs.

Pearson correlation (p=0.8578) was found between the natural logarithm of marginal damage costs from NH3 and NOx in the EAISUR estimates of across US counties, arising from the chemistry of ammonium particulate formation, coinciding human population exposure sites for concentrations of emission, and the same populations being exposed. Therefore, the individual distributions of $m_{i,a,NH3}$ and $m_{i,a,NOx}$ for each country, were fitted to lognormal distributions (Figure 22 to Figure 27) and treated as marginals of a joint lognormal distribution and jointly sampled using the block correlation matrix representing the i-jth entry between the NH3 or NOx marginal costs in country i and the NH3 or NOx costs in country j:

Annex A

$$\begin{bmatrix} \overbrace{\begin{matrix}1 & 0.58\\ 0.58 & 1\end{matrix}}^{NH3_i-NH3_j} & \overbrace{\begin{matrix}p & p\\ p & p\end{matrix}}^{NH3_i-NOx_j} \\ \begin{matrix}p & p\\ p & p\end{matrix} & \overbrace{\begin{matrix}1 & 0.72\\ 0.72 & 1\end{matrix}}^{NOx_i-NOx_j}\end{bmatrix}$$

Here p is the maximum value below 0.8578 (p was 0.634) such that the resulting covariance matrix is positive semi-definite (i.e., that the given correlation structure can be represented by a multivariate normal distribution).

The differences between the original samples of $m_{i,a,NH3}$ and $m_{i,a,NOx}$ and the outcome of joint sampling are exemplified in Figure 22 to Figure 27. For NH3 the uniform sampling of $m_{a,NH3}$ (which is chosen from a lack of any other information from [70]) widens the central mass of the distributions more, resulting in the lognormal fit undersampling the mid-range above the mean and oversampling the mode.

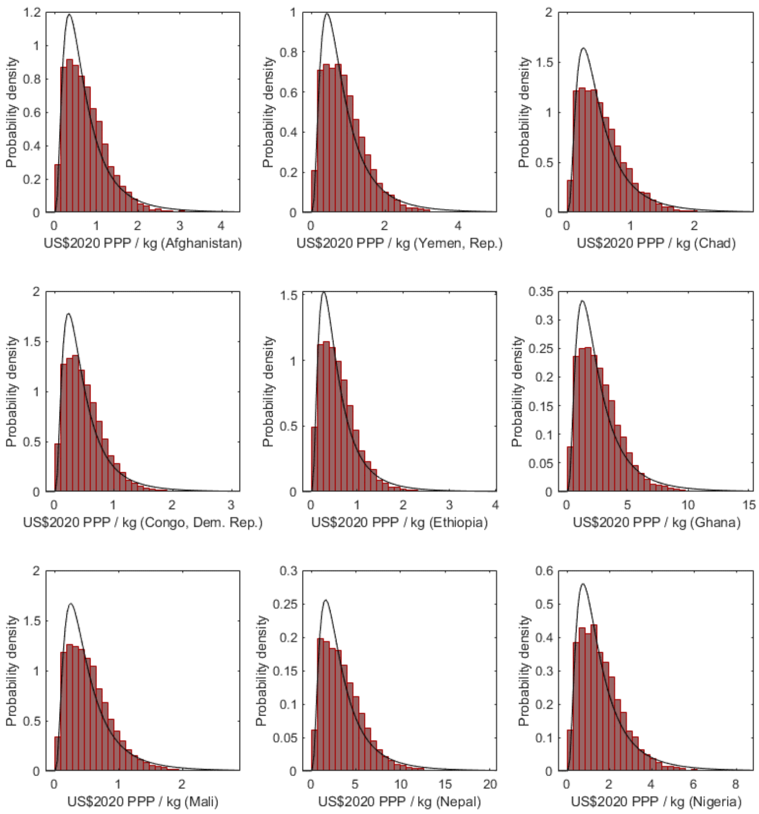

Figure 22: Lognormal marginals (black lines) of the joint resampling of $m_{i,a,NH3}$ for example countries. Red bars are histograms of the original samples of $m_{i,a,NH3}$ using a discounting adjustment factor, exposure adjustment factor, and the EU marginal damage value from Table 2

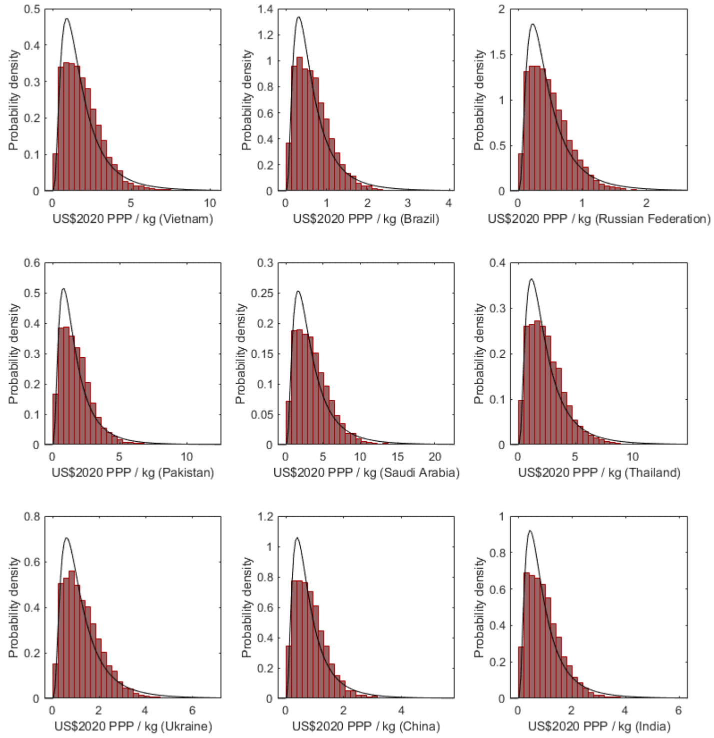

Figure 23: Lognormal marginals (black lines) of the joint resampling of $m_{i,a,NH3}$ for example countries. Red bars are histograms of the original samples of $m_{i,a,NH3}$ using a discounting adjustment factor, exposure adjustment factor, and the EU marginal damage value from Table 2

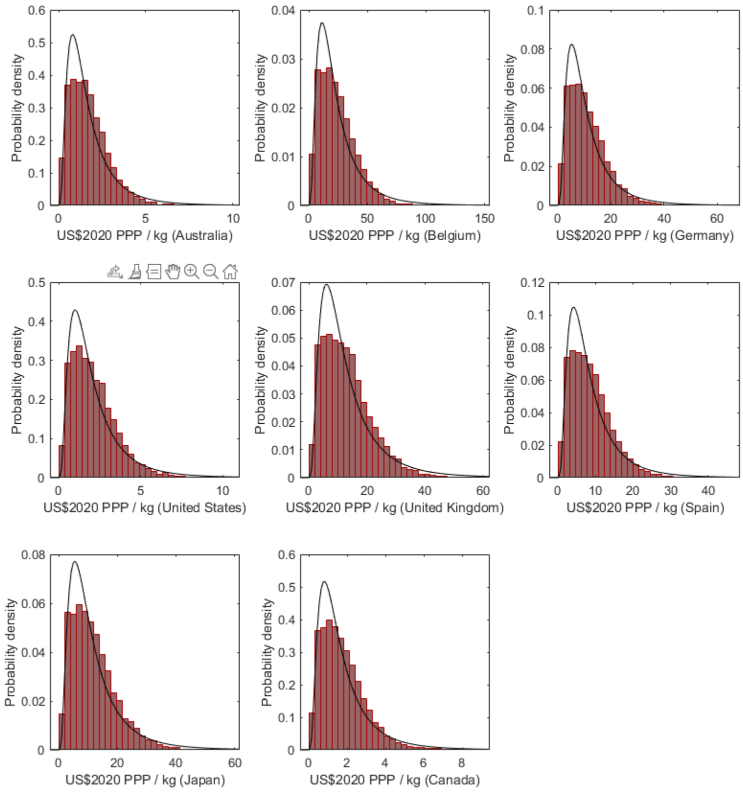

Figure 24: Lognormal marginals (black lines) of the joint resampling of $m_{i,a,NH3}$ for example countries. Red bars are histograms of the original samples of $m_{i,a,NH3}$ using a discounting adjustment factor, exposure adjustment factor, and the EU marginal damage value from Table 2.

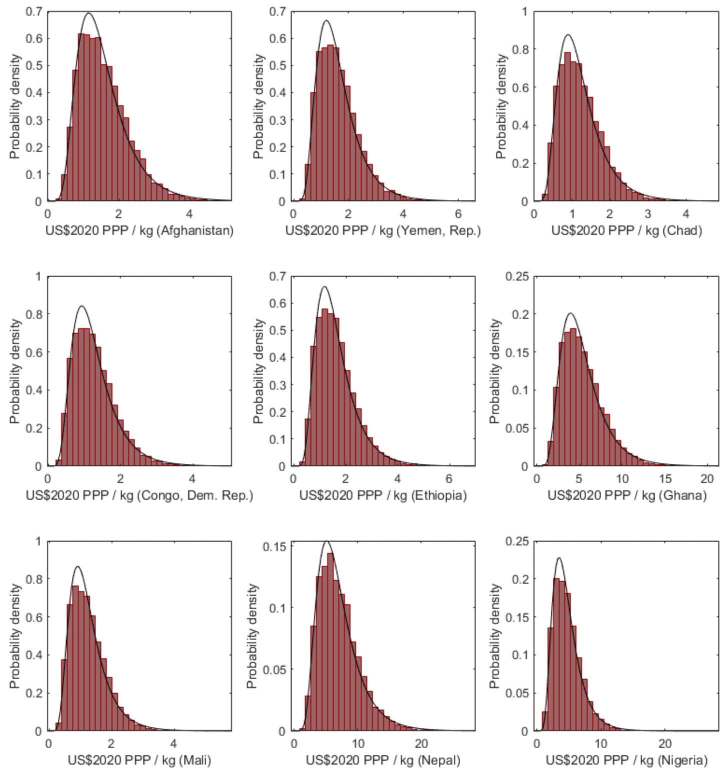

Figure 25: Lognormal marginals (black lines) of the joint resampling of $m_{i,a,NOx}$ for example countries. Red bars are histograms of the original samples of $m_{i,a,NOx}$ using a discounting adjustment factor, exposure adjustment factor, and the EU marginal damage value from Table 2.

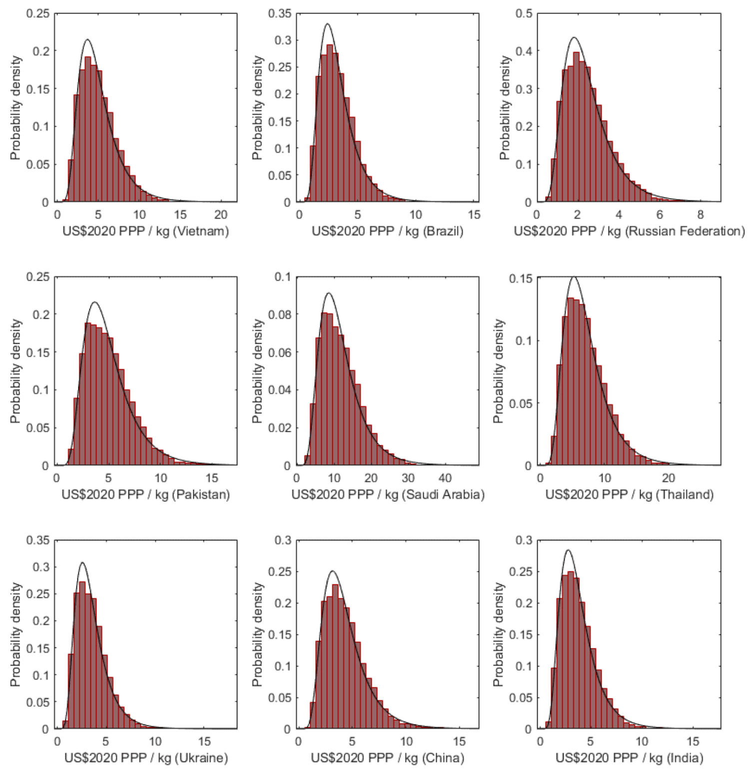

Figure 26: Lognormal marginals (black lines) of the joint resampling of $m_{i,a,NOx}$ for example countries. Red bars are histograms of the original samples of $m_{i,a,NOx}$ using a discounting adjustment factor, exposure adjustment factor, and the EU marginal damage value from Table 2.

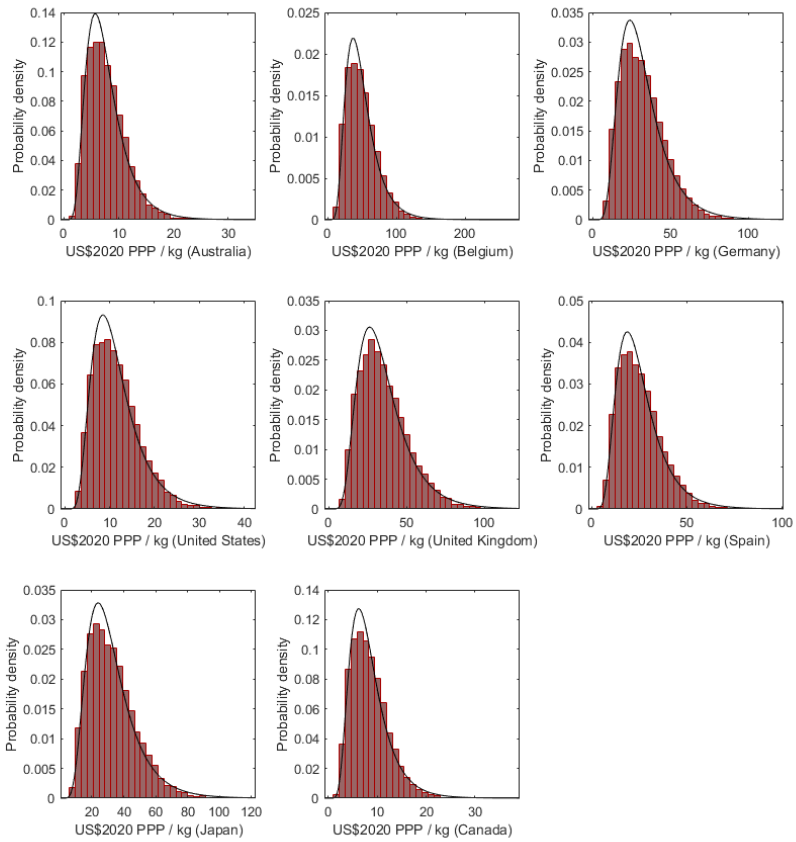

Figure 27: Lognormal marginals (black lines) of the joint resampling of $m_{i,a,NOx}$ for example countries. Red bars are histograms of the original samples of $m_{i,a,NOx}$ using a discounting adjustment factor, exposure adjustment factor, and the EU marginal damage value from Table 2.

4.10.6 Statistical fits for relationships between agricultural GVA and nitrogen run-off

Estimating damages from nitrogen run-off and deposition requires: (a) modelling of ecosystem service loss at a high spatial level of resolution and use values of ecosystem services, or (b) another proxy such as economic sector effected by nitrogen run-off for which there is coincident data.

We examined using a fixed proportion of agricultural GVA as damages. This was not chosen as the transfer method in the end as, in existing studies from the EU and the US, the agricultural sector is not necessarily the most affected by Nr run-off [97] [98]. The relationship with the agricultural sector is more on the production of Nr than the effect of Nr run-off.

Agricultural GVA shows relationships to Nr run-off through N inputs. The mean value of $m_{w,Nr}$ from Table 2 and the estimate of marginal benefit for the EU $mb_{EU} = 220$ \$US2020 PPP ($r^2 = 0.898$) / kg Nr run-off (Figure 28 left panel) would suggest $\tau = 7.5\%$ in ecosystem damages to the wider economy from Nr run-off in every 1 \$2020 USD PPP of marginal benefit in agriculture in the EU. This percentage should increase for economies like China, where additional run-off is associated with decreases in marginal benefit to agricultural value. N saturation to ecosystems involving surface and coastal water generally occurs as Nr run-off increases and marginal benefit to agricultural value of Nr run-off (through Nr input) decreases. Lacking data except for assessments for the EU, USA and China, there was no global data set available to examine the relationship to marginal agricultural benefit.

For Organisation for Economic Co-operation and Development (OECD) countries the OECD produces an environmentally adjusted multi-factor productivity measure and has a natural capital productivity component, however the change in GDP per pollutant includes only a limited list of air pollutants and the natural capital productivity component includes only subsoil resources.

Assuming a constant $\tau = 7.5\%$ of marginal benefit of agricultural GVA in ecosystem damages to the wider economy from Nr run-off, then estimating a functional form of marginal benefit of Nr run-off GVA could be used as a method for transfer of damage costs.

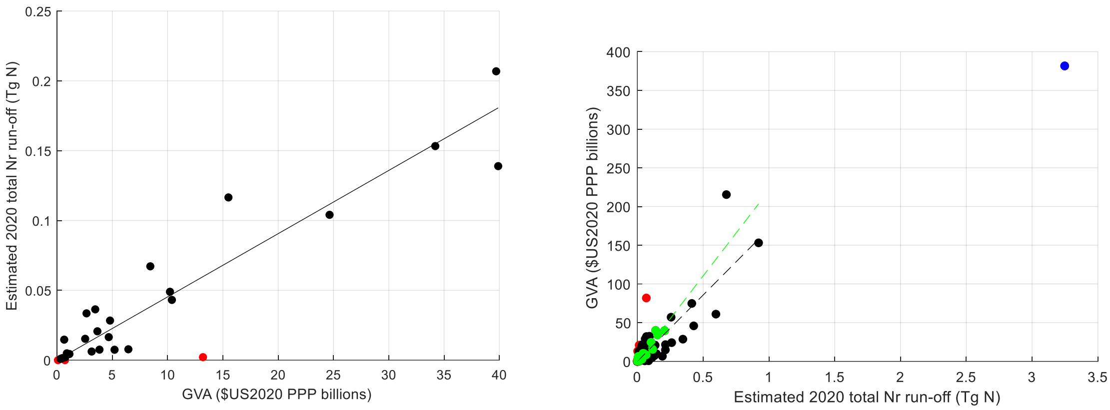

Figure 28: Statistical determination of marginal benefit for the EU27 countries of 2008 in left panel shows Nr run-off in 2000 versus GVA for agriculture in 2000 for EU27 with three outliers as red. The slope of OLS regression through the origin is 0.0045 (~1/220) and $r^2 = 0.898$. In the right panel of data points for all countries, Japan (red) is an outlier with high GVA and little run-off, and China (blue) with lower GVA relative to higher run-off is skewing the OLS fit in linear co-ordinates. The EU27 countries of the left panel are the green data points (reflected about the x=y line) and the slope of the green line is ~220. The residuals show high heteroscedasticity in the right panel and the linear fits are misleading in linear axes. An analysis using log-log axes was used below, which transformed the residuals to be approximately normally distributed.

The relationship between GVA for agriculture and Nr run-off to surface waters for all countries in 2000 was examined. China is an outlier to a generally superlinear relationship between GVA and total Nr run-off, and should be expected to have a higher proportion of damages from Nr to GVA than the method would describe. Data from 163 countries was used after removing outliers. A functional relationship between GVA and Nr run-off was used to smooth inconsistencies between a marginal damage for countries based on potential error in GVA reporting and Nr modelling, variation between years, or additional explanatory factors (only 70% of the variation is accounted for in Nr run-off). To fit a functional relationship that has value approximately 220 for EU economies but accounts for heteroscedasticity and uncertainty, data points were examined on a log-log scale and a Bayesian regression applied (Figure 30).

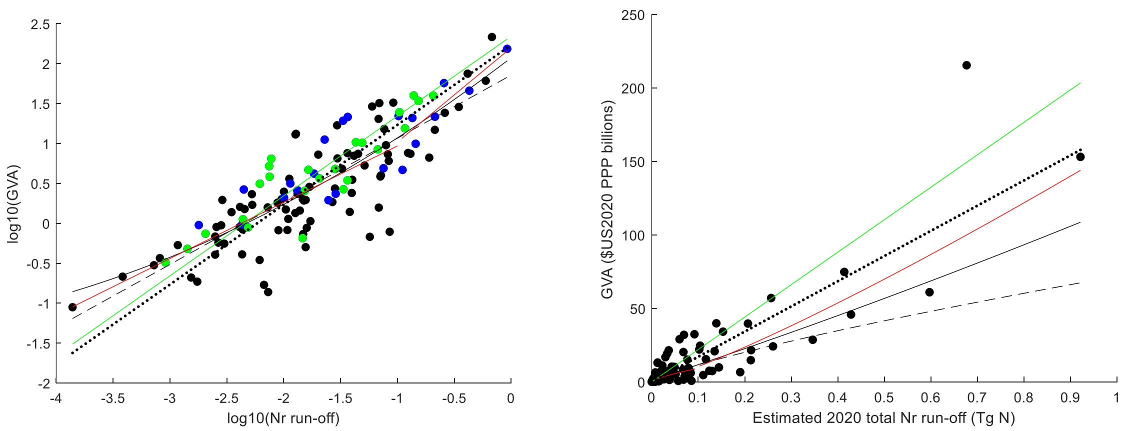

Figure 29: Left panel: the relationship of GVA to Nr run-off for 163 countries (EU27 green dots, very high HDI countries blue dots, and others black dots) including the EU. In log-log axes, residuals to linear (dashed black), piecewise linear (red), and

quadratic (black), were normal fits and all r^2 approximately 0.72. Piecewise linear and convex quadratic fits have slightly better fits statistics, demonstrating an eventual super-linear response in GAV to Nr run-off. Fitting between HDI >0.8 and HDI < 0.8 provided no better fits and almost identical slopes in log-log axes. Green solid line and black dotted line are the OLS linear fits for EU27 (green) and all (dashed black) transformed in log-log-axes. In the resolution of log-log axes r^2 OLS linear fits are approximately 0.45 in log-log axes, with greater positive residuals at lower GVA values, another demonstration of superlinear behaviour not seen in quadratic fitting in linear axes. Fitting assumptions, with no clear rationale of better fit statistics, cause a spread of uncertainty and fail to represent the full variance in potential models. We chose a Bayesian quadratic regression in log-log axis, which could capture uncertainty and linear regression in log-log and linear axes, and most of the behaviours of piecewise linear models.

Bayesian quadratic regression on the parameter space $\beta = (\beta_1, \beta_2, \beta_3)$ with $\beta_1 \geq 0, \beta_2 \geq 0$ and

$$\log_{10}(GVA(x)) = \beta_3 + \beta_2 x + \beta_1 x^2$$

offered the simplest way to capture model uncertainty in agricultural GVA against Nr run-off:

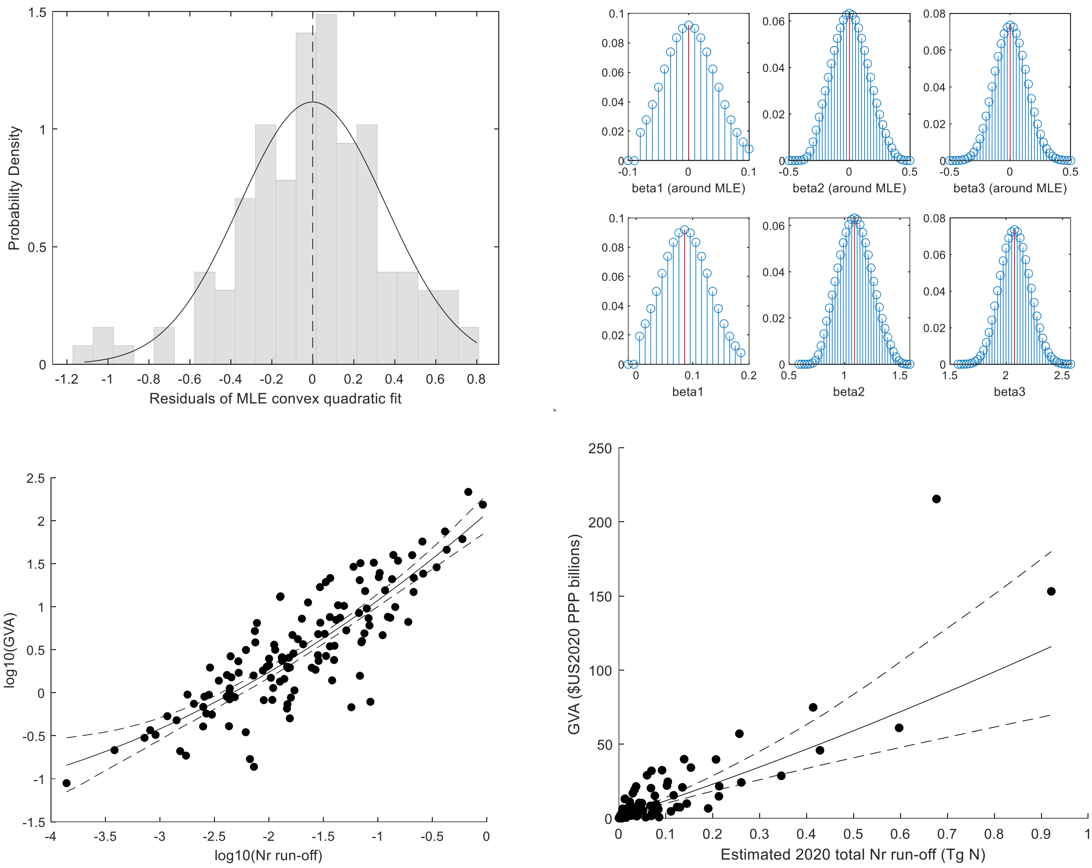

Figure 30: Bayesian quadrative regression. Top left panel shows residuals of the MLE convex quadratic fit in log-log axes which were a good fit for a normal distribution. Top right marginals of the joint distribution of parameters β. Bottom left panel, mean (black line) and 5th and 95th percentile bands for the model in log-log axes. Bottom right panel, mean (black line) and 5th and 95th percentile band of the model for GVA against Nr run-off.